ERRATA FOR SLAC-PUB-738 (REVISED)

P. 17, l. 10, third $\int$, replace $\int_0$ with $\int_0^\infty$

P. 23, l. 3, replace $\ldots G \int_0^1 \ldots$ with $\ldots G\,(N - 2\ell - 1)! \int_0^1 \ldots$

l. 7, replace $\ldots M^2 \sum_{j=1}^{N}$ with $\ldots M^2 - C(\alpha) \sum_{j=1}^{N} \ldots$

last line, following first = sign, replace $\sum_{j=1}^{N}$ with $C(\alpha) \sum_{J=1}^{N}$

P. 26, l. 11, read $C = \alpha_1 + \alpha_2 + \alpha_3 + \alpha_4 = 1$

P. 29, l. 5, replace $\int d\sigma\ \theta(-x) - \theta(-x-1)\ H(\sigma, -x)$ with $\int d\sigma\ [\theta(-x) - \theta(-x-1)]\ H(\sigma, -x)$

P. 47, l. 4, after last $\int$, replace $\int_{K_{min}}^{K_{max}}$ with $\int_{K_{min}}^{K_{max}} dK$

P. 65, between lines 13 and 14, insert: "k) L. S. Brown, 1969 Boulder Lectures"

P. 67, l. 9, change Gribor to Gribov

SLAC-PUB-738 (Revised)
February 1971

FORWARD COMPTON SCATTERING AMPLITUDE AS A SIMULTANEOUS ANALYTIC FUNCTION OF COMPLEX PHOTON MASS AND ENERGY*

Ashok suri

Stanford Linear Accelerator Center
Stanford University, Stanford, California 94305

and

Division of Natural Sciences
University of California, Santa Cruz, California 95060

(Submitted to Physical Review.)

*Work supported in part by the U. S. Atomic Energy Commission.

ABSTRACT

The analytic structures of the virtual forward Compton scattering amplitude as a function of one and two complex variables is investigated for various combinations of variables which involve the virtual photon mass. This is done both by using the DGS representation and by using the Feynman perturbation theory. The role and significance of complex Landau singularities is discussed. In general these are branch points but it is found that at t=0 some of these become poles. The effect of these complex singularities and of overlapping cuts on the ordinary single variable dispersion relations and the mass extrapolations in Vector Meson Dominance Model is explained.

Using the Cutkosky discontinuity formula for Feynman graphs the analytic structure of the discontinuities across various normal threshold cuts of the non-Born term part of this amplitude is deduced. One finds that the two variable analyticity of the amplitude implies a single variable analyticity for these discontinuities.

It is shown that in general the inelastic structure functions W and $\overline{W}$ cannot be expected to have a simply determinable analytic structure. But under certain conditions W and $\overline{W}$ can be identified with boundary values of the discontinuities across the s and u channel normal threshold cuts in the virtual forward Compton scattering amplitude, respectively. This is used to show that the contribution to W and $\overline{W}$ from certain types of Feynman graphs under certain conditions are analytic functions of one complex variable and only for such cases can one use crossing symmetry to relate the inelastic electron scattering structure functions and the annihilation structure functions.

The motion of the Landau singularities of νW_2 is shown to provide a possible explanation for its observed rapid approach to "scaling" for finite but large final state masses.

I. INTRODUCTION

In recent literature on inelastic electron scattering, increasing use has been made of analytic continuations of the inelastic electroproduction structure functions[1a,b,c] and single variable dispersion relations in the virtual photon mass q^2 for the virtual forward Compton scattering amplitude[1e,f] and for its integrated absorptive parts.[1g] Power series expansions in q^2 for fixed center-of-mass energy s have been used in the analysis of experimental data on these electroproduction structure functions.[1h] The Vector Meson Dominance Model (VDM) depends crucially on "smooth" analytic continuations in the mass q^2,[1i,j,k] and so do some theorems of current algebra.[1m] We would like to know the limitations and range of validity of all such analytic continuations, dispersion relations and power series expansions. For this purpose, we investigate the analytic structure of the virtual forward Compton scattering (VFC) amplitude T as an analytic function of one and two complex variables and demonstrate a method of deducing, in certain cases, the analytic structure of its discontinuities across fixed cuts and of the inelastic structure functions.

Our analysis is based on the Feynman perturbation theory,[2] and we only consider massive scalar particles. We ignore spin and renormalization since these do not affect the position of the singularities on the physical sheet. However, the strength (residues of poles and discontinuities across cuts) and the nature of these singularities does depend on spin, renormalization and the nature of the couplings. Besides these, renormalization can also affect the singularity structure on unphysical sheets. Our results therefore apply to the kinematic singularity free invariant amplitude and we hope that the physical sheet analyticity is valid even if the perturbation theory fails[2a,3] (as in the case of strong interactions). In this paper we do not attempt any rigorous proofs but simply demonstrate some important theorems and physical features relevant to the problem.

In Section II we collect the basic definitions used throughout the paper.

In Section III we start by giving a practical discussion of the DGS representation[4] and show how one can deduce the analyticity of the VFC amplitude directly from this representation for any combination taken as the pair of independent variables. The results are tabulated in Table I. From our analysis we find that the DGS representation implies the same analyticity for the full VFC amplitude as we obtain from the subsequent perturbative analysis. However for a single box diagram we do get a larger domain of analyticity than implied by the DGS representation. This is because in the absence of knowledge of the detailed structure of the DGS spectral function, the DGS representation is incapable of showing an analytic continuation with complex singularities except by giving an infinite cut along the whole real axis (which separates the whole complex plane into a pair of disjoint half-planes). We show how to determine the DGS spectral function for an arbitrary Feynman graph and use it to show that for the box diagram the DGS representation gives the same analytic structure as perturbation theory for the absorptive part of the box graph. This analysis also demonstrates a practical technique of determining whether the contribution of a particular Feynman graph to the inelastic structure functions[5] "scales" or not in the Bjorken limit.[1]

In Section IV we use well-known techniques[2,6,7] to determine the analytic structure of the Feynman integral for the box diagram with unstable external legs at t=0. On the basis of it we conjecture results for the complete VFC amplitude in all orders consisting of all possible Feynman graphs. The proof of these conjectures is left to a subsequent paper. The off mass shell continuation is defined by the Feynman integral and the physical boundary is determined by the Feynman prescription of giving an infinitesimal negative imaginary part to the masses of all internal legs which are presumed stable (the resonances can also be treated as stable particles for the purpose of determining the physical sheet singularities[6i]). Fixing t=0 is found very useful in trying to generalize our analysis to all orders because at t=0 the dual diagram[8] for the VFC amplitude is topologically similar to the dual diagram for the vertex function. Therefore the two amplitudes are required to have their Landau singularities similarly located (though their nature could be different). An analogous result does not hold for the second-type[9] or mixed singularities[7c] which are not determined by the usual dual diagrams. One expects[9a] that the pure second-type singularities in all orders stay away from the physical sheet and are located at the edges of the physical region (at s=0, $4M^2$, u=0, $4M^2$). However, we cannot make any definite statements about the mixed second-type singularities.[7c]

We indicate why we expect that an analysis of all orders of Feynman perturbation graphs at t=0 will show that besides the Born term poles the only Landau singularities on the physical sheet of the complex q^2 plane for fixed $s=s_R+i\epsilon$ (or vice-versa) are the s-independent normal q^2-threshold branch points (for real time-like $q^2 > 0$) and a set of complex anomalous singularities $q^2_\pm(s)$, which move with s, and correspond to the single loop box or triangle reduced diagrams. In particular this shows that the Landau singularities of the full VFC amplitude nearest to the origin and on the real plane are given by the lowest order Feynman graphs. This is a reflection of a similar well known result for the vertex function.[8e]

When all the external legs are stable (or when s is below the normal threshold) the VFC amplitude has only real singularities on the physical sheet. These real singularities are the Born term poles (due to weakly connected Feynman graphs which separate into two graphs on cutting a single line) and the normal and anomalous branch points. When the external legs are unstable some of these anomalous branch points move over into the complex plane to give the complex Landau singularities. We find that at t=0 some of these anomalous branch points coalesce to form simple anomalous poles (which come from the strongly connected graphs). We demonstrate this explicitly for the single loop box graph and give reasons why we believe this need not be true in similar situations for arbitrary Feynman graphs. This structure has important implications for ordinary single variable dispersion relations (with semi-infinite real cuts and poles) and for mass extrapolation in the Vector meson Dominance Model (VDM).[1i,j,k]

We find that ordinary single variable dispersion relation can cease to exist either when left and right hand cuts overlap giving a cut along the whole real axis or when we get complex anomalous singularities. Thus fixed ν dispersion relations in complex q^2 exist for all real ν while fixed real q^2 dispersion relations in ν cease to exist for $q^2 \geq 4\mu^2\left[1-(\mu^2/4M^2)\right]$. Similar results for other choices of variables are listed in Table I.

To study the mass extrapolation in VDM we consider the physical sheet analytic structure (see Fig. 1) of VFC amplitude in the complex q^2 plane for real s fixed above the threshold, i.e.: Re s $\geq (M+\mu)^2$, Im s $\to 0+$. From Fig. 17c and our subsequent discussion we will find that we have a real cut $\sum_z \equiv \left\{4\mu^2 \leq q^2 \leq \infty\right\}$ due to the normal q^2 threshold together with a moving (with s) overlapping cut $\sum_u \equiv \left[\frac{1}{2}(s-4M^2+u) \leq \text{Re } q^2 \leq \infty,\ \text{Im } q^2 \to 0+\right]$ due to the u channel normal threshold with the physical region squeezed between them. In addition we have the complex anomalous singularities like $q_A^2(s)$, the u channel Born poles $P_u^{(s)}$, and the vector meson resonance poles on the second sheet at

$m_\rho^2 - im_\rho \Gamma_\rho$. VDM requires an analytic continuation of the VFC amplitude from the ρ pole to the origin. For small s_R, $\sum_u$ overlaps $\sum_z$ squeezing the physical region between them and the above analytic continuation is not possible since the continuation path A leads off to the unphysical sheet in $\epsilon \to 0+$ limit. But for large s_R this cut moves to the right exposing the physical boundary and the analytic continuation is possible along a path B. This is the well known[1j] reason why VDM is expected to work for large real s only. Now the mass extrapolation assumption for VDM amounts to dominating the absorptive part across the normal q^2 cut $\sum_z$ by the ρ pole with a width (which parameterizes the effect of this cut), cutting off u-channel poles $P_u(s)$ by the form factor and ignoring the $\sum_u$ cut due to its distance. But VDM also ignores the contributions of the complex anomalous singularities. This we find to be unjustified because even though, at large real s, these anomalous singularities may have a small effect on the modulus of the VFC amplitude at $q^2=0$, due to their large (of order of s_R) distance from the origin, they can still have very significant effect on the phase of the amplitude (or its ratio of real to imaginary part). Related results for the case $t \neq 0$ have been recently obtained by Potter and Sullivan.[1k]

In contrast to the DGS representation, the advantage of our perturbative analysis is that we can deduce the single variable analyticity of the discontinuities of the non-Born term part (the strongly connected Feynman graphs) of the VFC amplitude across the various normal threshold cuts. The Born terms give non-analytic delta function contributions. The single variable analyticity of the discontinuities is found as a straight forward consequence of the two variable analyticity of the amplitude. These facts are apparent from the Cutkosky's discontinuity formula,[2a, 10] from which one can also show that the non-Born term parts (nonresonant final states) of the inelastic structure functions are a boundary value of the discontinuity functions on and only on the cut free part of the real axis, when the mass of the undetected final state is kept fixed. These facts are explained further in Section V. There we also discuss the special class of graphs for which the inelastic structure functions can be analytically continued from the scattering region to the annihilation region.[1b, c, ℓ]

In a separate publication[11] we discuss an interesting application of our analysis which is based on the observation that the physical x-sheet anomalous singularities $x_{\pm}(s)$ of $W(s,x)$ rapidly approach their s independent asymptotic position once s is large enough. We propose that this may provide an explanation of the rapid approach to "universality" of the inelastic electron scattering structure functions. A simple minded discussion of the physical basis of this proposal is given in Section IV.C and V.

Most of the sections of this paper can be read independent of each other. In particular we suggest Sections IV.C and V to those interested in practical applications of our analysis.

II. DEFINITIONS

The forward Compton scattering amplitude represents the process $\gamma N \rightarrow \gamma N$ when there is no four momentum transferred from the photon to the nucleon. This process is shown in Fig. 2. For future reference we list the relevant kinematic variables below (our metric is (1, -1, -1, -1) and $\hbar = C = 1$);

1. The photon mass $q^2 \equiv z$.
2. The nucleon mass $P^2 = M^2$ (fixed).
3. The energy of photon in the rest frame of the nucleon is proportional to $\nu \equiv 2q \cdot P$.
4. The direct channel center-of-mass energy equals

$$S \equiv (p_1+p_2)^2 = (q+P)^2 = z + \nu + M^2 .$$

5. The momentum transfers $t = (p_2+p_4)^2 = (P-P)^2 = 0$ (fixed)

$$u = (p_2+p_3)^2 = (P-q)^2 = z - \nu + M^2$$

These satisfy $s + u = 2z + 2M^2$.

6. The scaling variables are

$$\omega = \frac{2q \cdot P}{-q^2} = -\frac{\nu}{z} \qquad \text{and} \qquad x \equiv \frac{z}{\nu} = -\frac{1}{\omega} .$$

If we keep $P^2 = M^2$ and t=0 fixed we know from Lorentz invariance that T is a function of two invariants. We choose these to be either the set (z, ν) or the set (z, s) and study the analytic structure of $T(z, \nu)$ and $T(z, s)$ as functions of complex z, ν and s.

When the spins of the photon and the nucleon are considered, one finds that T is a multicomponent Lorentz tensor $T_{\mu\nu}^{(\alpha\beta)}$ where α, β are spinor indices and μ, ν are vector indices. Then one can use Lorentz invariance[2h,ℓ] to expand the tensor amplitude in terms of a complete set of linearly independent tensors $\left\{\mathscr{L}^{\alpha\beta}_{\mu\nu}(\mathrm{i})\right\}$ formed out of q_μ, P_μ, $\gamma^{(\alpha\beta)}_\mu$, and $\epsilon^{(\alpha)}_\mu$, as follows:

$$T^{(\alpha\beta)}_{\mu\nu} = \sum_{\mathrm{i}} \mathscr{L}^{(\alpha\beta)}_{\mu\nu}(\mathrm{i})\ T_{\mathrm{i}}$$

Here the coefficient T_{i} are scalar functions of linearly independent invariants and we call these invariant amplitudes. These are chosen to be free of kinematic singularities, which can be discovered applying conservation laws like four momentum conservation and gauge invariance.[1j, ℓ]

It is well known[2a, c] that the analytic structure of the invariant amplitudes is the same as that of a corresponding amplitude with all spins ignored. That spin is an "inessential complication" in the study of analyticity, is most easily understood in terms of the Feynman graphs in which spin just adds extra momentum dependent terms in the numerator of the integrand but does not affect the denominators whose zeros give the usual Landauian[6] and second-type singularities.[9] On the other hand, it should also be clear that spin will be very important important in the study of the asymptotic behavior[2a] which is an input for the dispersion relations. This will not concern us in the present paper. However, when discussing specific cases we should remember that these spin factors can lead to cancellations within a particular Feynman integral or between different ones in a sum of Feynman integrals. From now on we shall ignore all the spin factors and only consider scalar particles. Hence, our results will only apply to the kinematic singularity free invariant amplitudes. In the same spirit we will also assume as usual that the infrared and ultraviolet divergences have been removed by suitable cutoff.

III. RESULTS FROM THE DGS REPRESENTATION

Using the LSZ reduction formulae,[2h] the forward Compton scattering amplitude can be defined in three ways (ignoring spin).

$$T_R(q,P) \equiv \int d^4x\, e^{iq\cdot x} \langle P|\theta(x_0)\left[J_1(x),\, J_2(0)\right]|P\rangle$$

$$T_A(q,P) \equiv -\int d^4x\, e^{iq\cdot x} \langle P|\theta(-x_0)\left[J_1(x),\, J_2(0)\right]|P\rangle$$

or

$$T_T(q,P) \equiv \int d^4x\, e^{iq\cdot x} \langle P|T_+(J_1(x)\, J_2(0))|P\rangle$$

where $J_1(x)$ and $J_2(x)$ are local electromagnetic currents and T_+ the positive time ordering operator. For a stable nucleon these definitions agree for various physical values of the four momenta q and P. This is seen as follows:

$$\begin{aligned} T_+(J_1(x)\, J_2(0)) &= \theta(x_0)\left[J_1(x),\, J_2(0)\right] + J_2(0)\, J_1(x) \\ &= -\theta(-x_0)\left[J_1(x),\, J_2(0)\right] + J_1(x)\, J_2(0) \quad . \end{aligned}$$

Therefore

$$\begin{aligned} T_T(q,P) - T_R(q,P) &= \int d^4x\, e^{iq\cdot x} \langle P|J_2(0)\, J_1(x)|P\rangle \\ &= \sum_n (2\pi)^4\, \delta^{(4)}(q-P+P_n) \langle P|J_2(0)|n\rangle\langle n|J_1(0)|P\rangle \end{aligned}$$

Energy conservation and the stability of the physical nucleon of momentum P ($P^o \geq 0$) forbids it to decay into a physical single particle of momentum q ($q^o \geq 0$) and another system of momentum $P_n (P^o \geq 0)$. Therefore $P_n=0$, i.e.: the only intermediate state allowed is the vacuum. But $\langle P|J_2(0)|\Omega\rangle = 0$ from LSZ assumptions. Therefore in the physical region of s-channel ($q^o > 0$), $T_T(q,P) = T_R(q,P)$. Similarly in the physical region for the crossed channel ($q^o < 0$), $T_T(q,P) = T_A(q,P)$.

This shows that in the appropriate physical regions T_T coincides with $T_{R,A}$. For unphysical (and complex) values of the momenta one must define the amplitude T by means of an analytic continuation.[2m,n] Then the function T_T, T_R and T_A will simply be different boundary values in the appropriate regions of this unique analytic continuation T. To seek this analytic continuation it is convenient to start with T_R or T_A rather than T_T since the locality of the retarded (or advanced) commutator (i.e.: vanishing at space-like separations) allows its fourier transform to have a large domain of analyticity.[2] On the other hand it is perfectly possible to arrive at this unique analytic function T by analytic continuing any representation for the scattering amplitude which has the suitable analyticity and agrees with T_T in the physical regions. This fact will be used in our subsequent discussions in this section. We should observe that even though the Feynman perturbation theory is derived using the form $T_T(q \cdot P)$, the analytic structure obtained by analyzing connected Feynman diagrams reflects the analytic structure of the retarded (or advanced) commutator. This is because Feynman graphs involve positive energy particles and conserve four momentum so that the extra terms $J_2(0)\ J_1(x)$, or $J_1(x)\ J_2(0)$ are not seen in the diagrams contributing to the respective channels. To be precise, the connected Feynman diagrams correspond to the connected part of the retarded (or advanced) commutator defined by

$$\theta(\pm x_0) \langle P| \left[J_1(x),\ J_2(0) \right] |P\rangle_{\text{connected}} \equiv \theta(\pm x_0) \langle P| \left[J_1(x),\ J_2(0) \right] |P\rangle -$$
$$- \theta(\pm x_0)\ \delta^{(4)}(P-P') \langle \Omega | \left[J_1(x),\ J_2(0) \right] | \Omega \rangle$$

The term $\theta(\pm x_0)\ (P-P') \langle \Omega | \left[J_1(x),\ J_2(0) \right] | \Omega \rangle$ corresponds to the disconnected graphs shown in Fig. 3a.

When discussing analytic continuations we will be interested mainly in the cut structure of the amplitude in the complex planes. Since pole graphs do not affect such structures, we shall ignore them in all our discussions.

Let us now consider the amplitudes $T_R(q,P)$ and $T_A(q,P)$. Using the identity[2h, j] $e^{iq_0x_0}\,\theta(\pm x_0) \equiv \pm(2\pi i)^{-1}\int_{-\infty}^{\infty} dq_0'\, e^{iq_0'x_0}\left[q_0'-q_0 \mp i\epsilon\right]^{-1}$ (or a subtracted version), it is easy to show that T_R is analytic in the upper half q_0 plane and T_A is analytic in the lower half q_0 plane. We can define a function T which equals T_R in the upper half plane and T_A in the lower half plane. The two half planes are separated along the whole real axis with the discontinuity in T across real q^o axis being the absorptive part of T which equals

$$A(q,P) \equiv \int_{-\infty}^{\infty} d^4x\, e^{iqx} \langle P|\left[J_1(x),\, J_2(0)\right]|P\rangle = T(q_0+i\epsilon) - T(q_0-i\epsilon) \quad .$$

In case this discontinuity vanishes across some finite interval of the real q^o axis we can analytically connect T_R and T_A across this segment and then T defines a real analytic function of q^o, otherwise not. On the other hand if this absorptive part is nonzero along the whole real q^o axis then T_R and T_A are not analytically connected. However, we will see from the analysis of the Feynman graphs that one may still be able to define a analytic continuation of T_R (and a different one for T_A) into the lower half plane, but this continuation will have branch points in the complex plane (and corresponding complex cuts) and will not be a real analytic function. Here again we must remember that as long as we can find an analytic function which equals T_R or T_A in the appropriate physical regions it is a perfectly legitimate analytic continuation into the unphysical region, though the domains of different analytic continuations would be different. This fact will be very useful in understanding the Compton amplitude for $q^2 > 0$.

To understand the physical significance of the absorptive part A(q, P) we put in a complete set of physical (in or out) states, use translational invariance and integrate to get

$$A(q,P) \equiv \int d^4x\, e^{iq\cdot x} \langle P | \left[J_1(x),\ J_2(0) \right] | P \rangle$$

$$= (2\pi)^4 \sum_n \left[\delta^{(4)}(q+P-P_n) \langle P | J_1(0) | n \rangle \langle n | J_2(0) | P \rangle \right.$$

$$\left. - \delta^{(4)}(q-P+P_n) \langle P | J_2(0) | n \rangle \langle n | J_1(0) | P \rangle \right]$$

Now for all q^2 in the s-channel physical region ($q^o > 0$, $P^o > 0$, $P_n^o \geq 0$, see Fig. 4), energy conservation and stability of nucleon makes the second term vanish so we get for all q^2

$$A(q,P)_{\text{Physical}} = (2\pi)^4 \sum_n \delta^{(4)}(q+P-P_n) \langle P | J_1(0) | n \rangle \langle n | J_2(0) | P \rangle$$

The various parts of this commutator correspond to the various classes of connected unitarity diagrams C, P and D shown in Fig. 3. Its disconnected part (Fig. 3a) is not needed for the present considerations. These parts are real quantities defined as

$$C(q,P) = (2\pi)^4 \sum_k \delta^{(4)}\ (q+P-P_k) \langle P | J_1(0) | k \rangle_c \langle k | J_2(0) | P \rangle_c$$

$$D(q,P) = (2\pi)^4 \sum_\ell \delta^{(4)}\ (q-P_\ell) \langle \Omega | J_1(0) | \ell \rangle_c \langle \ell, P | J_2(0) | P \rangle_c$$

$$+ \langle P | J_1(0) | P, \ell \rangle_c \langle \ell | J_2(0) | \Omega \rangle_c$$

$$P(q,P) = (2\pi)^4 \sum_m \delta^{(4)}\ (q-P-P_m) \langle \Omega | J_1(0) | P, m \rangle_c \langle m, P | J_2(0) | \Omega \rangle_c$$

$$A(q,P) = C(q,P) + D(q,P) \pm P(q,P)$$

where the subscript c denotes connected part of the matrix element. From Fig. 3b, c, d, we observe that the unitarity diagrams for C, P and D are topologically similar to the Cutkosky discontinuity diagrams for the discontinuities across various s, u and z channel normal threshold cuts respectively. The relationship between C, P, D and $\mathrm{disc}_s\, T$, $\mathrm{disc}_u\, T$, $\mathrm{disc}_z\, T$ respectively will be discussed later.

Using the LSZ reduction techniques its easy to show the crossing relation

$$C(q, P) = \pm\, P(q, -P)$$

where (+) or (-) sign refers to a Boson or Fermion target $|P\rangle$ respectively reflecting the Pauli principle. For $q^o > 0$, $q^2 < 0$, C is like the structure function W for inelastic electron scattering ($e^- + N \rightarrow e^- + \text{anything}$). For $q^o > 0$, $q^2 > 0$, P is like the annihilation structure function $\overline{W}$ for the reaction ($e^+e^- \rightarrow N + \text{anything}$). Its clear that to use this crossing relation we need to analytically continue the two sides of the equation to common domains. If the existance of such analytic continuation can be established, then it can be used to connect inelastic electron scattering and annihilation structure functions. The regions in which these functions are nonzero are shown in Fig. 4. In region I only C contributes. In region II, (C+D) contribute. In region III, IV and V (C+D+P) contribute. In region VI (P+D) contribute. In region VII P contributes and in region VIII none contribute and thus the commutator must vanish. This is because kinematics require that C contributes for $s \geq 0$ (in fact M^2), P contributes for $u \geq 0$ (and $z \geq 0$, but may be analytically continued into region VII keeping u fixed), and D contributes for $z \geq 0$. We should observe that C, D and P cannot vanish identically in any finite subregion of the unphysical region IV if they are analytic functions. But this does not restrict the value of their sum which represents the full commutator and need not be analytic. A similar remark applies to regions III and V. Thus the vanishing of the sum (C+D+P) in regions III, IV and V (as indicated by Bjorken's analysis[1b, d, f] for the asymptotic limit functions) together with analyticity could be expected to impose rather strong restrictions on the functional form of C, D and P.

To study the support of the absorptive part $A(q, P)$ it is convenient to use the DGS representation[4] which is derived on the following assumptions:

1. Microcausality $[J_1(x), J_2(0)] = 0$ for all $x^2 < 0$ (space-like)
2. Rapidly vanishing asymptotic behavior in α for

$$G(\alpha, \beta) \equiv \iint_{-\infty}^{\infty} d(x^2)\, d(Px)\, e^{-i\alpha x^2}\, e^{-\beta(P\cdot x)} \langle P|\left[J_1(x), J_2(0)\right]|P\rangle$$

(we shall assume the unsubtracted form)

3. T P or C invariance

Nakanishi[4] has shown that every connected Feynman diagram satisfies a DGS representation so that we should expect the results obtained from the DGS representation to be valid for each perturbation diagram. This is discussed further at the end of this section.

The DGS representation for the fourier transform of a causal commutator states that

$$A(q, P) \equiv \int d^4x\, e^{iq\cdot x} \langle P|\left[J_1(x), J_2(0)\right]|P\rangle$$

$$= \int_{-1}^{1} d\beta \int_{-\beta^2 P^2}^{\infty} d\sigma\, \epsilon(P\cdot q + \beta P^2)\, \delta(q^2 + 2\beta q\cdot P - \sigma) \sum_{n=0}^{N} H_n(\sigma, \beta)(P\cdot q + \beta P^2)^n$$

where $H(\sigma, \beta)$ is real, irrespective of the nature of currents because of T P or C invariance. The terms for $n > 0$ correspond to terms in A which do not vanish as $|\nu| \to \infty$ for fixed z or $|z| \to \infty$ for fixed ν (where we express the polynomials in z by those in ν using their linear dependence due to $\delta(z+\nu-\sigma)$).[4d, i, j] For example such terms can arise when spin is not ignored. They would also occur when the commutator has Schwinger terms (since fourier transform of $(d^n/d(x^2)^n)\ \delta(x^2)$ is $(q^2)^n$). Using crossing symmetry of the whole Compton amplitude (which require symmetry under $\nu \to -\nu$) we can also show that $H(\sigma, -\beta) = H(\sigma, \beta)$.

We will be concerned with the case when the nucleon is massive and stable and we will ignore the subtraction terms, since they are known not to affect the analytic structure of the matrix elements. With these restrictions we can write (using our notation)

$$A(q,P) \equiv \int d^4x\ e^{iq\cdot x} \langle P|\left[J_1(x), J_2(0)\right]|P\rangle = \int_{-1}^{1} d\beta \int_0 d\sigma\, \epsilon\left(\frac{\nu}{2} + \beta M^2\right) \delta(z+\beta\nu - \sigma)\ H(\sigma, \beta)$$

The physical region in the real (z, ν) plane and the support of the spectral function $H(\sigma, \beta)$ in real (σ, β) plane are shown in Figs. 4 and 5.

From their representation for $A(z, \nu)$, DGS are also able to derive a representation for T_R which is

$$T_{\substack{R\\A}}(q,P) = \int_{-1}^{1} d\beta \int_0^{\infty} d\sigma \frac{H(\sigma, \beta)}{z + \beta\nu - \sigma \pm i\left(\frac{\nu}{2} + \beta M^2\right)} + \begin{array}{l}\text{Real Polynomial } P(z,\nu)\\ \text{in } z \text{ and } \nu\end{array}$$

The support of $H(\sigma, \beta)$ is deduced from the behavior of the commutator in the physical region. The physical region (where Energy $\geq$ mass) is $\nu^2 \geq 4M^2 z$. The s-channel reactions lie in $s \equiv z + \nu + M^2 \geq M_s^2$ and the u-channel reactions in $u = z - \nu + M^2 \geq M_u^2$. For $M_s - M > 0$ and $M_u - M > 0$ these two regions are disjoint and this nucleon stability condition is crucial to our analysis (if these conditions are violated the analyticity is reduced drastically). The support Σ of $H(\sigma, \beta)$ is bounded by $-1 \leq \beta \leq 1$, $\sigma \geq 2\mu M\beta + \mu^2$ and $\sigma \geq -2\mu M\beta + \mu^2$ assuming $M_s = M_u = (M+\mu)^2$ where μ is the pion mass. Σ is shown in Fig. 5.

For every point in the (z,ν) plane the absorptive part $A(z,\nu)$ receives contribution from the integral along the line in the (σ,β) plane given by the equation

$$z + \beta\nu - \sigma = 0$$

The parabola $\nu^2 = 4M^2 z$ generates a set of lines in the (σ,β) plane which have as their envelope the parabola $\sigma = -\beta^2 M^2$. The part of the line $s = z + \nu + M^2 = M_s^2$ in the physical region generates a pencil of lines through $(\sigma = M^2 - M_s^2,\ \beta = -1)$ lying between tangents of positive slope and the line $\beta = +1$. Similarly the line $u = z - \nu + M^2 = M_u^2$ gives the tangent to $\sigma = -\beta^2 M^2$ through $(\sigma = M^2 - M_u^2,\ \beta = +1)$. All the lines generated by points in $\nu^2 \geq 4M^2 z$ intersect the parabola (or at least touch it) and the ϵ-function changes sign inside the parabola (or at the point of contact) where $H(\sigma,\beta)$ vanishes. Also in the support of $H(\sigma,\beta)$, $\epsilon(\nu/2 + \beta M^2) = \epsilon(\nu)$ for ν lying in the physical region of the (z,ν) plane.

Using the fact that due to the stability of the nucleon the s-channel physical region (where the term $\langle P| J_1(x)\ J_2(0) |P\rangle$ contributes) is disjoint from the u-channel physical region (where the term $\langle P| J_2(0)\ J_1(x) |P\rangle$ contributes) DGS show that one can write

$$T_T(q,P) = \int_{-1}^{1} d\beta \int_0^\infty d\sigma \frac{H(\sigma,\beta)}{z + \beta\nu - \sigma + i\epsilon} = -\int_0^1 d\beta \int_{-z}^\infty d\nu'\ H(z+\nu',\beta) \left[\frac{1}{\nu' - \beta\nu - i\epsilon} + \frac{1}{\nu' + \beta\nu - i\epsilon}\right]$$

$$-\frac{1}{\pi} \operatorname{Im} T_T(q,P) = \int_{-1}^{1} d\beta \int_0^\infty d\sigma\ \delta(z + \beta\nu - \sigma)\ H(\sigma,\beta)$$

We see that DGS representation for $T_{R,A}$ defines a function which is analytic in the physical region $\left(\text{since there the sign of } \left(\frac{\nu}{2} + \beta M^2\right) \text{ is fixed}\right)$ but due to the presence of $i\left(\frac{\nu}{2} + \beta M^2\right)\epsilon$ it cannot be continued to unphysical values of ν since $\left(\frac{\nu}{2} + \beta M^2\right)$ can go through a zero and change sign. On the otherhand the representation obtained for T_T is continuable to the unphysical ν regions provided Im T_T

vanishes over a real interval. To determine the support of Im T_T we use the fact that the nonvanishing contribution to the integral defining Im T_T comes from the intersection of the line $z+\beta\nu-\sigma=0$ with the support of $H(\sigma,\beta)$. From Fig. 6 we observe that for arbitrary fixed real ν and z variable or for z fixed less than μ^2 and ν variable we can always find a pencil of such lines corresponding to a real z interval or real ν interval respectively, which do not intersect the support and therefore gives a vanishing value of Im T_T. In such cases the DGS representation for T_T defines a real analytic function of z for arbitrary fixed real ν with a cut along a part of real z axis. Similarly for fixed real $z<\mu^2$ we get a real analytic function of ν. But if we fix $z>\mu^2$ then the line $z+\beta\nu-\sigma=0$ always intersects the support for all real ν and in general we will get a nonzero Im T_T for all real ν. In this case we do not have a real analytic function of ν but instead a function which has a cut along the entire real axis and the DGS representation for T_T can not be used to continue in ν from the upper half plane to the lower half plane. However, as we shall see in the analysis of Feynman graphs, we may still be able to find an analytic continuation of the amplitude from the upper half ν-plane to the lower half ν-plane, but this continuation will have complex branch points and correspondingly cuts in the complex plane. At this point we should note that in the case $z>\mu^2$, the nonvanishing of Im T_T for all real ν may not imply the nonvanishing of A for all real ν. This is because for certain ν in the unphysical region $\epsilon\left(\frac{\nu}{2}+\beta M^2\right)$ can change sign on $z+\beta\nu-\sigma=0$ inside the support and so may cause the integral for A to vanish.

A similar analysis in Fig. 7 shows that for fixed $s>(M+\mu)^2$ the amplitude is not a real analytic function of z and for fixed $z>\mu^2$ the amplitude is not a real analytic function of s. Of course below these thresholds (which are the lower bounds on actual thresholds) we do get the amplitude to be a real analytic function of one variable. The reason is that for fixed s as we vary z the σ-intercept of the integration line rises while its slope decreases and (for say $s > (M+\mu)^2$) this can cause the integration line to intercept the support for all real z. In fact we observe that whenever a variable is such that varying it can cause this intercept to rise simultaneously with falling slope we can expect to get a nonreal analytic function (above the threshold for the fixed variable). On the other hand if the intercept falls simultaneous with falling slope, then we may expect a real analytic function. Using these rules we can analyze the amplitude for any combination of a pair of invariant variables and the results are indicated in Table I.

We thus see that the representation for T_R derived from the DGS representation for A defines an analytic function in the physical region but does not provide an analytic continuation of $T_{R,A}$ to the unphysical regions. Instead the representation for T_T is in a continuable form and the two agree on the various physical regions. Since T is defined to be the analytic continuation to unphysical region of the physical region amplitude (T_R or T_T) we choose the DGS representation for T_T to define T for all z and ν (or z and s, etc.). Hence in general we have

$$T(z,\nu) = P(z,\nu) + \int_0^\infty d\sigma \int_{-1}^{1} d\beta \, \frac{\left\{ \sum_{m=0}^{M} \nu^m h_m(\sigma,\beta) + \sum_{n=0}^{N} (z+\beta\nu-\sigma)^n \tilde{h}_n(\sigma,\beta) \right\}}{z+\beta\nu-\sigma}$$

for all z and ν. $T_T(z,\nu)$ is always a boundary value (at Im $z > 0$, Im $\nu > 0$ in the s-channel physical region; at Im $z > 0$, Im $\nu < 0$ in the u-channel physical region) of an analytic function $T(z,\nu)$ of two complex variables. As we have seen, it may not always be a boundary value of a real analytic function of one complex variable when the other variable is fixed above certain real values. We also note that this analytic continuation is conjugate symmetric in the two complex variables, i.e.:

$$T(z^*, \nu^*) = T^*(z, \nu)$$

This property will also be reflected by the analytic continuations obtained from Feynman graphs. This does not necessarily imply that the physical amplitudes $T(z, \nu_R \pm i\epsilon)$ or $T(z_R \pm i\epsilon, \nu)$ are real analytic functions of one complex variable.

Now

$$A(z,\nu) = \int_{-1}^{1} d\beta \int_0^\infty d\sigma\, \epsilon\left(\frac{\nu}{2} + \beta M^2\right) \delta(z + \beta\nu - \sigma)\, H(\sigma, \beta)$$

$$= \begin{cases} \displaystyle\int_{-1}^{1} d\beta \int_0^\infty d\sigma\, \delta(z + \beta\nu - \sigma)\, H(\sigma,\beta) & \begin{cases}\text{for } \nu > 0 \text{ and } (z,\nu) \text{ in the} \\ \text{physical region } (\nu^2 \geq 4M^2 z)\end{cases} \\ \displaystyle -\int_{-1}^{1} d\beta \int_0^\infty d\sigma\, \delta(z + \beta\nu - \sigma)\, H(\sigma,\beta) & \big\{\text{for } \nu < 0 \text{ and } (z,\nu) \text{ in the physical region} \\ \displaystyle\int_0^1 d\beta \int_0^\infty d\sigma\, \delta(z - \sigma) \left\{H(\sigma,\beta) - H(\sigma,-\beta)\right\} = 0 & \big\{\text{for } \nu = 0 \text{ and any } z \end{cases}$$

while

$$I(z,\nu) = -\frac{1}{\pi} \operatorname{Im} T(z,\nu) = \int_{-1}^{1} d\beta \int_0^\infty d\sigma\, \delta(z + \beta\nu - \sigma)\, H(\sigma,\beta)$$

$$= \text{disc } T_R = A, \qquad \text{in the s-channel physical region}$$

$$= \text{disc } T_A = -A, \qquad \text{in the u-channel physical region}$$

Thus the absorptive parts $A(z,\nu)$ and $I(z,\nu)$ agree in the various physical regions. They can differ in the unphysical region $\nu^2 < 4M^2 z$, and here $I(z,\nu)$ need not represent the commutator. But in the unphysical region the definition of the fourier transform of the commutator is arbitrary since neither the DGS representation nor any general principles indicate any analyticity for these absorptive parts, and so we have no a priori criterion to choose one over the other. Thus different representations of the commutator in the unphysical region which agree on the physical region will give the same amplitude and the same physics. Since we have chosen a particular representation for the amplitude on the, a priori, basis of analyticity, it is convenient to choose its total imaginary part $I(z, \nu)$ to define the commutator even in the unphysical region. One advantage of such definition is that the analytic continuation of the amplitude into a particular complex domain is unique and so has a unique imaginary part. In the particular case of a real analytic function (only real cuts) the total discontinuity across the real cut gives the imaginary part. For an analytic function with complex cuts (as is needed to define analytic continuation of the amplitude in case the DGS indicates nonvanishing imaginary part across whole real axis) the imaginary parts in the real region on the physical sheet are related to the discontinuities across the complex cuts[7] also. This will become clear when we discuss Feynman graphs. As an example we should note the fact that since the DGS representation for T tells us that T is a real analytic function of z for all fixed real ν we can, therefore, unambiguously define the imaginary part $I(z, \nu)$ as the total discontinuity across the (real) cuts in the z plane for any real z and ν and we can take this to define the commutator for all real z and ν.

Before we conclude this section we discuss the Nakanishi's[4c] method of deriving the DGS representation from the Nambu[2, 6a, b, c] representation for an arbitrary order Feynman graph for the virtual forward Compton scattering amplitude and apply the results to the box graph of Fig. 8a. In particular we explicitly demonstrate how to use this representation to study the "scaling" of the contribution of any Feynman graph to the inelastic structure functions W.

For an arbitrary Feynman graph, with N internal legs and ℓ independent loops, for the VFC amplitude the Nambu representation[2a, 6abc] is written as

$$T(z,s,M^2) = \lim_{E \to 0+} G \int_0^1 \frac{\prod_{i=1}^{N} d\alpha_i \, \delta\left(\sum_{i=1}^{N} \alpha_i - 1\right) C(\alpha_j)^{N-2\ell-2}}{\left[D(\alpha_j, z, s, M^2) + i\epsilon \, C\right]^{N-2\ell}}$$

where G is a constant. For a u-channel graph the variable s is replaced by u. Applying circuit theory[2a, 6] one can show that the discriminant

$$D(\alpha_1, \ldots \alpha_N, z, s, M^2) = \xi_s(\alpha_1, \ldots, \alpha_N)\, s + \xi_z(\alpha_1, \ldots, \alpha_N)\, z + \xi_u(\alpha_1, \ldots, \alpha_N)\, u$$

$$+ \xi_M(\alpha_1, \ldots, \alpha_N)\, M^2 - \sum_{j=1}^{N} \alpha_j m_j^2$$

while $C(\alpha_i)$ is a sum of products of $\{\alpha_i\}$ and for[3a]

$$0 \le \alpha_i \le 1 \qquad \xi_\nu\left(\{\alpha_j\}\right) \ge 0 \qquad \nu = s, z, u, M, \qquad \{j\} = 1, 2, \ldots, N$$

and

$$C\left(\{\alpha_i\}\right) \ge 0$$

Again we define

$$\eta(\alpha_i) = \xi_s(\alpha_i) + \xi_z(\alpha_i) + \xi_u(\alpha_i) \ge 0$$

$$\phi(\alpha_i) = \frac{\xi_s(\alpha_i) - \xi_u(\alpha_i)}{\xi_s(\alpha_i) + \xi_z(\alpha_i) + \xi_u(\alpha_i)}, \qquad -1 \le \phi(\alpha_i) \le 1$$

$$\psi(\alpha_i, m_i^2, M^2) = \frac{\sum_{j=1}^{N} \alpha_j m_j^2 - \left(\xi_s(\alpha_i) + \xi_u(\alpha_i) + \xi_M(\alpha_i)\right) M^2}{\xi_s(\alpha_i) + \xi_z(\alpha_i) + \xi_u(\alpha_i)}$$

and use $s = z + \nu + M^2$ and $u = z - \nu + M^2$ to write

$$D = \eta \left\{ z + \phi\nu - \psi \right\}$$

To get a representation with a DGS type of denominator we use the identity

$$1 = \int_{-\infty}^{\infty} d\beta \quad (\beta - \phi) \int_{-\infty}^{\infty} d\sigma \quad (\sigma - \psi)$$

and

$$\int_{-\infty}^{\infty} d\sigma \frac{\delta(\sigma-\psi)}{(A-\sigma)^{n+1}} = \frac{(-1)^n}{n!} \int_{-\infty}^{\infty} d\sigma \frac{\frac{\partial^n}{\partial\sigma^n} \delta(\sigma-\psi)}{(A-\sigma)}, \qquad n \geq 1$$

after n partial integrations.

We use $\delta(\sum_i \alpha_i - 1)$ to extend the α_i integrations to infinity and assume suitable convergence properties so as to be able to interchange the order of α_i, β, σ integrations to get

$$T(z, s, M^2) = G \int_{-\infty}^{\infty} d\beta \int_0^{\infty} \prod_{i=1}^{N} d\alpha_i \frac{C(\alpha_j)^{N-2\ell-2} \delta\left(\sum_{i=1}^{N} \alpha_i - 1\right) \delta(\beta-\phi)}{\eta^{N-2\ell}} \int_{-\infty}^{\infty} d\sigma \frac{\delta(\sigma-\psi)}{(z+\beta\nu-\sigma)^{N-2\ell}}$$

$$= \frac{G(-1)^{N-2\ell-1}}{(N-2\ell-1)!} \int_{-\infty}^{\infty} d\beta \int_{-\infty}^{\infty} d\sigma \frac{\int_0^{\infty} \prod_{i=1}^{N} d\alpha_i \frac{C(\alpha_j)^{N-2\ell-2} \delta\left(\sum_{i=1}^{N} \alpha_i - 1\right) \delta(\beta-\phi)}{\eta^{N-2\ell}} \frac{\partial^{N-2\ell-1}}{\partial\sigma^{N-2\ell-1}} \delta(\sigma-\psi)}{z + \beta\nu - \sigma}$$

If we define the DGS spectral function

$$H(\sigma, \beta) = \frac{G(-1)^{N-2\ell-1}}{(N-2\ell-1)!} \int_0^{\infty} \prod_{i=1}^{N} d\alpha_i \frac{C(\alpha_j)^{N-2\ell-2} \delta\left(\sum_{i=1}^{N} \alpha_i - 1\right) \delta(\beta-\phi)}{\eta^{N-2\ell}} \frac{\partial^{N-2\ell-1}}{\partial\sigma^{N-2\ell-1}} \delta(\sigma-\psi)$$

we get the DGS representation

$$T(z,\nu) = \int_{-\infty}^{\infty} d\beta \int_{-\infty}^{\infty} d\sigma \frac{H(\sigma,\beta)}{z+\beta\nu-\sigma}$$

To find the support of the spectral function $H(\sigma,\beta)$ we use the delta functions and note that by its definition

$$-1 \leq \phi \leq 1 \qquad \text{for} \qquad 0 \leq \alpha_i \leq 1$$

implying that $H(\sigma,\beta)$ is nonzero only for $0 \leq \beta \leq 1$. Similarly $H(\sigma,\beta)$ is nonzero only for $\psi_{min} \leq \sigma \leq \psi_{max}$ where $\psi_{min(max)}$ is the minimum (maximum) value of ψ subject to the constraint that $\phi=\beta$ lie at a fixed given value in the interval $[-1,1]$.

Therefore the support of $H(\sigma,\beta)$ is the two dimensional region

$$\left\{-1 < \beta \leq 1, \qquad \psi_{min} \leq \sigma \leq \psi_{max}\right\}$$

To get a feel for the representation we determine its spectral function for some example.

For poles of the form $T(z,\nu) = C/z-m^2$ we get $H(\sigma,\beta) = C\,\delta(\beta)\,\delta(\sigma-m^2)$.

For poles of the form

$$T(z,\nu) = \frac{1}{s-m^2} \pm \frac{1}{u-m^2}$$

we get

$$H(\sigma,\beta) = \left\{\delta(\beta-1) \pm \delta(\beta+1)\right\} \delta(\sigma-m^2+M^2)$$

while

$$H(\sigma,\beta) = \theta(1-\beta^2)\frac{\partial}{\partial\sigma}\delta(\sigma-m^2+M^2)$$

gives

$$T(z,\nu) = \frac{2}{(s-m^2)(u-m^2)}$$

Now we use this method to determine the explicit DGS representation for the box diagram of Fig. 8a. Here N=4, ℓ=1

$$\xi_s = \alpha_2\alpha_4$$

$$\xi_z = \alpha_4(\alpha_1+\alpha_3)$$

$$\xi_M = \alpha_2(\alpha_1+\alpha_3)$$

while

$$\xi_u \equiv 0$$

$$\eta = \alpha_4(\alpha_1+\alpha_2+\alpha_3) = \alpha_4(1-\alpha_4)$$

$$\phi = \frac{\alpha_2}{\alpha_1+\alpha_2+\alpha_3} = \frac{\alpha_2}{1-\alpha_4} \quad , \qquad 0 \le \frac{\alpha_2}{1-\alpha_4} \le 1$$

$$\psi = \frac{\sum_{i=1}^{4} \alpha_i m_i^2 - \alpha_2(1-\alpha_2) M^2}{\alpha_4(1-\alpha_4)} = \frac{(1-\alpha_2)\mu^2 + \alpha_2^2 M^2}{\alpha_4(1-\alpha_4)}$$

$$C = \alpha_1+\alpha_2+\alpha_3+\alpha_4$$

So the DGS representation is

$$B(z,\nu) = \int_0^1 d\beta \int_{-\infty}^{\infty} d\sigma \frac{H(\sigma,\beta)}{z+\beta\nu-\sigma}$$

where

$$H(\sigma,\beta) = -G \int_0^{\infty} \prod_{i=1}^{4} d\alpha_i \frac{\delta\left(\sum_{i=1}^{4}\alpha_i - 1\right)\delta(\beta-\phi)}{\eta^2} \frac{\partial}{\partial\sigma}\delta(\sigma-\psi)$$

Performing the α_1 and α_3 integrations using one delta functions gives

$$H(\sigma,\beta) = -G\int_0^1\int_0^1 d\alpha_2\, d\alpha_4 \frac{(1-\alpha_4-\alpha_2)\,\theta(1-\alpha_4-\alpha_2)}{\alpha_4^2(1-\alpha_4)^2}\,\delta\left(\beta - \frac{\alpha_2}{1-\alpha_4}\right)\frac{\partial}{\partial\sigma}\delta(\sigma-\psi)$$

Put $1-\alpha_4=\alpha$ and $\frac{\alpha z}{\alpha}=y$ and use the θ-functions to get

$$H(\sigma,\beta) = -G\int_0^1 \frac{d\alpha}{(1-\alpha)^2}\int_0^1 dy(1-y)\ \delta(y-\beta)\ \frac{\partial}{\partial\sigma}\delta\left(\sigma - \frac{(1-\alpha y)\mu^2+\alpha^2 y^2 M^2}{\alpha(1-\alpha)}\right)$$

Use a delta function to do the y integration to get

$$H(\sigma,\beta) = -G\left[\theta(\beta)-\theta(\beta-1)\right](1-\beta)\int_0^1 \frac{d\alpha}{(1-\alpha)^2}\frac{\partial}{\partial\sigma}\delta\left(\sigma - \frac{(1-\beta\alpha)\mu^2+\beta^2\alpha^2 M^2}{\alpha(1-\alpha)}\right)$$

Assuming we can interchange the order of integration and differentiation we get

$$H(\sigma,\beta) = -G\left[\theta(\beta)-\theta(\beta-1)\right](1-\beta)\frac{\partial}{\partial\sigma}\int_0^1 \frac{d\alpha}{(1-\alpha)^2}\delta\left(\sigma - \frac{\beta^2\alpha^2 M^2-\beta\alpha\mu^2+\mu^2}{\alpha(1-\alpha)}\right)$$

Call

$$I(\sigma) \equiv \int_0^1 \frac{d\alpha}{(1-\alpha)^2}\ \delta\left(\sigma - \frac{\beta^2\alpha^2 M^2-\beta\alpha\mu^2+\mu^2}{\alpha(1-\alpha)}\right) = \int_0^\infty d\alpha\ \frac{\left[\theta(\alpha)-\theta(\alpha-1)\right]}{(1-\alpha)^2}\ \delta(g(\alpha))$$

We define

$$g(\alpha) = \sigma - \frac{\beta^2\alpha^2 M^2-\beta\alpha\mu^2+\mu^2}{\alpha(1-\alpha)} \equiv \left(\sigma+\beta^2M^2\right)\frac{(\alpha-\alpha_+)(\alpha-\alpha_-)}{\alpha(\alpha-1)}$$

where

$$\alpha\pm(\sigma,\beta) = \frac{(\sigma+\beta\mu^2)\pm\sqrt{\sigma^2+2\mu^2(\beta-2)\ \sigma-\beta^2\mu^2(4M^2-\mu^2)}}{2(\sigma+\beta^2M^2)}$$

$$g'(\alpha) = (\sigma+\beta^2M^2)\left\{\frac{(2\alpha-\alpha_+-\alpha_-)}{\alpha(\alpha-1)} - \frac{(\alpha-\alpha_+)(\alpha-\alpha_-)(2\alpha-1)}{\alpha^2(\alpha-1)^2}\right\}$$

Doing the α integration we get

$$I(\sigma) = \frac{\left[\theta(\alpha_+) - \theta(\alpha_+ -1)\right]}{|g'(\alpha_+)|(1-\alpha_+)^2} + \frac{\left[\theta(\alpha_-) - \theta(\alpha_- -1)\right]}{|g'(\alpha_+)|\,(1-\alpha_-)^2}$$

where the θ functions are interpreted to vanish if $\alpha_\pm$ are complex.

To see the use of having the explicit form of the DGS function we calculate

$$\lim_{\nu \to \infty} \nu \operatorname{Im} B(z,\nu) \qquad \text{for } z < 0 \qquad \text{and } x = \frac{z}{\nu} \text{ fixed}$$

We expect from our calculation in Section IV that for $z < 0$

$$\lim_{\nu \to \infty,\ x \text{ fixed}} \nu \operatorname{Im} B(z,\nu) = \lim_{\nu \to \infty} \frac{\nu}{2i} \operatorname{disc}_s B(z,\nu)$$

$$= (\text{Const}) \frac{(1+x)\left[\theta(-x) - \theta(-x-1)\right]}{M^2 x^2 + \mu^2 x + \mu^2}$$

To calculate this from the DGS representation we note that

$$\operatorname{Im} B(z,\nu) = -\pi \int_{-\infty}^{\infty} d\sigma \int_{-\infty}^{\infty} d\beta\, H(\sigma,\beta)\ \delta(z+\beta\nu-\sigma)$$

Doing the β integration and using the support of $H(\sigma,\beta)$ we get

$$\lim_{\nu \to \infty} \frac{\nu \operatorname{Im} B(z,\nu)}{(-\pi)} = \lim_{\nu \to \infty} \int_{-\infty}^{\infty} d\sigma \left[\theta\left(\frac{\sigma}{\nu} - x\right) - \theta\left(\frac{\sigma}{\nu} - x - 1\right)\right] H\left(\sigma, \frac{\sigma}{\nu} - x\right)$$

Assuming we can interchange the order of integration and the limit and assuming that the limit of a product of distributions is the product of their limits we get

$$\lim_{\nu \to \infty} \frac{\nu \operatorname{Im} B(z,\nu)}{(-\pi)} = \int_{-\infty}^{\infty} d\sigma \left[\theta(-x) - \theta(-x-1)\right] \lim_{\nu \to \infty} H\left(\sigma, \frac{\sigma}{\nu} - x\right)$$

Now one may be tempted to claim without further assumption[1f] that

$$\lim_{\nu \to \infty} H\left(\sigma, \frac{\sigma}{\nu} - x\right) = H(\sigma, -x)$$

But it is important to note that this could be false since $H(\sigma, \beta)$ is a distribution which is defined as a limit of a sequence. So to use the above result we must assume that we can interchange the limit $\nu \to \infty$ and the limit of the sequence defining the distribution. Assuming this we get

$$\lim_{\nu \to \infty} \nu \operatorname{Im} B(z,\nu) = -\pi \int_{-\infty}^{\infty} d\sigma \quad \theta(-x) - \theta(-x-1) \quad H(\sigma, -x)$$

Substituting the $H(\sigma, -x)$ obtained for the box graph we get

$$\lim_{\nu \to \infty} \nu \operatorname{Im} B(z,\nu) = \pi G \left[\theta(-x) - \theta(-x-1)\right] (1+x) \int_{-\infty}^{\infty} d\sigma \frac{\partial}{\partial\sigma} I(\sigma)$$

$$= \pi G \left[\theta(-x) - \theta)-x-1)\right] (1+x) \left\{I(+\infty) - I(-\infty)\right\}$$

Now $I(-\infty) = 0$ since the delta function cannot be satisfied for $0 \leq \alpha \leq 1$.

To calculate $I(+\infty)$ we note that

$$\alpha_{\pm}(\sigma, \beta) \sim \frac{(\sigma - x\mu^2) \pm \left(\sigma - x\mu^2 - 2\mu^2 + 0\left(\frac{1}{\sigma}\right)\right)}{2(\sigma + x^2M^2)} , \quad \sigma \to +\infty$$

so that

$$\alpha_+ \sim \frac{\sigma - x\mu^2 - \mu^2}{\sigma + x^2 M^2} + 0\left(\frac{1}{\sigma^2}\right)$$

$$\alpha_- \sim \frac{\mu^2}{\sigma + x^2 M^2} + 0\left(\frac{1}{\sigma^2}\right)$$

Then

$$I(\sigma) = \frac{\left[\theta(\alpha_+) - \theta(\alpha_+ - 1)\right] |\alpha_+|}{(\sigma + x^2M^2)(1-\alpha_+)|\alpha_+ - \alpha_-|} + \frac{\left[\theta(\alpha_-) - \theta(\alpha_- - 1)\right] |\alpha_-|}{(\sigma + x^2M^2)(1-\alpha_-)|\alpha_+ - \alpha_-|}$$

$$\underset{\sigma \to \infty}{\sim} \frac{1}{M^2x^2 + \mu^2 x + \mu^2}$$

Therefore

$$\lim_{\nu \to \infty} \nu \, \mathrm{Im} \, B(z,\nu) = \pi G \, \frac{\left[\theta(-x) - \theta(-x-1)\right](1+x)}{M^2 x^2 + \mu^2 x + \mu^2}$$

which agrees with the result obtained by direct laborious calculation of the discontinuities. This demonstrates the utility of having the explicit form of the DGS spectral function of any Feynman graph for studying the "scaling" of its contribution to the inelastic structure functions.[1] For this purpose one should also include spin which has the effect of altering the function $C(\alpha)$ and adding external momentum dependent factors in the numerator,[9a] but the technique for obtaining the DGS representation remains unchanged. We should also be careful about the infrared and ultraviolet divergences.[2a, 6]

The above result also shows that the complex anomalous poles in the discontinuities indicated by our general analysis are also shown by the DGS representation when the explicit form of the spectral function is calculable. On the other hand, in spite of being equivalent to the Nambu representation, the DGS representation in its general form is very inconvenient to continue into the unphysical region due to the apparently singular nature of its spectral function. That is why, for example, the resonance poles on the second sheet are hard to represent in the DGS form.

IV. RESULTS FROM PERTURBATION THEORY

To understand what happens to the analyticity of the amplitude T when its absorptive part is nonzero on the entire real axis we study the analytic structure of the Feynman integral represented by the box diagram of Fig. 8. This is the simplest graph exhibiting a nontrivial cut structure. Since spin is unimportant in our discussions, we take all particles to be scalars and the internal masses in Fig. 8a are chosen to reflect the $t=0$ symmetry of the graph. The generalized Mandelstam representations in the complex s and t planes for this diagram have been extensively studied by several authors in cases when one fixed external mass is unstable or when a pair of equal external masses are unstable[12] (like off-mass-shell forward Compton amplitude). Unfortunately these representations do not display the analytic structure at $t=0$ in the complex mass plane and so we have to start afresh.

A. The Bjorken-Landau-Cutkosky Method

We use the Bjorken-Landau-Cutkosky method[6] for analyzing the singularities of integrals. The details of this method are very clearly explained in the first two chapters of the book ELOP[2a,c] and hence omitted here. We simply outline the method to establish notation and terminology.

It is well known[2,6-10] that the singularities (in the space of complex external variables) of the analytic continuations of integrals, like the Feynman integral, arise when the singularities of its integrand moving as functions of the external variables, either lie at an "end point" of integration or two (or more) of them "pinch" the integration hypercontour between them so that it cannot be distorted without crossing one of them. This is because if such situations did not arise in all the integrations, then we could use the Cauchys theorem to deform the contour away from the singularities of integrand to define an analytic function.

This analytic function would analytically continue the Feynman integral since the distortion of the hypercontour is equivalent to moving the external variables away from the singular point of the Feynman integral. The original integral is then a boundary value of this analytic continuation.

Such analysis applied to the Feynman integral shows that all its singularities are given by a set of equations first obtained by Bjorken[2e] and Landau[8a] which require that

1. For each internal line i of the Feynman graph either $q_i^2 = m_i^2$ or $\alpha_i=0$ where $\{\alpha_i\}$ are the Feynman parameters; and
2. For each loop j of internal momenta $\sum_{(j)} \alpha_i q_i = 0$ where $\sum_{(j)}$ denotes summation along the jth loop of internal momenta.

For a given Feynman graph the leading singularity corresponds to all $\alpha_i > 0$ (no $\alpha_i=0$). The q-orders lower singularities correspond to q of the $\alpha_i=0$ and the remaining $\alpha_j > 0$, and are shared by the reduced or contracted graphs in which the q lines with $\alpha_i=0$ have been shrunk to a point. The location of the complete set of singularities is given by the leading singularities of the original graph together with all its reduced graphs.

The physical boundary is determined by the Feynman prescription of giving all the internal masses an infinitesimal negative imaginary part $(m_i^2 \rightarrow m_i^2 - i\epsilon)$.

The solutions of Landau equations with all $\alpha_i \geq 0$ correspond to singularities of the Feynman integral with undistorted hypercontour. In the presence of several branch points the definition of the various sheets of the complex domain depends on the choice of the cuts attached to these branch points. We define the "physical sheet" as the sheet of the normal threshold cuts which carries the physical boundary. Normal thresholds, in general, are the lowest order singularities of a given Feynman integral and they lie in the physical region.[6p] We collectively call the higher order singularities the anomalous singularities. The anomalous singularities found on the physical sheet are the ones which move onto it during the process of analytic continuation. Amongst the various possible methods[2a, c, 6d] for the anomalous singularities to come on the physical sheet the most common is the mechanism of "critical intersections" and much less common ones are the mechanisms of "cusps" and "acnodes".[13] The type of graphs or the conditions under which cusps and acnodes have been found do not seem to occur for the scattering amplitude at t=0, since its dual diagram is topologically similar to that of a vertex. We therefore, assume their absence and restrict our discussion to the mechanism of critical intersection which corresponds to a pinch moving onto the undistorted hypercontour past an end point. With this mechanism the only anomalous singularities found on the physical sheet are the ones which climb onto it through the normal threshold cuts or through the cuts attached to the (lower order) branch points which have previously come onto the physical sheet through the normal thresholds. The required condition for one Landau singularity to change sheets by moving through the cut attached to another Landau singularity is that their Landau curves "touch effectively" (or intersect critically). For two Landau curves to "touch effectively" they must touch and at the point of touch have identical values for all the Feynman parameters α_i. It is easy to prove that the intersection (if it occurs) of any Landau curve with any one order lower Landau curve is necessarily effective. But as we will see (in Figs. 13 and 14) that once an effective touch is established one must check that the singularity does in fact cross the lower order cut.

These singularities can be poles or branch points depending on various factors like the dimensionality of space time, the redundancy in the Landau equation for a given graph, spin, form factors and nature of the couplings. The poles and the branch points can be distinguished in practice by one of two methods. Either we calculate the discontinuity (using the Cutkosky formula[10]) across the given singularity and see if it is finite or a delta function. A delta function discontinuity indicates a pole. Alternatively we calculate the discontinuity across a lower order singularity and in it see explicitly the presence of the pole due to the given higher order singularity.[7c]

The singularities obtained from the solution of the Landau equations fall into three main classes which are conveniently categorized in terms of the Nambu representation (see Section III). These are the Landau singularities ($D=0$, $C\neq 0$) or the mixed or pure non-Landauian (or second type) singularities ($D=0$, $C=0$). The Landau singularities[6,8] correspond to pinches and end point singularities when all the components of the loop momenta are finite. The second-type[9,7c] singularities correspond to a wide class of special solutions of the Landau equations which correspond to pinches when either all (pure) or some (mixed) components of the loop momenta are infinite. In the present paper we shall mainly concern ourselves with the Landau singularities since very little is known about the Reimann sheet properties of the second-type singularities. The presence or absence of the second-type singularities depends on the dimensionality of space time but can also be affected by spin and derivative couplings. It has been expected[9a] that the pure second-type singularities for a scattering graph always stay away from the physical sheet and their position can be found in terms of the momenta p_i of the external legs only. They are located at the edges of the physical region (s or $u = 0,\ 4M^2$) where

(i) $\det (p_i \cdot p_j) = 0$ $\qquad$ ($i, j=1, 2, \ldots$ E = number of external legs)

and

(ii) $p_j \cdot \sum_{i=1}^{E} p_i = 0$ $\qquad$ and $\qquad$ $\left(\sum_{i=1}^{E} p_i\right)^2 = 0$

The situation regarding the mixed second-type singularities[7c] is not so clear. They originate on the unphysical sheet, since they need $C(\alpha)$ for a subgraph to vanish (and $C(\alpha)$ being a sum of products of α's cannot vanish for $\alpha > 0$). But it is not known in general whether they come onto the physical sheet through a cut on the physical sheet, when an analytic continuation is performed. The necessary conditions for this to occur are that the second-type singularity curve either has an "effective intersection" with some other curve that is itself singular on the physical sheet or that the curve contains acnodes or cusps.[2a, 13]

The reason the second-type singularities can be important even if they stay on the second sheet is that the discontinuities in general display the singularities of both the physical and the second sheet, and in fact that is how the second-type singularities were discovered. It is the lack of knowledge of the second sheet singularities that restricts us to discussing only the single variable analyticity of the discontinuities which only involves the ordinary and virtual[2c] anomalous singularities on the physical sheet of the amplitude.

B. The Box Diagram

Consider the general box diagram of Fig. 8. Using the Feynman parameters and doing the loop integration we obtain the "Nambu Representation" for this graph to be

$$B(p_1, p_2, p_3, p_4) = (\mathrm{Const}) \int_0^1\int_0^1\int_0^1\int_0^1 \frac{d\alpha_1 d\alpha_2 d\alpha_3 d\alpha_4 \; \delta(\alpha_1+\alpha_2+\alpha_3+\alpha_4-1)\; C^0}{D^2}$$

where

$$D = \alpha_2\alpha_4 s + \alpha_1\alpha_3 t + \alpha_4\alpha_1 P_1^2 + \alpha_1\alpha_2 P_2^2 + \alpha_2\alpha_3 P_3^2 + \alpha_3\alpha_4 P_4^2 - \left(\sum_{n=1}^{4}\alpha_i\right)\left(\sum\alpha_i m_i^2\right)$$

$$C = \alpha_1 + \alpha_2 + \alpha_3 + \alpha_4 \; .$$

If we define the variables

$$y_{ij} = -\frac{q_i \cdot q_j}{m_i \; m_j} \equiv y_{ji}\,, \qquad y_{ii} = -1$$

then for the single loop box graph the equation of the surface of Landau singularities is given by

$$\det\,(y_{i,j}) = 0$$

and the vanishing of the various minors of $\det\,(y_{i,j})$ corresponds to the lower order singularities due to the reduced graphs shown in Fig. 9. For future reference we list the equations for the various Landau surfaces in the two dimensional complex space of external variables, starting with the leading singularity.

1. The "Box singularity" which corresponds to Fig. 8 or 9a: —

In this case we need $m_1 = m_3 = \mu$

$$\det y_{ij} = -\frac{t}{\mu^2}\;\mathscr{D}_3(t) \qquad \text{where}$$

$$\mathscr{D}_3(t) \equiv \begin{vmatrix} -1 & \dfrac{M^2-\mu^2-m_2^2}{2\mu\; m_2} & \dfrac{s-m_2^2-m_4^2}{2m_2\; m_4} \\[2ex] \dfrac{M-\mu^2-m_2^2}{2\mu\, m_2} & -1+\dfrac{t}{4\mu^2} & \dfrac{z^2-\mu^2-m_4^2}{2\mu\; m_4} \\[2ex] \dfrac{s-m_2^2-m_4^2}{2m_2\, m_4} & \dfrac{z-\mu^2-m_4^2}{2\mu\; m_4} & -1 \end{vmatrix}$$

At fixed t=0 the Box singularity is given by the equation

$$\mathscr{D}_3^{(0)} = 0 \qquad \text{and} \qquad m_1 = m_3$$

which is identical to the equation of the physical sheet "Triangle singularity" corresponding to the reduced graph of Fig. 9b. For $t\neq 0$ one defines a complex cut joining[14c] the box branch point ($1/\sqrt{\xi}$ type) and the Triangle branch point ($\ln \xi$ type). But in the t=0 case these two points coincide giving a collapsed cut which, as we will see later, acts like a simple pole[14c, d] and could have dominating effect in the appropriate regions.

2. The "Triangle singularities" corresponding to Figs. 9b, c_1, c_2: —

Corresponding to Fig. 9b we have the anomalous threshold surface Σ_A whose equation $\mathscr{D}_3^{(0)}=0$ can be written as

$$M^2z^2 + (M^2-m^2+\mu^2)\, z\nu + \mu^2\nu^2 + \Delta z = 0$$

where

$$\Delta \equiv \left[M^2-(m+\mu)^2\right]\left[M^2-(m-\mu)^2\right]$$

The shape of its conic section with the real plane (z_R, ν_R) is determined by the discriminent which turns out to be Δ. It is an ellipse, parabola or hyperbola according as $\Delta \lesseqgtr 0$. It is easy to see by an analysis similar to that for the triangle graph in ELOP, that the condition for this triangle singularity to be on the physical sheet of the VFC amplitude is $\Delta < 0$, i.e.: an elliptic curve with the normal threshold surfaces as tangent planes. This then restricts m to be $|M-\mu| < m < M+\mu$. Figures 10, 11, and 12 show the real section of this surface Σ_A under various conditions. To obtain the solution of the above equation for general masses we recommend that the reader use the method of dual diagrams.[8] To draw the complex parts of Σ_A requires another two dimensions. To get over this difficulty we use the searchline method. We imagine a plane in the complex (z, ν) space. This is

$$\nu = \psi z + \eta \quad , \qquad \psi, \eta \ \text{real}$$

$$\mathrm{Im}\,\nu = \psi\,\mathrm{Im}\,z$$

It intersects the real conic section of the quadratic surface $\sum_A$ in the real (z_R, ν_R) planes at two unique points. If its slope is kept fixed and the intercept η increased the line moves upwards in a direction perpendicular to itself and the two points of intersection form a pair of continuous curves on the Landau surface. Eventually these two real intersections with the search line coalesce and after that they are no longer real and become a pair of complex conjugate points, with the imaginary parts of their coordinates related by the above equation. Nothing is missed since every complex point lies on one and only one search line.

Using such search lines we discover that attached to the positive gradient arcs of the real conic sections are two parts of a complex surface with $\frac{\mathrm{Im}\,\nu}{\mathrm{Im}\,z} = \psi > 0$ while attached to the negative gradient real arcs are two parts of a complex surface with $\frac{\mathrm{Im}\,\nu}{\mathrm{Im}\,z} = \psi < 0$. Along horizontal tangents $\psi = 0$, $\mathrm{Im}\,\nu = 0$, $\mathrm{Im}\,z$ arbitrary while along vertical tangent $\psi = \infty$, $\mathrm{Im}\,\nu$ = arbitrary, $\mathrm{Im}\,z = 0$.

In using this description of the Landau surface to perform analytic continuation it is frequently important to distinguish the directions along which we approach the real section. For this purpose we define the following limits[2c] onto the real section. When we approach the real domain along $\mathrm{Im}\,s/\mathrm{Im}\,z > 0$ we call it the "corresponding half plane limit" and when we approach along $\mathrm{Im}\,s/\mathrm{Im}\,z < 0$ we call it the "opposite half plane limit". Furthermore, the limit onto the real section of the Landau surface that is defined by giving z, s (or z, ν) small imaginary parts whose relative sign is the same as that which they take on the attached complex Landau surface (i.e.: the same as the sign of the slope of the search line) will be called the "appropriate limit". When their relative sign is opposite to that taken on the attached complex Landau surface we call it the "inappropriate limit". It is easy to see that these limits are different if and only if the sections of the real axes being approached in both variables lie in a cut, i.e.: the real section lies in a crossed cut.

If the complex Landau surface is not singular on the physical sheet, then the appropriate limit cannot be singular. If the inappropriate limit is singular then the singularity is found just past the real boundary of the physical sheet approached by going through the real cut (Fig. 12b). Such arcs of real singularities (Fig. 12a) which are singular in the inappropriate limit (and hence lie in the region of crossed cuts) are called virtual singularities. These virtual singularities are present in the non-Euclidean region ($\lambda(z, s, M^2) > 0$) on the real axis (when $\epsilon \to 0$) which lie inside the crossed normal threshold cuts. Their presence is, therefore, not important for the discussion of the domain of analyticity on the physical sheet of the amplitude, though they are near its physical boundary (which lies above or below the cut). On the other hand, their importance for the study of the discontinuities is seen by the fact that in the limit $\epsilon \to 0+$

$$\mathrm{disc}_s\, T(z_R + i\epsilon', s_R) \equiv T(z_R + i\epsilon', s_R + i\epsilon) - T(z_R + i\epsilon', s_R - i\epsilon)$$

So we are simultaneously taking the corresponding and opposite half plane limits of the amplitude T and therefore $\mathrm{disc}_s\, T$ will carry both the ordinary (appropriate limit) and virtual (inappropriate limit) anomalous singularities of T.

To find which segments of this four (real) dimensional surface Σ_A is singular on the physical sheet we use the fact that the Feynman parameters α vary continuously on this surface so knowing the α's at its effective intersections with the lower order singularity (the normal threshold tangents) we can deduce the α's on the whole real conic section of Σ_A. In particular the real segment (solid lines in Figs. 10, 11 and 12) with all $\alpha \geq 0$ is singular on the physical sheet. The complex segment occurs on analytic continuation by distorting the hypercontour when α's are complex.

At $t=0$ the singularities corresponding to the reduced graphs in Figs. $9c_2$ and c_1 are found to coincide with the normal z threshold (Fig. 9e) and the normal M^2-threshold (Fig. 9f) respectively.

3. The s-channel normal threshold corresponds to Fig. 9d, and gives the plane

$$s-M^2 = z+\nu \geq 2\mu M+\mu^2$$

and

$$\mathrm{Im}\, s=0 \,, \qquad \mathrm{Im}\, z = -\mathrm{Im}\, \nu$$

4. The z-channel normal threshold corresponds to Figs. $9c_2$, e giving the plane

$$z \geq 4\mu^2 \,, \qquad \mathrm{Im}\, z=0 \,, \qquad \nu \text{ arbitrary}$$

This completes the description of the whole Landau surface of B.

To establish the analytic continuation of B in two complex variables we just have to show that we can start from the physical boundary and find a singularity free path to continue the Feynman integral into the complex unphysical domain making suitable detours when we hit its singularities. To discover the physical boundary we use the Feynman prescription to find

$$\begin{aligned} \mathrm{Im}\, D = {} & (\alpha_2\alpha_4 + \alpha_4\alpha_1 + \alpha_4\alpha_3)\ \mathrm{Im}\, z \\ & + (\alpha_2\alpha_4)\ \mathrm{Im}\, \nu \\ & + (\alpha_2 \textstyle\sum \alpha_i)\, \epsilon \,, \qquad \epsilon \to 0+ \end{aligned}$$

Therefore the physical boundary of a Feynman integral with real internal masses is

$$\mathrm{Im}\, z > 0 \,, \quad \mathrm{Im}\, \nu > 0$$

The two variable analyticity is then easily established using techniques explained in ELOP. To see that this continuation is conjugate symmetric, i.e.: $B(z, \nu) = B^*(z^*, \nu^*)$, we just have to note that the properties of all the complex segments of the Landau surface are invariant under complex conjugation. So that if we start at some real point (z_R, ν_R) and continue to some point (z, ν) the distortion of the α-hypercontour forced on us, if any, when we meet singularities will just be the complex conjugate of that forced on us if we continue instead by a complex conjugate path to the complex conjugate point (z^*, ν^*) and thus the value of B obtained at (z^*, ν^*) will just be the complex conjugate of that obtained at (z, ν).

To establish the analyticity in one complex variable keeping the other fixed in the physical region we have to study the singularities on a particular search line $z = z_R + i\epsilon$ or $\nu = \nu_R + i\epsilon$. In such cases the Landau curves shown in Figs. 10 and 11 give physical sheet singularities while the Landau curves of Fig. 12 do not contribute since they are singular in only the inappropriate limit on the real (z, ν) plane.[2c, 6d, k] Therefore, from now on we will not consider them any more, but remember that these virtual singularities occur in the discontinuity since the whole of the real arc in Fig. 12a on which the points E and F lie is singular in the inappropriate limit. These singularities are nonsingular in the appropriate limit because during the process of analytic continuation they never cross a cut to come onto the sheet chosen as the physical sheet, as shown in Fig. 12b.

If we consider $B(z, \nu_R + i\epsilon)$ as an analytic function of z. Figure 13a shows the location of various branch points for various values of ν_R. The solid lines indicate the motion of these branch points on the physical sheet while the dotted lines indicate their motion on the unphysical sheets. We see that $\sum_z$ gives a fixed branch point z_N on the real axis at $z = 4\mu^2$. $\sum_s$ gives a branch point ν_N of $z = 2\mu M + \mu^2 - \nu_R$ which moves just below the real axis. The anomalous branch point A corresponding to the triangle singularity $\sum_A$ is on the unphysical sheet when $\nu_R < -2\mu^2$. As ν_R is increased A crosses over into the physical sheet through the cut attached to z_N and when ν_R increases through $\nu_R = 2\mu M - \mu^2 - \frac{\mu^3}{M}$ A again crosses over into the unphysical sheet through the cut attached to the moving branch point ν_N which leads A beyond this point. So ultimately for large ν_R we are left with the two branch points ν_N and z_N. In the limit $\epsilon \to 0+$, ν_N lies on the real axis. $B(z, \nu_R + i\epsilon)$ therefore has only real cuts attached to the branch points z_N and ν_N, and is therefore a real analytic function for all fixed ν_R.

When we consider $B(z_R + i\epsilon, \nu)$ as an analytic function of ν. Figure 13b shows the location of various branch points for various values of z_R. For $z_R < 2\mu^2 + \frac{\mu^3}{M}$ the branch point ν_N due to $\sum_s$ lies just below the real axis on physical sheet while the branch point A due to $\sum_A$ lies on the unphysical sheet. As we increase z_R through $2\mu^2 + \frac{\mu^3}{M}$ the branch point A moves below the real axis and then crosses over onto the physical sheet through the cut attached to the ν_N branch point. As z_R is increased more the two branch points move infinitesimally below the real axis (A below ν_N) till we reach $z_R = 4\mu^2$. Beyond this value of z_R, the branch point moves to finite distance below the real axis and since it does not cross any cuts in this process it stays on the physical sheet. This corresponds to the complex segment of $\sum_A$ attached to AB. Thus for $z_R > 4\mu^2$, in the limit $\epsilon \to 0+$ we get a real branch point ν_N and a complex branch point A at ν_A, and $B(z_R + i\epsilon, \nu)$ is no longer a real analytic function of ν. This is consistent with what we expected from our discussion of the DGS representation and also shows that the reason DGS representation indicates a nonreal function of ν for $z_R > \mu^2$ (lower bound to $4\mu^2$) is that the analytic continuation acquires complex branch points. At this point we should note the importance of keeping ϵ nonzero and determining the magnitude of the imaginary parts of various branch points (using search lines). If in the above discussion A was above ν_N then as we would go through $z_R = 4\mu^2$ A would move down and cross over onto the unphysical sheet through the cut attached to A. It is because A is below ν_N that it remains on the physical sheet as a complex branch point.

We can similarly discuss the analytic structure of B as a function of one variable while the other is fixed for various sets of variables. The motion of singularities in the case (z, s) shown in Figs. 9 and 14 and Table I indicate the results for all such possible sets of variables.

C. The Blankenbecler-Nambu-Mandelstam Method[14]

To obtain further insight into the origin and nature of these complex anomalous singularities we consider the fixed t=0 dispersion relation for our box diagram which in the nonanomalous case (say z < 0) is

$$B(s,z) = \frac{1}{2\pi i}\int_{(m_2+m_4)^2}^{\infty} ds' \, \frac{\mathrm{disc}_s\, B(s',z)}{s'-s} \quad , \qquad t=0$$

Using the Cutkosky's discontinuity formula,[10] assuming a coupling constant g at each vertex in Fig. 8 and defining at t=0, $q_1^2 = q_3^2 \equiv \kappa$, $q_2^2 \equiv \beta$, $q_4^2 = \tau$, $m_1 = m_3 = \mu$ we get

$$\mathrm{disc}_s\, B(s,z) = \frac{ig^4}{(2\pi)^4}\,\frac{\pi(-2\pi i)^2}{2\sqrt{\lambda(s,z,M^2)}}\int_{\beta_{min}}^{\beta_{max}} d\beta\, \delta(\beta - m_2^2)\,\theta(q_2^o)\int_{\tau_{min}}^{\tau_{max}} d\tau\, \delta(\tau - m_4^2)\,\theta(q_4^o)\int_{\kappa_{min}}^{\kappa_{max}} d\kappa \frac{1}{(\kappa-\mu)^2}$$

where $\beta_{\substack{min\\max}}$, $\tau_{\substack{min\\max}}(\beta)$ and $\kappa_{\substack{min\\max}}(\tau,\beta)$ are the extrema relative to q_3^μ when two of the three squared four momenta are kept fixed. They can be shown[2a, 10] to be determined by the Landau equation:

$$\alpha_2 q_2^\mu + \alpha_3 q_3^\mu + \alpha_4 q_4^\mu = 0$$

where the α's serve as Lagrange's undetermined multipliers.

From these equations we determine the integration limits to be as follows

$$\beta_{min} = 0 \qquad \beta_{max} = \infty$$

$$\tau_{min} = 0 \qquad \tau_{max} = (\sqrt{s} - \sqrt{\beta})^2$$

$$\kappa_{\substack{max\\min}}(s,z,M^2;\tau,\beta) = M^2+\beta - (z-M^2-s)(\tau-\beta-s)/(2s)$$

$$\pm \sqrt{\lambda(s,\beta,\tau)\,\lambda(s,z,M^2)}/(2s)$$

where the triangle function is

$$\lambda(x,y,z) \equiv x^2+y^2+z^2 - 2xy - 2yz - 2zx$$

$$= \left[x - (\sqrt{y}+\sqrt{z})^2\right]\left[x - (\sqrt{y}-\sqrt{z})^2\right]$$

and the masses of the external legs are

$$p_1^2 = p_4^2 = z \qquad p_2^2 = p_3^2 = M^2$$

Integrating we get

$$\mathrm{disc}_s\, B(s,z) = \frac{-ig^4}{8\pi}\, \frac{\sqrt{\lambda\left(s,m_2^2,m_4^2\right)}}{f(s,z)}\, \theta\left[s-(m_2+m_4)^2\right]$$

where

$$f(s,z) \equiv \mu^2\left[s-s_+(z)\right]\left[s-s_-(z)\right] = m_2^2\left[z-z_+(s)\right]\left[z-z_-(s)\right]$$

$$s_\pm(z) = m_2^2 + m_4^2 - \frac{\left(M^2-m_2^2-\mu^2\right)\left(z-m_4^2-\mu^2\right)}{2\mu^2} \pm \frac{1}{2\mu^2}\sqrt{\lambda\left(M^2,m_2^2,\mu^2\right)\lambda\left(z,m_4^2,\mu^2\right)}$$

$$z_\pm(s) = m_4^2+\mu^2 - \frac{\left(M^2-m_2^2-\mu^2\right)\left(s-m_2^2-m_4^2\right)}{2m_2^2} \pm \frac{1}{2m_2^2}\sqrt{\lambda\left(M^2,m_2^2,\mu^2\right)\lambda\left(s,m_2^2,m_4^2\right)}$$

If we use this expression for $\mathrm{disc}_s\, B(s,z)$ without the θ-function to define it for all real s then it is an analytic function of z for fixed real s (though it need not be analytic in s). We can use this to define the analytic continuation of $B(s,z)$, for all z, by varying z and suitably distorting the integration contour to avoid the approaching singularities of $\mathrm{disc}_s B$. As we increase z from small values to a point above its normal threshold cut (i.e.: $\mathrm{Im}\, z = +i\epsilon$, $\mathrm{Re}\, z > (m_2+\mu)^2$) the path followed by the poles in $\mathrm{disc}_s B$ due to $f(s,z)=0$ are shown in Figs. 15, 16, and to avoid it we must distort the integration path as shown. The final position of this pole (determined by the fixed z) then determines the anomalous threshold, which being a solution of a quadratic equation, can be in the complex s plane. The complex conjugate root of f does not cross the integration contour and so gives no singularity of the amplitude on the physical sheet. If we has increased z to a point below the cut (i.e.: $\mathrm{Im}\, z = -i\epsilon$, $\mathrm{Re}\, z > (m_2+\mu)^2$) then the anomalous threshold would be in the complex conjugate position.

By similar techniques one can deduce the single variable analyticity of the integrated absorptive part

$$R(z) = \int_{(m_2+m_4)^2}^{\infty} ds' \, \mathrm{disc}_s B(s',z)$$

It is easy to see that the roots of $f(s,z)$ represents the anomalous singularities given by the Landau equations. In the present case of single loop box graph at $t=0$, this singularity turns out to be a pole. This is a peculiarity of fixing $t=0$ when $q_1^2=q_2^2$ causes a double pole in the integrand of the Feynman integral. The double pole on first (κ) integration gives a simple pole which survive the remaining (τ, β) integrations by successively pinching with the remaining simple poles. For general $t \neq 0$ this singularity is a cut joining the triangle and box branch points of $\mathrm{disc}_s B$.[14c,d] This cut collapses to a pole when $t \to 0$. We find no such poles on the physical sheet for multilooped Feynman graphs. This is easy to understand if we focus our attention on one momentum loop and lump the remaining integrations together. Then a sufficient condition to get a pole in the final amplitude (irrespective of the sheet it lies on) is that the starting integrand have a double (or higher order) pole so that the "first (κ) integration" yields at least a simple pole. Then the integrands for the remaining two (β and τ) integrations must be such that they do not "smooth" this pole into a cut on successive integrations. This requires that these remaining integrands provide pinching poles. Hence only a single loop Feynman graph at t=0 whose four legs are elementary particles ($1/p^2-m^2+i\epsilon$) or resonances ($1/p^2-m^2+im\Gamma$) can, in general, give such anomalous poles.

Using similar arguments one can show that inclusion of spin turns these anomalous poles into a poles into a pole plus a cut at the same point, and that inclusion of form factors can "smooth" out these Landau singularities.

For applications to the study of "scaling"[1] of the inelastic structure functions it is convenient to know the analytic structure of $\mathrm{disc}_s B$ for fixed real s in the complex x-plane. The Landau singularities of $\mathrm{disc}_s B(s,x)$ are located at

$$x_\pm(s) = z_\pm(s)/\left\{s - M^2 - z_\pm(s)\right\}$$

and they move as we vary s. From the above formula we see that when s is large compared to a suitable combination of the internal masses,[11] these singularities $x_\pm(s)$ move rapidly to positions extremely close to their asymptotic position $x_\pm(\infty)$. The rapidity of this approach to "asymptopia" can be deduced from the above equations. In a separate publication[11] we discuss how these observations could provide a possible explanation for a rapid approach to "universality" (or s-independence) of the inelastic electron scattering structure functions.

To intuitively understand this explanation of "Universality" let us consider the following model of discontinuity of a box diagram (t=0) with spin, for large real s and fixed $x = z/\nu$

$$\mathrm{disc}_s \widetilde{B}(s,x) \equiv \frac{\mathrm{const}}{\sqrt{\lambda(s,z,M^2)}} \int_0^\infty d\beta\ \delta(\beta - m_2^2)\ \theta(q_2^o) \int_0^s d\tau\ \delta(\tau - m_4^2)\ \theta(q_4^o) \int_{\kappa_{min}}^{\kappa_{max}} \frac{\kappa}{(\kappa - \mu^2)^2}$$

where $\sqrt{\lambda(s,z,M^2)}$ represents the second type singularity at the edge of the physical region and the factor of κ is the effect of spin. Integrating we get

$$\sqrt{\lambda(s,z,M^2)}\ \mathrm{disc}_s \widetilde{B}(s,x) \propto F(s,x) = \ln \left(\frac{\kappa_{max}(s,x) - \mu^2}{\kappa_{min}(s,x) - \mu^2} \right)$$

$$+ \mu^2 \left[\frac{1}{\kappa_{min}(s,x) - \mu^2} - \frac{1}{\kappa_{max}(s,x) - \mu^2} \right]$$

where as $s \to \infty$ for fixed finite x

$$\left[\kappa_{min}(s,x) - \mu^2\right] \longrightarrow -\frac{\mu^2}{(x+1)} (x + 1 + s/\mu^2)$$

$$\left[\kappa_{max}(s,x) - \mu^2\right] \longrightarrow \Sigma_2(x) = \text{a quadratic s-independent function of x}$$

This shows that singularities in $F(s,x)$ arise when the edges of the allowed phase space $\kappa_{\substack{max \\ min}}$ approach the exchanged mass μ^2. For large finite s the singularity $(\kappa_{min} - \mu^2) = 0$ is very far (at $x = -1 - s/\mu^2$) from the region of interest $-1 \leq x \leq 0$ in the complex x-plane. On the other hand the singularities $(\kappa_{max} - \mu^2) = 0$ are close to the experimental region and s-independent since the edge κ_{max} of the phase space has stopped moving. So if we assume that the variations with s in the "shape" of the function $F(s,x)$ versus x, are controlled by the motion of the nearby singularities, then we should expect F to attain a universal s-independent shape once $\kappa_{max}(s,x)$ is s-independent. However, the s-dependence of the overall magnitude of F(s, x) is determined by all its singularities and will, in particular, be affected by the distant s-dependent singularity $(\kappa_{min}-\mu^2) = 0$. In case (like above) this distant singularity is giving a divergent contribution due to ultraviolet divergence in the graph, the magnitude of F will diverge as $s \to \infty$. This is the source of "nonscaling" behavior in certain field theoretic models of inelastic electron scattering.[1n]

We may choose to take the philosophy that the ultraviolet divergences are a disease of the theory rather than of nature and assume that there exists a realistic causal and unitary S-matrix theory without such divergences. Then we know[3] that the physical sheet analytic structure (i.e.: the position of the singularities but not their nature) obtained from finite order Feynman perturbation theory (with a cutoff) is expected to be the same as that obtained from this unitary s-matrix theory. In such a theory the experimental data in the region $-1 \leq x \leq 0$ should be expected to show the effects of the nearby singularities $(\kappa_{max}-\mu^2 = 0)$, rather than the effects of the distant singularities $(\kappa_{min}-\mu^2 = 0)$ which are obtained in the asymptotic models based on summing leading ultraviolet divergences.[1n] This provides the motivation for constructing models[11] of inelastic electron scattering structure functions which are based on their analytic structure and dominant singularities.

It is easy to generalize these arguments to arbitrary graphs, and specially those that correspond to a peripheral production of the intermediate state. In this way one can also see why the physical x-sheet singularities correspond to box or triangle shaped reduced graphs.

D. Single Variable Dispersion Relations for the Full VFC Amplitude

As far as dispersion relations[1,2] are concerned, we find that one can always write fixed real ν_R dispersion relation in z for the amplitude B with integrals over only real contours and real poles, as long as the asymptotic behavior is "decent" enough to be handled by a finite number of subtractions. Also because of the Sugawara-Kanazawa theorem[2h,m,n] one just needs to check the asymptotic behavior in only one direction in the complex z-plane. On the other hand in case of real s_R fixed above the normal threshold there are complex singularities in z and the above theorems fail. In such cases one can again use the Cauchy theorem to write dispersion-like relations but now one must include the contribution of the complex cuts. We must also independently check that the contribution from the circle at infinity does in fact vanish, or can be taken into account by a suitable number of subtractions. This can usually be done with the help of a wider class of the maximum-modulus theorems called the Phragmén-Lindelöf theorems.[2m,n]

To see what happens in a realistic model of the full scattering amplitude we consider a combination of the s-channel and the u-channel box diagrams of Fig. 17a at t=0, each of which can be obtained from the other by the simple interchange $\nu \to -\nu$. We will now find that our analysis will give the same analytic structure as expected on the basis of the DGS representation.

The possible physical sheet Landau singularities for such a combination T are shown in Fig. 17b in terms of the complex variables (z, ν). By methods already explained, it is easy to see that the physical region amplitude is a boundary value of an analytic function of two complex variables. The physical boundaries are (Im $z > 0$, Im $\nu > 0$, $\nu > 0$) for the s-channel physical region and (Im $z > 0$, Im $\nu < 0$, $\nu < 0$) for the u-channel physical region.

We have to be careful when we consider the single variable analyticity in ν keeping $z = z_R + i\epsilon$ fixed. In such cases the DGS representation for $T(z_R + i\epsilon, \nu)$ indicates a cut along the whole real ν-axis when $z_R > \mu^2$. But this does not, a priori, rule out the possibility of finding an analytic continuation in ν with complex singularities but a large domain of analyticity. In fact we saw that such an analytic continuation does exist for the s-channel box diagram. But when we consider the amplitude $T(z_R + i\epsilon, \nu)$ to be the combination of the s-channel and the u-channel box graphs we find that the ν-plane analytic structure to be as shown in Fig. 18. We find that for $z > 2\mu M + \mu^2$ the s-channel normal cut $\sum_s$ overlaps the u-channel normal cut $\sum_u$ and the physical region of the combined amplitude T (which is above the $\sum_s$ cut and below the $\sum_u$ cut when these cuts are chosen parallel to the real ν-axis) is squeezed between these two normal cuts and vanishes in the limit $\epsilon \to 0+$. Clearly under such circumstances we cannot determine the physical value of the amplitude as the boundary value of such an analytic continuation in one complex variable. One way to rectify this situation would be by defining a different analytic continuation by distorting the cuts, but then we would risk exposing the singularities on the unphysical sheet, since during the deformation of cuts these unphysical singularities could cross through onto the physical sheet. The other choice is to consider an analytic continuation in ν which is separated by a cut along the whole real ν-axis, the s-channel physical region being just above this cut and the u-channel physical region just below. This, we would observe, is precisely what happens in the case of the DGS representation. On the other hand if we fix $\nu = \nu_R$, Im $\nu = 0$ and consider the analyticity in z we find that we do get a real analytic function of z for any ν inspite of the u-channel cuts and that the physical boundary of this real analytic function of one complex variable is Im $z > 0$, i.e.: $z = z_R + i\epsilon$. The location of the physical boundary is most easily deduced from the expressions for the imaginary parts of the denominators in the Nambu representation of the s and u channel box diagrams. These are, respectively, of the form

$$\mathrm{Im}\, D_{(s)} = (a+b)\,\mathrm{Im}\, z + b\,\mathrm{Im}\,\nu + c$$
$$= a\,\mathrm{Im}\, z + b\,\mathrm{Im}\, s + c$$

and

$$\mathrm{Im}\, D_{(u)} = (a+b)\,\mathrm{Im}\, z - b\,\mathrm{Im}\,\nu + c$$
$$= (2b+a)\,\mathrm{Im}\, z - b\,\mathrm{Im}\, s + c$$

where $a > 0$, $c > 0$, $b \geq 0$ and $\epsilon \longrightarrow 0+$.

If we consider the pair of variables (z, s) we find that we again run into the problem of overlapping cuts in the complex s-plane if we fix $z = z_R + i\epsilon$ with $z_R > (2\mu M + \mu^2)$. At $z_R > 4\mu^2 \left[1 - (\mu^2/4M^2)\right]$ this function ceases to be real analytic in s because of anomalous thresholds. Similarly if we fix $s = s_R$, $\mathrm{Im}\, s = 0$ we get a real analytic function of z only if $s < (M+\mu)^2$.

From this discussion we conclude that for the full forward Compton scattering amplitude we cannot expect much more single variable analyticity than that implied by the DGS representation and shown in Table I.

V. THE ANALYTIC STRUCTURE OF DISCONTINUITIES AND INELASTIC STRUCTURE FUNCTIONS

The two variable analyticity of the amplitude $T(s,z)$ implies a single variable analyticity of the difference $\left\{T(s_1,z) - T(s_2,z)\right\}$ in the complex z plane if we keep s_1 and s_2 fixed. Cutkosky[10] used this fact, in the framework of Feynman perturbation theory, to determine the single variable analyticity of the discontinuities of the amplitude across fixed cuts. He showed that the singularities of a given Feynman integral $F(\xi)$ which are also the singularities of the discontinuity $F_m(\xi)$ (across the cut due to the reduced graph with m legs on mass shell) are those which correspond to the (reduced and full) Landau diagrams in which lines have been added to the given reduced diagram which defined the original singularity. The other Landau singularities of $F(\xi)$ appear on both sheets (corresponding to the given fixed cut) and their cuts cancel when we calculate the difference. The singularities of F which correspond to the reduced graphs with additional internal lines i, $i > m$ on mass shell, appear on only one of the two adjacent sheets connected by the branch point corresponding to the reduced graph with m lines on mass shell (e.g., the anomalous threshold due to triangle graphs moves from second to first sheet of normal thresholds due to bubble graphs). This discontinuity can also carry the non-Landauian singularities. These facts can readily be seen from the structure of the Cutkosky formula for calculating discontinuities (remembering that in applying this formula one integrates in the physical region and then analytically continues into the unphysical domain). This formula can also be used to calculate the discontinuity $F_{m,m'-m}(\xi)$ of the discontinuity function $F_m(\xi)$ across a (fixed) cut corresponding to a reduced graph in which the additional internal lines i, $m < i \le m'$ are also on mass shell, and we find that

$$F_{m,m'-m} \equiv F_{m'} = (-2\pi i)^{m'} \int\!\cdot\!\cdot\!\int \frac{\prod_{\text{loops}} (d^4k)\, \delta(q_1^2-\mu_1^2)\, \theta(q_1^o) \ldots \delta(q_{m'}^2-\mu_{m'}^2)\, \theta(q_{m'}^o)}{(q_{m'+1}^2-\mu_{m'+1}^2) \ldots (q_N^2-\mu_N^2)}$$

(the sign of $F_{m,m'-m}(\xi)$ is, in fact, defined by this relation). This result can be obtained by the following replacement in the original Feynman integral

$$\frac{1}{(q^2-\mu^2)^{r+1}} \longrightarrow \frac{(-2\pi i)\, \theta(q^o)}{r!} \frac{d^r}{d(\mu^2)^r}\, \delta(q^2-\mu^2)$$

The Cutkosky formula defines an analytic function of the internal masses and external invariants whose domain of analyticity must be found by analytic continuation. This in general, could be a very difficult problem. But in the special case when we are interested in the single variable analyticity in the second variable of the discontinuity across a fixed cut in the first variable (like normal s-threshold cut) the problem is much simpler. Then it only requires the knowledge of the ordinary and virtual anomalous singularities on the physical sheet of the second variable (like complex z-plane). This will become clear from our discussion and Cutkosky's analysis. In practice we are interested in the various boundary values of this function. For example $\text{disc}_s\, T(z_R+i\epsilon,\, s_R)$ across only the normal s-cut is one such boundary value above the real z cut which corresponds to giving all internal masses a small negative imaginary part when one starts to encounter singularities on the real axis. (This is because disc_s T is of the form T^2.) These small imaginary parts are inessential on the cutfree region of the real axis. On the other hand we observe from their definition that the inelastic structure functions are a different boundary value whose boundary is discovered by the prescription of putting $m_i^2 \to m_i^2 - i\epsilon$ for the internal masses in initial state and $m_f^2 \to m_f^2 + i\epsilon$ for the internal masses in the final state, when one encounters real singularities.

(This is because they are of the form $|T|^2$.) The mixed nature of this prescription makes it difficult to determine the boundary for arbitrary graphs.[7c, 10] But in the regions of the real axis where the discontinuities are cutfree (and pure imaginary) the $\pm i\epsilon$ are irrelevant so that their values will agree (up to factors of i) with those of the various inelastic structure functions defined by similar formula, even though the imaginary part of the amplitude in this region is a sum of different discontinuities across various cuts and not a boundary value of any discontinuity function. This follows from the conjugate symmetry ($T^*(s^*, z^*) = T(s, z)$) of the VFC amplitude from which we see that

$$\begin{aligned} \mathrm{disc}_s\, T(s_R, z) &\equiv T(s_R + i\epsilon, z) - T(s_R - i\epsilon, z) \\ &= -\left[\mathrm{disc}_s\, T(s_R, z^*)\right]^* \end{aligned}$$

Hence, on the cutfree part of the real z-axis we can reach the point $z^* = z = z_R$ where

$$\mathrm{disc}_s\, T(s_R, z_R) = -\left[\mathrm{disc}_s\, T(s_R, z_R)\right]^* = \text{pure imaginary}$$

This is not possible on parts of the real z-axis lying inside a cut. Similarly we find that

$$2i\, \mathrm{Im}\, T(s_R + i\epsilon, z_R + i\epsilon) = \left[\mathrm{disc}_s\, T(s_R, z_R + i\epsilon)\right]^* - \mathrm{disc}_z\, T(s_R + i\epsilon, z_R)$$

In this formula $\mathrm{disc}_s\, T$ represents the contribution of the connected direct channel graphs of Fig. 3b while $\mathrm{disc}_z\, T$ gives the contribution of the semi-disconnected graphs of Fig. 3d, to the total imaginary part of the VFC amplitude. Since by definition $\mathrm{Im}\, T(s_R + i\epsilon, z_R + i\epsilon)$ must be real, hence

$$\begin{aligned} \mathrm{Re}\left[\mathrm{disc}_s\, T(s_R, z_R + i\epsilon)\right] &= \mathrm{Re}\left[\mathrm{disc}_z\, T(s_R + i\epsilon, z_R)\right] \\ &= \frac{1}{2}\, \mathrm{disc}_z \left[\mathrm{disc}_s\, T(s_R, z_R)\right] \end{aligned}$$

which is related to the imaginary part that the inelastic electron scattering structure functions develop due to the presence of the double discontinuity graphs (like the semi-disconnected graphs) when we try to continue the structure function to the annihilation region (where z is time-like).

Thus we see why a simple relation between the discontinuities or the structure functions and the imaginary parts of the amplitude only holds in cases when the amplitude is real analytic ($T^*(s^*,z) = T(s,z)$) rather than when it is conjugate symmetric ($T^*(s^*,z^*) = T(s,z)$).

Using the Cutkosly formula we can identify $\mathrm{disc}_s\, T$, $\mathrm{disc}_u\, T$ and $\mathrm{disc}_z\, T$, on their cutfree sections of the real axes, with the non-Born term parts of the structure functions $C(s,z)$, $P(u,z)$ and $D(z,s)$ respectively. The conventional function W and $\overline{W}$ are trivially related to C and P respectively. The Born terms give non-analytic delta function contributions to C, P and D.

To understand the main features of the analytic structure of the discontinuities we first consider the example of $\mathrm{disc}_s\, B$. This was explicitly evaluated in the last section. We leave the detailed discussion of higher order to a subsequent publication. We find from this calculation that for fixed real $s_R > (m_2+m_4)^2$, $\mathrm{disc}_s\, B(s_R,z)$ is analytic in the whole z plane except for a pair of anomalous singularities at $f(s_R,z) = 0$. For $s_R < (m_2+m_4)^2$, $\mathrm{disc}_s\, B(s_R,z) = 0$. Since $\mathrm{disc}_s\, B(s_R,z)$ is not required to be analytic in s_R, this sudden disappearance of anomalous singularities for $s_R < (m_2+m_4)^2$ should not be surprising. When $\lambda(M^2,m_2^2,\mu^2) < 0$ (Euclidean case) the anomalous singularities are at complex conjugate points $z_\pm(s)$. When $\lambda(M^2,m_2^2,\mu^2) > 0$ (non-Euclidean case) the anomalous singularities represents a pair of virtual anomalous singularities on the real axis. We note that there are no cuts along the real z-axis in $\mathrm{disc}_s\, B(s_R,z)$ even though $B(s_R,z)$ does have a cut $(m_4+\mu)^2 \le z \le \infty$. This just reflects the fact that

$\text{disc}_s\ B(s_R, z)$ must only contain ordinary and virtual singularities of B which correspond to adding lines to the reduced graphs defining disc_s B. It could have real cuts for $z > 0$ if the virtual singularities were branch points or if it had vertex corrections like in graphs of Fig. 19. The real cuts would join the pairs of virtual branch points and extend to infinity from normal threshold branch points.

For fixed z_R the above formula of $\text{disc}_s\ B(s_R, z_R)$ was used without the θ function to define it for all s and we noticed that it had both the s-channel normal threshold branch points (instead of only one like the amplitude). This is easily understood by the fact that in using to continue this formula to s below $(m_2+m_4)^2$ we necessarily cross over into the unphysical sheet in the s plane of one of the amplitudes $B(s_R \pm i\epsilon,\ z_R)$ and therefore as a function of s the disc_s B necessarily exposes the singularities on both the physical and the adjacent unphysical sheet. This is also seen from the definition

$$\text{disc}_s\ B = B_{IIs} - B_{Is}$$

where the numerical subscript denote the sheet of the normal s-threshold cut. We see that disc_s B must carry the singularities of both the first and the second s-sheets. This complicates the analysis of its analyticity in the complex s-plane and that is why we restrict ourselves to the complex z-plane keeping s fixed.

Keeping ν fixed also complicates the analytic structure in the complex z-plane since

$$\text{disc}_\nu\ B(\nu_R, z) = \text{disc}_s\ B(s_R - z_R - M^2, z)$$

From this relation it is clear that the analyticity of this function cannot be simply related to the single variable analyticity of any amplitude since for fixed ν_R, complexifying z requires simultaneous complexification of s_R and, as indicated above, this exposes all the singularities on the unphysical sheet of s plane all of which are not known to us. Besides the Landau singularities, the unphysical s-sheets can carry the second type singularities and also the singularities which come from the divergence of the sum of the perturbation series.[15]

Thus great care must be exercised when discussing the single variable analytic continuations of the discontinuities across moving branch cuts to make sure that analytic continuations are meaningful (that is, there exists a reason for the discontinuity to be an analytic function of one variable) and that the singularities coming from the unphysical sheets of the amplitude are correctly taken into account.

We should, however, observe that since the discontinuities across given fixed normal cuts do not have these normal branch points, the inclusion of crossed channel diagrams does not affect their single variable analyticity, like it did for the amplitude.

To summarize we find that in general $\mathrm{disc}_s\, T(s_R, z)$, $\mathrm{disc}_u\, T(u_R, z)$ and $\mathrm{disc}_z\, T(z_R, s)$ across the respective fixed normal s, u or z threshold cuts are analytic functions of the second complex variable when we fixed s, u or z, respectively, at real values. Besides the real normal threshold cuts (coming from double discontinuity graphs like those of Fig. 19) they carry the ordinary (complex) and virtual (real) anomalous singularities. On the other hand the non-Born term parts of the inelastic structure functions $C(s_R, z)$, $P(u_R, z)$ and $D(z_R, s)$ are boundary values of these discontinuity functions, respectively, on and only on the cutfree part of the real axis.

Since there are no real singularities for space like $z_R < 0$ the non-Born team part of the inelastic electron scattering structure function $W^{NB}(s_R, z_R)$ $\left(\text{or } C(s_R, z_R)\right)$ for fixed real s_R is a boundary value on the real z axis of an analytic function in the experimentally accessible region $z_R < 0$. This is not true in general for time like $z_R > 0$ due to the presence of double discontinuity graphs (like Fig. 19) causing real cuts in region $z_R > 0$ and due to the presence of real virtual anomalous singularities. If, however, for some dynamical reason the contribution of the double discontinuity graphs (like the semi-disconnected graphs) vanishes and the real cut joining the pairs of virtual anomalous singularities lies out of the time like region of interest, then in this cutfree time like region the $W^{NB}(s_R, z_R)$ is again a boundary value of an analytic function. An example of such dynamical reason[1c,ℓ] is the transverse momentum cutoff and $s \to \infty$ limit in the Drell-Levy-Yan model which causes the graphs like those of Fig. 21 to give vanishing contribution.

As far as the complex part of the z-plane of $\mathrm{disc}_s\, T(s_R, z)$ is concerned, we find from the formula for $z_\pm(s)$ that the complex anomalous box singularities move towards the right ($\mathrm{Re}\, z > 0$) or left ($\mathrm{Re}\, z < 0$) half-plane according as $(M^2 - m_2^2 - \mu^2)$ is negative or positive. For a single loop Feynman graph baryon conservation requires $(M^2 - m_2^2 - \mu^2)$ to be negative so that the left half z-plane is singularity free. This inequality is even stronger for box singularities from multilooped Feynman graphs (Fig. 20) since m_2 and μ now represent the sum of the masses of reduced legs $\sqrt{\beta}$ and $\sqrt{\kappa}$ respectively. Thus one is justified in expanding W^{NB} as a Taylor series in z for fixed real s in the region $\mathrm{Re}\, z < 0$.[1h]

As an interesting application of these ideas we study whether we can use the general crossing relation between the inelastic electron scattering structure function W and the annihilation structure function $\overline{W}$ to relate inelastic electron scattering to annihilation.[1c] Crossing implies that

$$W(s=u, \omega) = \pm\, \overline{W}(u=s, -\omega)$$

where the Pauli principle gives positive sign for scattering off bosons and negative sign for scattering off fermions. The inelastic electron scattering experiments measure $W(s,\omega)$ for $s > (m_2+m_4)^2$ and $1 < \omega < +\infty$ while for the annihilation cross section we need $\overline{W}(u,\omega)$ for $u > (m_2+m_4)^2$ and $-1 < \omega < 0$ which can be obtained from the crossing relation if we know $W(s=u,\omega)$ for $s > (m_2+m_4)^2$ and $0 < \omega < 1$. But for a general graph $\mathrm{disc}_s\, T(s,\omega)$ for fixed real s has a normal threshold (real) cut $\omega_{th} \leq \omega \leq +1$ together with real cuts joining pair of virtual anomalous singularities that lie in the region $\omega \leq +1$. Therefore in general the boundary value (above the cut) of $\mathrm{disc}_s\, T(s,\omega)$ for fixed real s, does not represent $W^{NB}(s,\omega)$ in the region $\omega \leq +1$ due to the presence of real cuts and so the crossing relation cannot be used.

However, if the amplitude T is restricted to the class of t-channel ladders with point couplings[1c,n] (corresponding to a multiperipheral production of intermediate states) then $\mathrm{disc}_s\, T$ is free from the normal threshold cuts in ω. One still has the real cuts connecting the virtual singularities in the region $\omega < +1$ but these generally lie at a finite distance away from $\omega=+1$. Under such condition we obtain a cutfree interval from $\omega_c < \omega < \infty$ with $\omega_c < 1$ where the boundary value of $\mathrm{disc}_s\, T$ gives $C(s,\omega)$. We can therefore use crossing to obtain $P(u=s,\omega)$ in the limited region $-1 \leq \omega < -\omega_c$. This result for finite energies is the analog of the result obtained by Drell, Levy and Yan[1c,ℓ] for asymptotic energies. On the other hand we find no reason at finite energies for the analyticity conjectured by Pestieau and Roy.[1b]

Further discussion of the analytic structure of the discontinuities and the inelastic structure function will be undertaken in separate publications. There we will use the method of dual diagrams[8] to generalize the analysis to all orders of Feynman perturbation graphs at t=0 and show that the only Landau singularities that come on the physical sheet of the complex z-plane for fixed $s=s_R \pm i\epsilon$

(or vise-versa) are the s-independent normal z-threshold branch points (for real time like $z > 0$) and a set of anomalous singularities $z_\pm(s)$, which move with s, and correspond to the single loop box or triangle reduced diagrams. Their equation is given by

$$z_\pm(s) = \tau + \kappa - (M^2 - \beta - \kappa)(s - \tau - \beta)/(2\beta) \pm 1/(2\beta)\sqrt{\lambda(M^2,\beta,\kappa)\lambda(s,\tau,\beta)}$$

where β, τ and κ are the squares of the sum of the masses of the bottom, top and vertical reduced legs respectively as shown in Fig. 20.

In case (Euclidean) the lower vertex is internally and externally stable, then $\lambda(M^2,\beta,\kappa) < 0$ and $z_\pm$ represent a pair of complex conjugate ordinary anomalous Landau singularities when $\lambda(s,\tau,\beta) > 0$ (i.e., $s > (\sqrt{z} + \sqrt{\beta})^2$). On the other hand, in case (pseudo-Euclidean) $\lambda(M^2,\beta,\kappa) > 0$ then $z_\pm$ represent a pair of virtual anomalous singularities on the time like part of the real x-axis. The physical z-sheet is defined to be the sheet of the normal z-threshold cuts (or the lowest order Landau singularities) that carries the physical boundary. The box and triangle singularities are coincident at t=0.

These facts follow[2c, 6, 8] from the following consequences of the Landau equations and four momentum conservation:

1. The dual diagram for the VFC amplitude (t=0) has to be drawn in a two-dimensional plane and is triangular (Figs. 20, 21).

2. A two-dimensional dual diagram with ℓ internal dual vertices (corresponding to ℓ independent loop momenta) and N internal dual prongs (corresponding to N different internal line momenta) must satisfy $N \leq 2\ell + 1$ to give a nontrivial solution of the Landau equations.

3. A p pronged internal dual vertex must be drawn in a (p-1) dimensional space. Each prong could be multiple internal lines like OA and OC in Fig. 20. This condition is called "tautening" of the dual diagram.

The only anomalous singularities found on the physical sheet are the ones which can climb onto this sheet through the normal threshold cuts or through the cuts attached to the branch points which have previously come onto the physical sheet through the normal thresholds. The sufficient condition[2a, c, 6] for one Landau singularity to change sheets by moving through the cut attached to another Landau singularity is that their Landau curves, "touch effectively" (or intersect critically). This need not be a necessary condition if we have acnodes or cusps, in the Landau curves. Here we assume their absence.[13]

For two Landau curves to "touch effectively" they must touch and at the point of the touch have identical values for <u>all</u> the Feynman parameters α. It is eacy to see that, in the Euclidean region, for two Landau curves to touch, the dual diagram of the higher order singularity at the point of touch must simultaneously form the dual diagram for the lower order singularity being touched. For this reason the leading singularity of Fig. 22 cannot touch the one order lower singularities of Fig. 23. This geometric criterion for touching is sufficient for our proof since Landau and Okun and Rudin have shown that in a theory with stable internal lines the multilooped reduced graphs with dual diagrams like in Fig. 22 give leading singularities in the Euclidean region only. Only the single loop reductions can give singularities in both the Euclidean (ordinary) and the pseudo-Euclidean (virtual) regions.[8] For example of Figs. 22 and 23, the leading singularity of Fig. 22 cannot touch the one order lower singularity of Fig. 23 because of the tautening of the internal dual vertex O_1 (or O_2). On the other hand it can touch the two orders lower singularity at $z = (DO_2+O_2A)^2$ but this touch is not effective if M is stable so that the angle $0 < AO_1B < \pi$. For it to be effective we need $\alpha_{O_1O_2}=0$, which cannot happen if the above condition is satisfied by the angle AO_1B. This just reflects the fact that the reduced diagram corresponding to O_1O_2 line being absent cannot be singular unless both z and M^2 are simultaneously unstable. On the other hand the lower order singularity corresponding to a single loop reduction of Fig. 23 can come onto the physical sheet at P through the normal z-threshold cut.

We wish to thank R. Blankenbecler, J. D. Bjorken, S. D. Drell, M. Nauenberg, K. G. Wilson, M. Einhorn, R. Haymaker and T.-M. Yan for very fruitful discussions.

REFERENCES AND FOOTNOTES

1. a) H. Abarbanel, M. L. Goldberger, and S. B. Treiman, Phys. Rev. Letters 22, 500 (1969)

   b) J. Pestieau and P. Roy, Phys. Letters 30B, 483 (1969)

   c) S. D. Drell, D. J. Levy, T.-M. Yan, Phys. Rev. Letters 22, 744 (1969); Phys. Rev. 187, 2159 (1969); D1, 1035 (1970); D1, 1617 (1970); S. D. Drell and T.-M. Yan, Report No. SLAC-PUB-808

   d) J. D. Bjorken, Phys. Rev. 179, 1547 (1969)

   e) R. Chanda, S. Sen and D. P. Majumdar, University of Maryland preprint NYO-3399-217 (SU-1206-217) (1969)

   f) J. M. Cornwall, D. Corrigan and R. E. Norton, UCLA prepring (1970); R. Jackiw, R. Van Royan and G. West, MIT preprint (1970)

   g) T. P. Cheng and Wu-ki Tung, IAS preprint (1970)

   h) M. Nauenberg, Phys. Rev. Letters 24, 625 (1970)

   i) J. J. Sakurai, Currents and Mesons (University of Chicago Press)

   j) J. D. Sullivan, University of Illinois, Urbana preprint (1970)

   k) W. T. Potter and J. D. Sullivan, CERN preprint Ref Th-1213 (1970)

   l) P. V. Landshoff, CERN preprint Ref Th-1154 (1970)

   m) S. L. Adler and R. F. Dashen, Current Algebras (W. A. Benjamin)

   n) S. J. Chang and P. M. Fishbane, University of Illinois preprint (1970).

2. a) R. J. Eden, P. V. Landshoff, D. I. Olive and J. C. Polkinghorne, The Analytic S-Matrix (Cambridge University Press, New York, 1966) and references therein. We will refer to this book as ELOP.

   b) R. J. Eden, High Energy Collisions of Elementary Particles (Cambridge University Press, New York, 1967)

c) 1961 Brandeis Summer Lectures in Theoretical Physics (W. A. Benjamin) Lectures by R. J. Eden, pp. 1-101 and J. C. Polkinghorne, pp. 102-167

d) Dispersion Relations, Scottish Universities' Summer School (Oliver and Boyd, 1960) Edited by G. R. Screaton

e) J. D. Bjorken and S. D. Drell, Relativistic Quantum Fields, (McGraw Hill)

f) Dispersion Relations and Their Connections with Causality, Course 29, Internation School of Physics, Enrico Fermi (1964) Lectures by P. V. Landshoff

g) K. Nishijima, Fields and Particles (W. A. Benjamin)

h) G. Barton, Introduction to Advanced Field Theory (Interscience) and Dispersion Techniques in Field Theory (W. A. Benjamin)

i) L. Klein, Dispersion Relations and Abstract Approach to Field Theory (Gordon and Breach)

j) R. Hagedorn, Introduction to Field Theory and Dispersion Relations (W. A. Benjamin)

k) R. F. Streater and A. S. Wightman, PCT, Spin and Statistics and All That (W. A. Benjamin)

l) A. O. Barut, The Theory of the Scattering Matrix (Macmillan)

m) E. C. Titchmarsh, The Theory of Functions (Oxford University Press)

n) E. Hille, Analytic Function Theory, Vol. I and II.

3. J. C. Polkinghorne, Nuovo Cimento 23, 360 (1962); 25, 901 (1962); Phys. Rev. 128, 2459 and 2898 (1962), and ELOP, Section 4.1, 4.10, 4.11.

4. a) S. Deser, W. Gilbert, and E. C. G. Sudarshan, Phys. Rev. 115, 731 (1959); Phys. Rev. 117, 266 (1960); Phys. Rev. 117, 272 (1960)

b) M. Ida, Prog. Theo. Phys. 23, 1151 (1960)

c) N. Nakanishi, Supp. Prog. Theo. Phys. No. 18, 1 (1961), Section 16; Prog. Theo. Phys. 26, 337 (1961); Prog. Theo. Phys. 26, 927 (1961); J. Math. Phys. 3, 1139 (1962); Phys. Rev. 127, 1380 (1962); J. Math. Phys. 4, 1385 (1963); J. Math. Phys. 5, 1458 (1964)

d) J. M. Cornwall and R. E. Norton, Phys. Rev. 173, 1637 (1968), and Phys. Rev. 177, 2548 (1969)

e) B. Schroer and P. Stichel, Commun. Math. Phys. 3, 258 (1966)

f) R. Jost and H. Lehman, Nuovo Cimento V, 1598 (1957)

g) F. J. Dyson, Phys. Rev. 110, 1460 (1958)

h) We would like to thank Dr. M. B. Einhorn and Dr. M. J. Creutz for some very useful discussions about the DGS representation.

i) J. Schwinger, Phys. Rev. Letters 3, 296 (1959)

j) K. Johnson, Nucl. Phys. 25, 431 (1961).

5. a) S. D. Drell and J. D. Walecka, Ann. Phys. 28, 18 (1964)

b) M. Gourdin, Nuovo Cimento 21, 1094 (1961).

6. a) N. Nakanishi, Supp. Prog. Theo. Phys. No. 18, 1 (1961)

b) J.S.R. Chisholm, Proc. Camb. Phil. Soc. 48, 300 (1952)

c) T. Appelquist, Ann. Phys. (N.Y.) 54, 27 (1969)

d) R. J. Eden, Phys. Rev. 119, 1763 (1960); 121, 1567 (1961)

e) R. J. Eden, P. V. Landshoff, J. C. Polkinghorne and J. C. Taylor, Phys. Rev. 122, 307 (1961)

f) P. V. Landshoff, Phys. Letters 3, 116 (1962)

g) J. Cunningham, Rev. Mod. Phys. 36, 833 (1964)

h) P. V. Landshoff, J. C. Polkinghorne and J. C. Taylor, Nuovo Cimento 19, 939 (1961)

i) E. S. Sarachik, Nuovo Cimento 51A, 949 (1967)

j) J. Tarski, J. Math. Phys. 1, 149 (1960)

k) L. F. Cook and J. Tarski, J. Math. Phys. 3, 1 (1962); Phys. Rev. Letters 5, 585 (1960)

l) D. Bessis and F. Pham, J. Math. Phys. 4, 1253 (1963)

m) R. E. Norton, Phys. Rev. 135, B1381 (1964)

n) P. Collas and R. E. Norton, Phys. Rev. 160, 1346 (1967)

o) S. Coleman and R. E. Norton, Nuovo Cimento 38, 438 (1965)

p) G. Barton and C. Kacser, Nuovo Cimento 21, 593 and 1001 (1961).

7. a) R. Blankenbecler and J. Tarski, Phys. Rev. 125, 782 (1962)

b) J. D. Bjorken and J. D. Walecka, Ann. Phys. 38, 35 (1966)

c) I. T. Drummond, Il Nuovo Cimento 24, 248 (1962); 29, 720 (1963).

8. a) L. D. Landau, Nucl. Phys. 13, 181 (1959)

b) L. B. Okun and A. P. Rudik, Nucl. Phys. 14, 261 (1960)

c) M. Fowler, J. Math. Phys. 3, 936 (1962)

d) P. V. Landshoff, Nucl. Phys. 20, 129 (1960)

e) J. C. Taylor, Phys. Rev. 117, 261 (1960)

f) Refs. 2c and 2d.

9. a) D. B. Fairlie, P. V. Landshoff, J. Nuttall and J. C. Polkinghorne, J. Math. Phys. 3, 594 (1962); Phys. Letters 3, 55 (1962)

b) P. Federbush, J. Math. Phys. 6, 825 (1965).

10. R. E. Cutkosky, J. Math. Phys. 1, 429 (1960); Phys. Rev. Letters 4, 624 (1960).

11. Ashok suri, Report No. SLAC-PUB-820 (October 1970) (to be published in Phys. Rev. Letters, January 25, 1971).

12. a) C. Fronsdal, K. Mahanthappa and R. E. Norton, Phys. Rev. 127, 1847 (1962); J. Math. Phys. 4, 859 (1963)

b) J. N. Islam, J. Math. Phys. 3, 1098 (1962).

13. a) R. J. Eden, P. J. Landshoff, J. C. Polkinghorne and J. C. Taylor, J. Math. Phys. 2, 656 (1961)

b) D. I. Olive and J. C. Taylor, Nuovo Cimento 24, 814 (1962)

c) J. N. Islam, J. Math. Phys. 4, 872 (1963)

d) N. Nakanishi, J. Math. Phys. 4, 1539 (1963).

14. a) R. Blankenbecler and Y. Nambu, Nuovo Cimento 18, 595 (1960)

b) S. Mandelstam, Phys. Rev. Letters 4, 84 (1960); Phys. Rev. 115, 1741 (1959)

c) V. N. Gribor, M. V. Terentev and K. A. Ter-Martirosyan, Soviet Phys. JETP 13, 229 (1961)

d) R. Oehme, Nuovo Cimento 13, 778 (1959)

e) G. Wanders, Nuovo Cimento 17, 535 (1960); 18, 580 (1960)

f) R. C. Brunet, University of Montreal preprint (1970).

15. R. Blankenbecler, private communications. See also Refs. 2a and 3.

TABLE I

THE SINGLE VARIABLE ANALYTICITY OF T OBTAINED FROM THE DGS REPRESENTATION

The pair of independent variables	The slope and intercept of integration line $\sigma = \beta\nu + z$	Single variable analyticity of the forward Compton amplitude T: fixed real variable	complex variable	Analytic structure in the one complex variable implied by DGS representation*
(z,ν)	slope $= \nu$	$z = z_R$	ν	Real analytic for $z_R < \mu^2$; cut along the whole real ν axis for $z_R > \mu^2$
	intercept = z	$\nu = \nu_R$	z	Real analytic for all ν_R
(z, s)	$\nu = s - M^2 - z$	$z = z_R$	s	Real analytic for $z_R < \mu^2$; cut along the whole real s axis for $z_R > \mu^2$
	z	$s = s_R$	z	Real analytic for $s_R < (M+\mu)^2$; cut along the whole real z axis for $s_R > (M+\mu)^2$
(ν, s)	ν	$\nu = \nu_R$	s	Real analytic for all ν_R
	$z = s - M^2 - \nu$	$s = s_R$	ν	Real analytic for $s_R < (M+\mu)^2$; cut along the whole real ν axis for $s_R > (M+\mu)^2$
(z,ω)	$\nu = -\omega z$	$z = z_R$	ω	Real analytic for $z < \mu^2$; cut along the whole real ω axis for $z > \mu^2$
	z	$\omega = \omega_R$	z	Real analytic for all ω_R
(ν, ω)	ν	$\nu = \nu_R$	ω	Real analytic for all ν_R
	$z = -\nu/\omega$	$\omega = \omega_R \neq 0$	ν	Real analytic for all $\omega_R \neq 0$
(ω, s)	$\nu = \frac{-\omega(s-M^2)}{(1-\omega)}$	$\omega = \omega_R$	s	Real analytic for all $_R$
	$z = \frac{s-M^2}{(1-\omega)}$	$s = s_R$	ω	Real analytic for $s < (M+\mu)^2$; cut along the whole real ω axis for $s > (M+\mu)^2$

*Note: When there is a cut along the whole real axis, one may still be able to define T as an analytic function in the whole complex plane, but it will then have complex singularities.

FIGURE CAPTIONS

1. The analytic structure of the virtual forward Compton scattering amplitude in the complex q^2-plane for fixed real s.
2. The virtual forward Compton scattering amplitude.
3. The unitarity and discontinuity diagrams.
4. The various physical regions for the forward Compton amplitude. The experimentally accessible areas show the different reactions which involve parts of the forward Compton amplitude in the definition of its inelastic form factors. (H is any hadronic system.)
5. The support Σ of the DGS weight function $H(\sigma, \beta)$.
6. The integration line $z + \beta\nu - \sigma = 0$ for various z and ν.
7. The integration line $z + \beta(s-M^2-z) - \sigma = 0$ for various z and s.
8. The direct channel box diagram (a) for special masses (b) for general masses.
9. The reduced graphs for the leading and lower order Landau singularities for the direct s-channel box diagram.
10. The Landau curves in the real (z, ν) plane for the case m=M. The equation of the ellipse AB A'B' is

$$M^2 z^2 + \mu^2 z\nu + \mu^2 \nu^2 - \mu^2 (4M^2 - \mu^2)\, z = 0$$

and the coordinates of the points of tangency are

$$A = (4\mu^2, -2\mu^2)\ ; \qquad B = \left(2\mu^2 + \frac{\mu^3}{M},\ 2\mu M - \mu^2 - \frac{\mu^3}{M}\right)$$

$$A' = (0, 0)\ ; \qquad B' = \left(2\mu^2 - \frac{\mu^3}{M},\ 2\mu M - \mu^2 + \frac{\mu^3}{M}\right)$$

11. The Landau curves in the real (z,s) plane for the case $m=M$. The equation of the ellipse $AB\,A'B'$ is

$$M^2z^2 + \mu^2(\mu^2-3M^2-s)\,z + \mu^2(s-M^2)^2 = 0$$

and the coordinates of the points of tangency are

$$A = (4\mu^2,\ M^2+2\mu^2) \quad ; \qquad B = \left(2\mu^2 + \frac{\mu^3}{M}\ ,\ (M+\mu)^2\right)$$

$$A' = (0, M^2) \quad ; \qquad B' = \left(2\mu^2 + \frac{\mu^3}{M}\ ,\ (M-\mu)^2\right)$$

12. a) The real section of Landau surfaces for $m \geq M+\mu$ when we get an hyperbola.

b) Virtual singularities close to the physical boundary of $\mathrm{disc}_s\, B(z, s_R)$.

13. a) The single variable analyticity of $B(z, \nu_R + i\epsilon)$ in the z plane.

b) The single variable analyticity of $B(z_R + i\epsilon\ , \nu)$ in the ν plane.

14. a) The single variable analyticity of $B(z, s_R + i\epsilon)$ in the z plane.

b) The single variable analyticity of $B(z_R + i\epsilon\ , s)$ in the s plane.

15. The motion of the pole in $\mathrm{disc}_s\, B(s_R, z)$ as z is increased, and the accompanying distortion of the integration contour.

16. The single variable analyticity of $\mathrm{disc}_z\, B(z_R, s)$ in the s plane, of $\mathrm{disc}_s\, B(z, s_R)$ in the z plane and of $\mathrm{disc}_s\, B(s_R, \omega)$ in the ω plane.

17. The analytic structure of the sum of direct and crossed channel box diagrams.

18. The single variable analytic structure of $T(z_R + i\epsilon\ , \nu)$ in the ν plane showing the overlap of the normal cuts.

19. Typical double discontinuity graphs leading to real cuts in the discontinuity functions.

20. Typical reduced Feynman graphs leading to anomalous box or triangle singularity at $t=0$ and the corresponding "tautened" dual diagram.

21. The dual diagrams for Feynman graphs representing scattering amplitudes and vertex functions.

22. Typical possible dual diagram for leading singularities of VFC amplitude.

23. Dual diagrams of one order lower singularities. P represents the point of "effective touch".

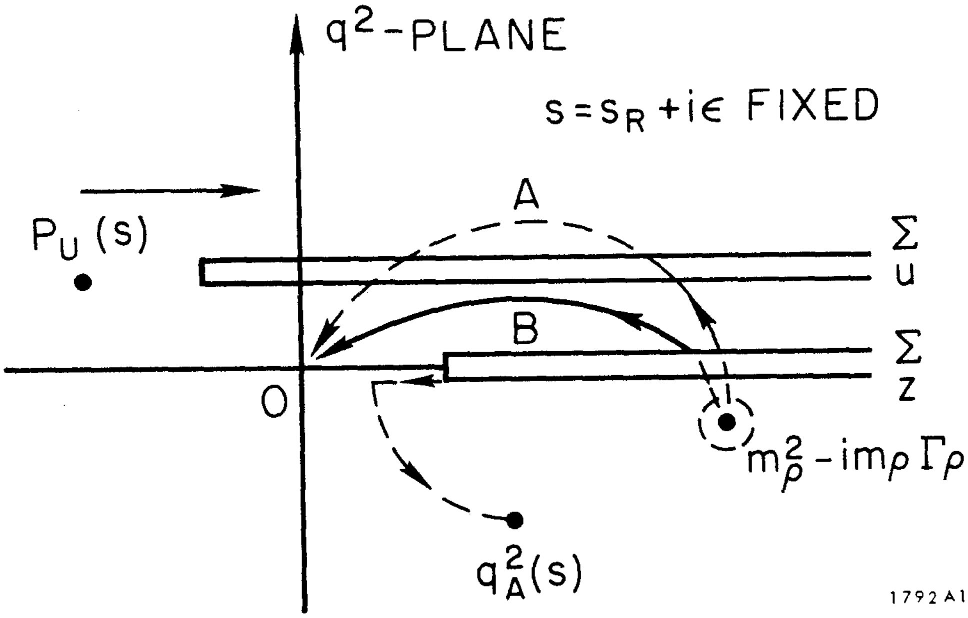

Fig. 1

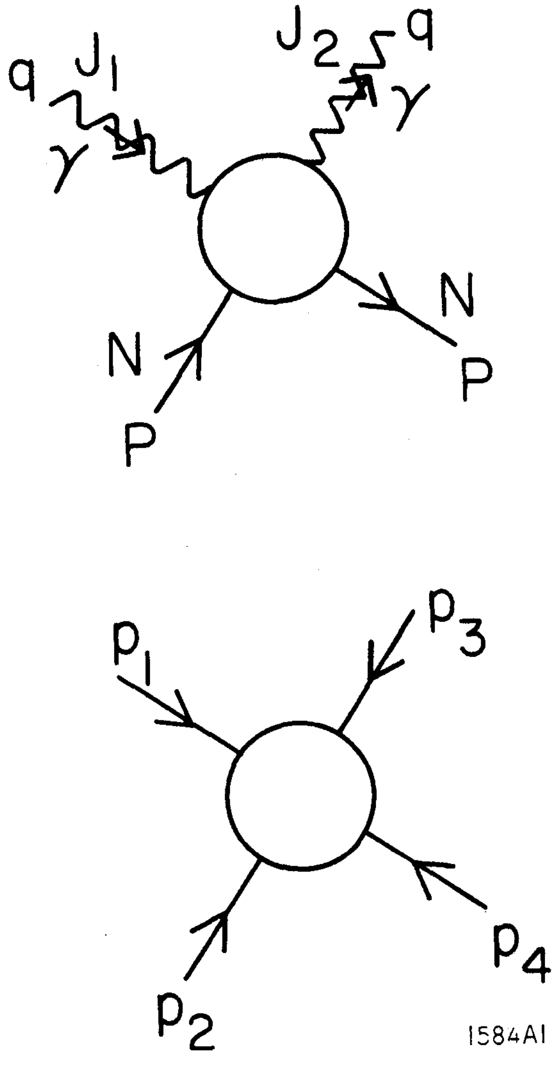

Fig. 2

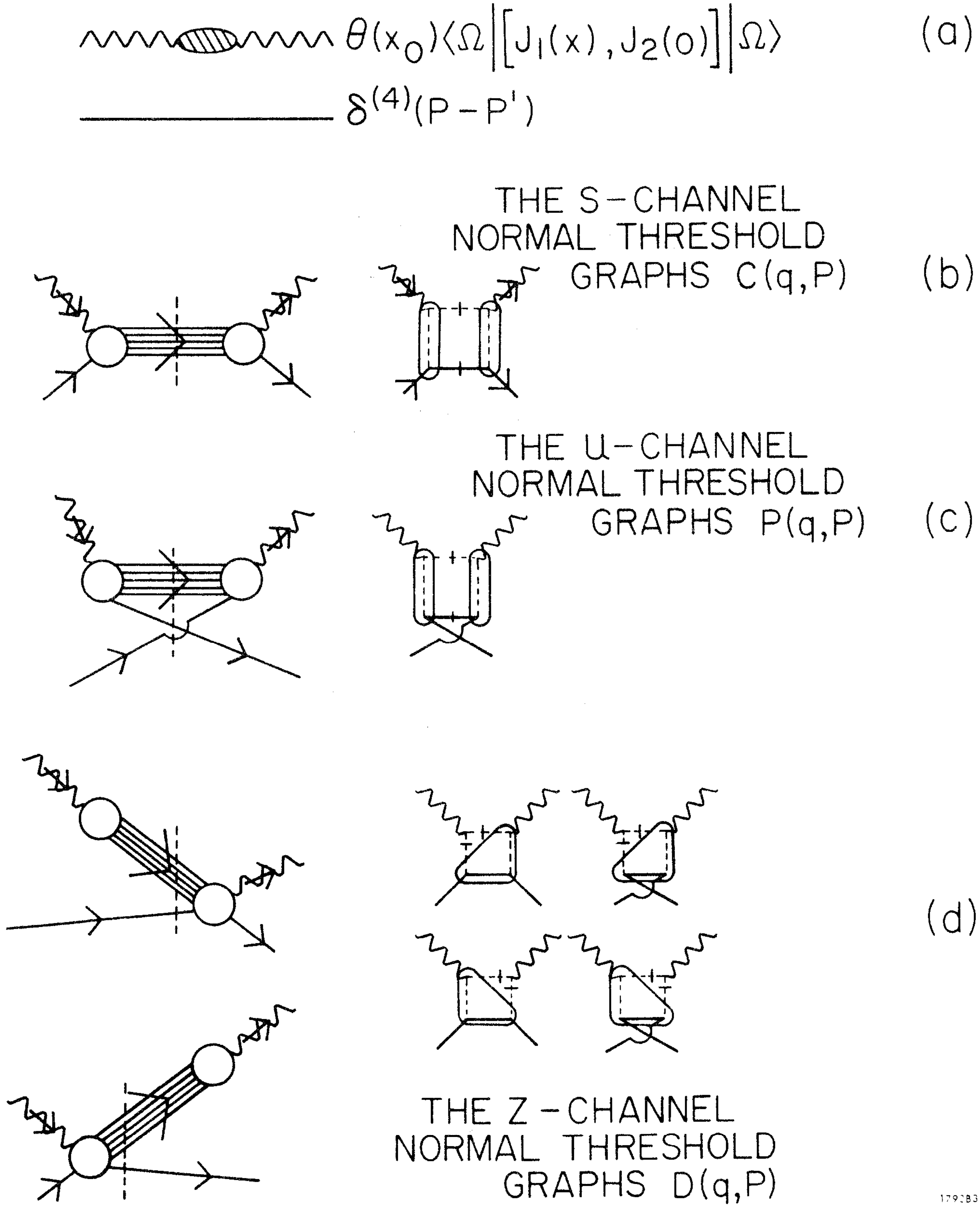

$\theta(x_0)\langle\Omega|[J_1(x), J_2(0)]|\Omega\rangle$
(a)
$\delta^{(4)}(P-P')$
THE S-CHANNEL NORMAL THRESHOLD GRAPHS C(q,P)
(b)
THE U-CHANNEL NORMAL THRESHOLD GRAPHS P(q,P)
(c)
(d)
THE Z-CHANNEL NORMAL THRESHOLD GRAPHS D(q,P)

Fig. 3

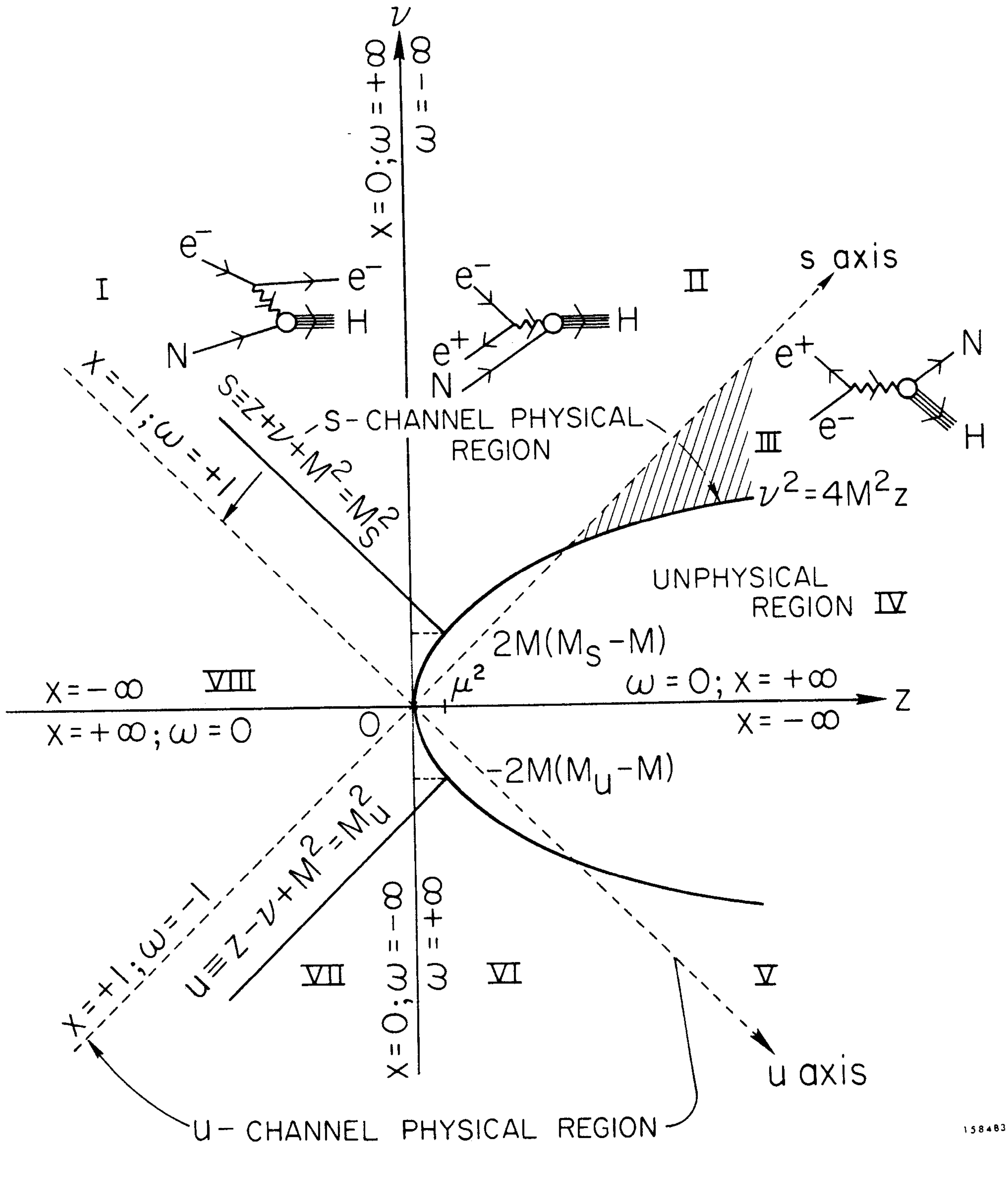
ν
x = 0; ω = +∞
ω = −∞
e⁻
e⁻
H
N
e⁻
e⁺
N
H
I
II
s axis
e⁺
e⁻
N
H
x = −1; ω = +1
S ≡ Z + ν + M² = M_S²
S - CHANNEL PHYSICAL REGION
III
ν² = 4M²z
UNPHYSICAL REGION IV
2M(M_S − M)
μ²
x = −∞
VIII
ω = 0; x = +∞
Z
x = +∞ ; ω = 0
O
x = −∞
−2M(M_u − M)
u ≡ Z − ν + M² = M_u²
x = +1; ω = −1
ω = −∞
ω = +∞
x = 0;
VII
VI
V
u axis
U − CHANNEL PHYSICAL REGION
158483

Fig. 4

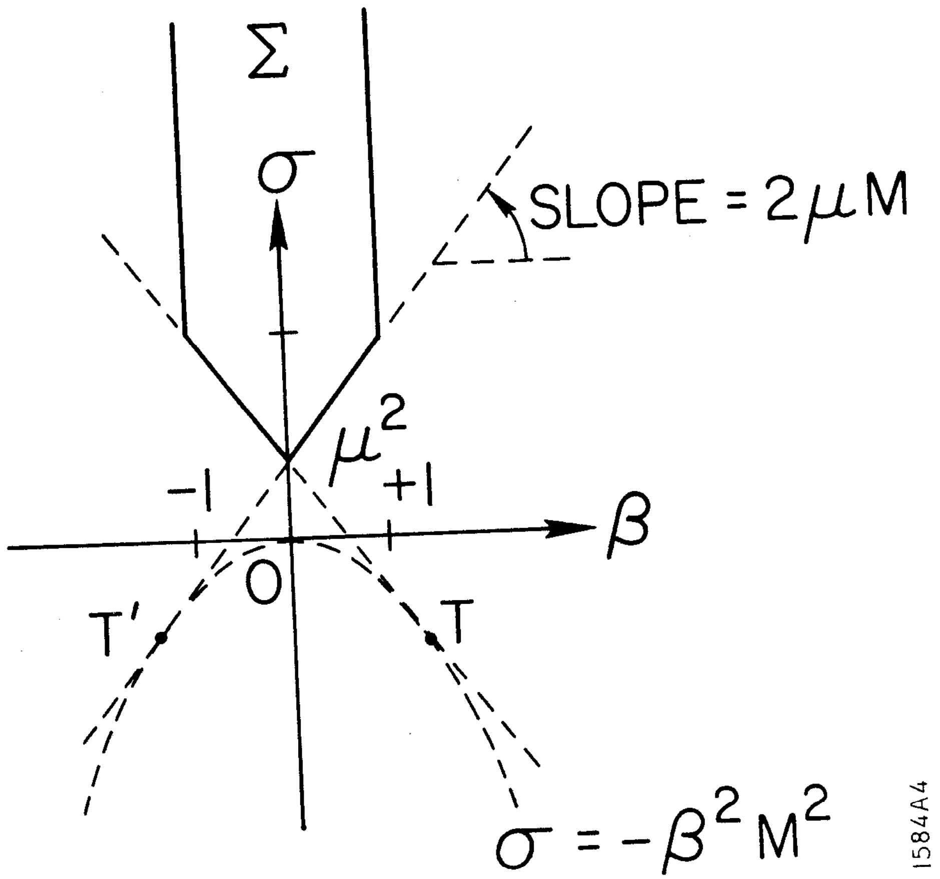

Fig 5

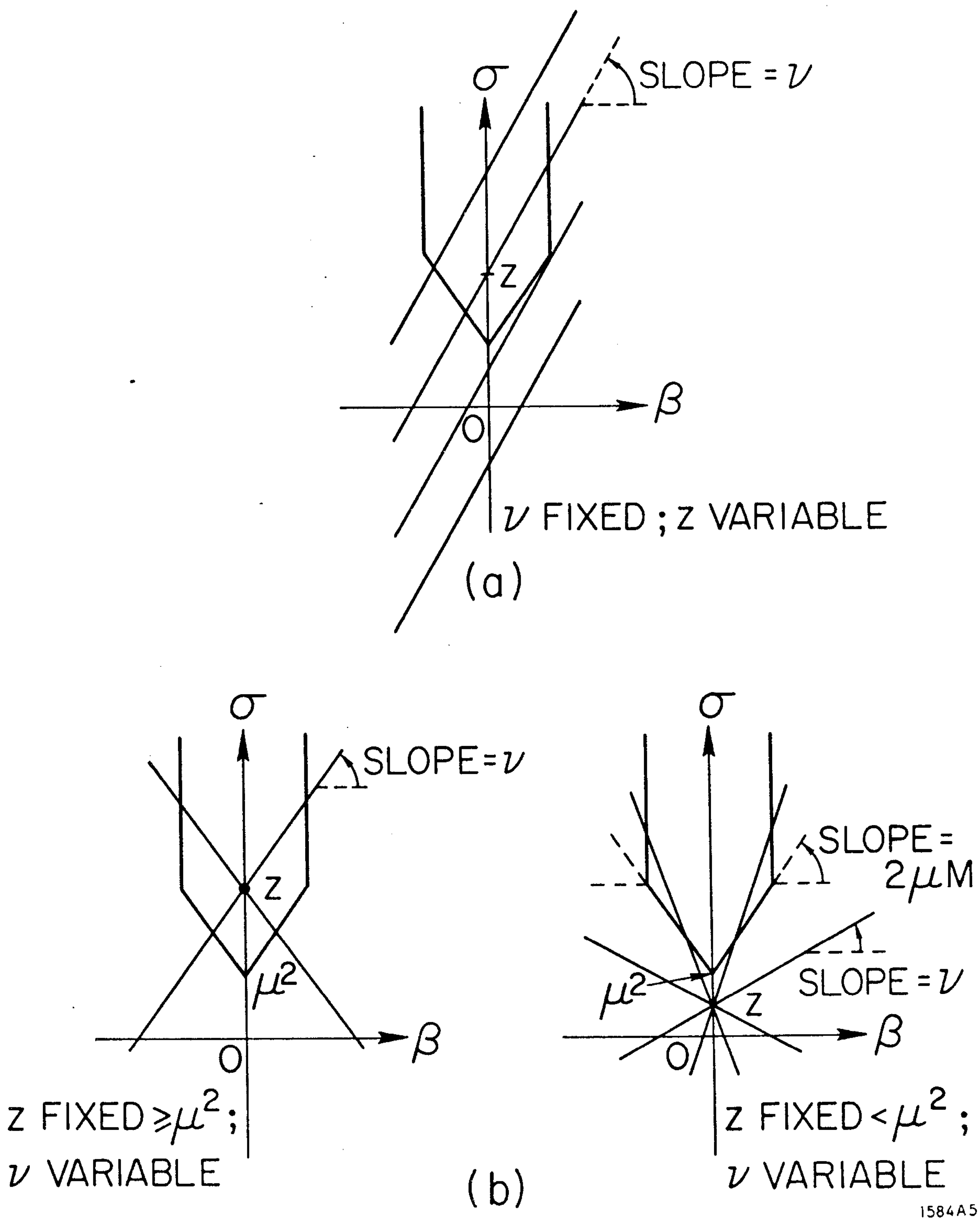

σ
SLOPE = ν
z
O
β
ν FIXED ; z VARIABLE
(a)
σ
SLOPE=ν
z
μ²
O
β
z FIXED ≥μ² ;
ν VARIABLE
σ
SLOPE =
2μM
SLOPE = ν
μ²
z
O
β
z FIXED <μ² ;
ν VARIABLE
(b)
1584A5

Fig. 6

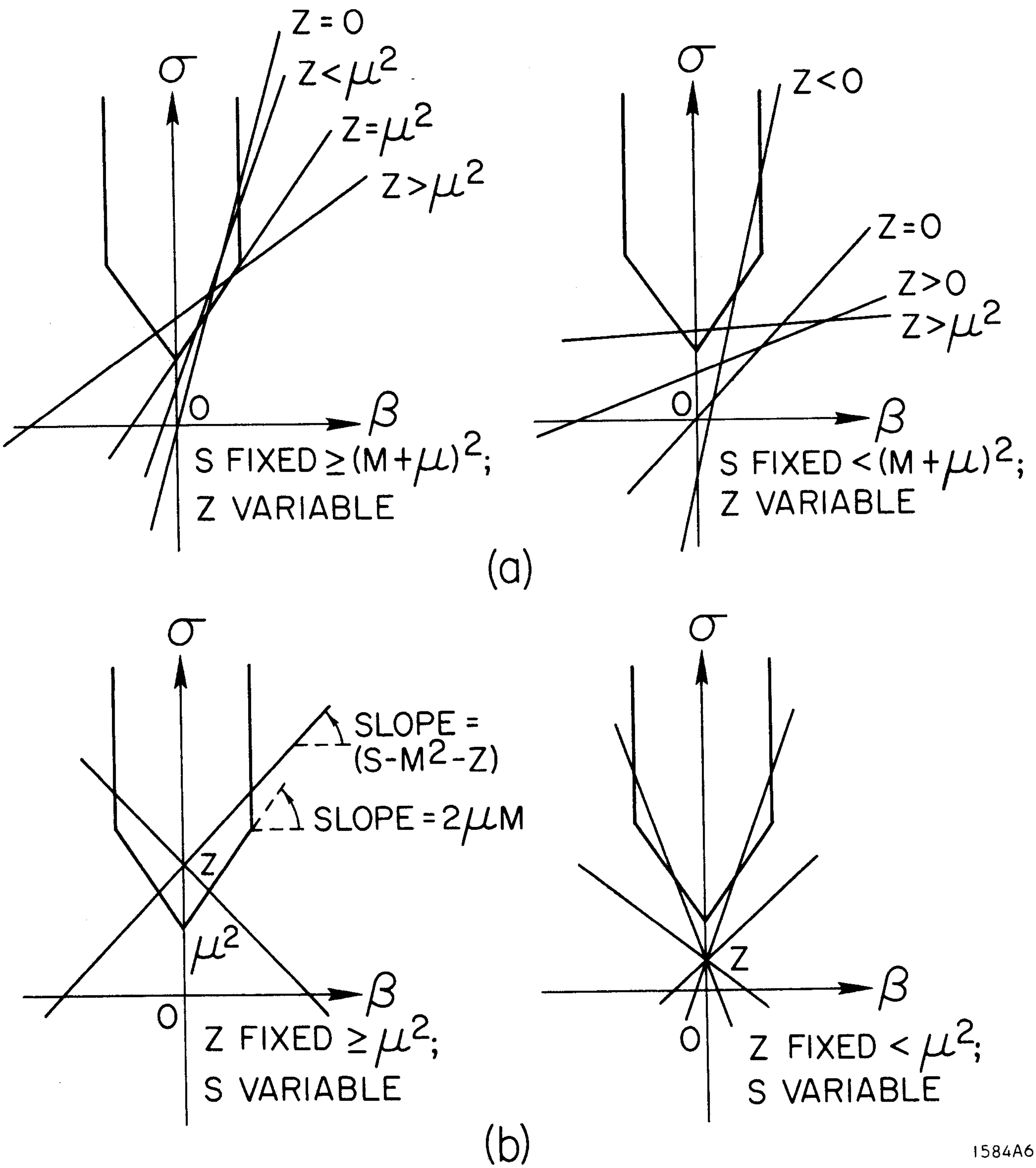

Z = 0
Z < μ²
Z = μ²
Z > μ²
σ
β
0
S FIXED ≥ (M + μ)²;
Z VARIABLE
Z < 0
Z = 0
Z > 0
Z > μ²
S FIXED < (M + μ)²;
Z VARIABLE
(a)
SLOPE =
(S-M²-Z)
SLOPE = 2μM
Z
μ²
Z FIXED ≥ μ²;
S VARIABLE
Z FIXED < μ²;
S VARIABLE
(b)
1584A6

Fig. 7

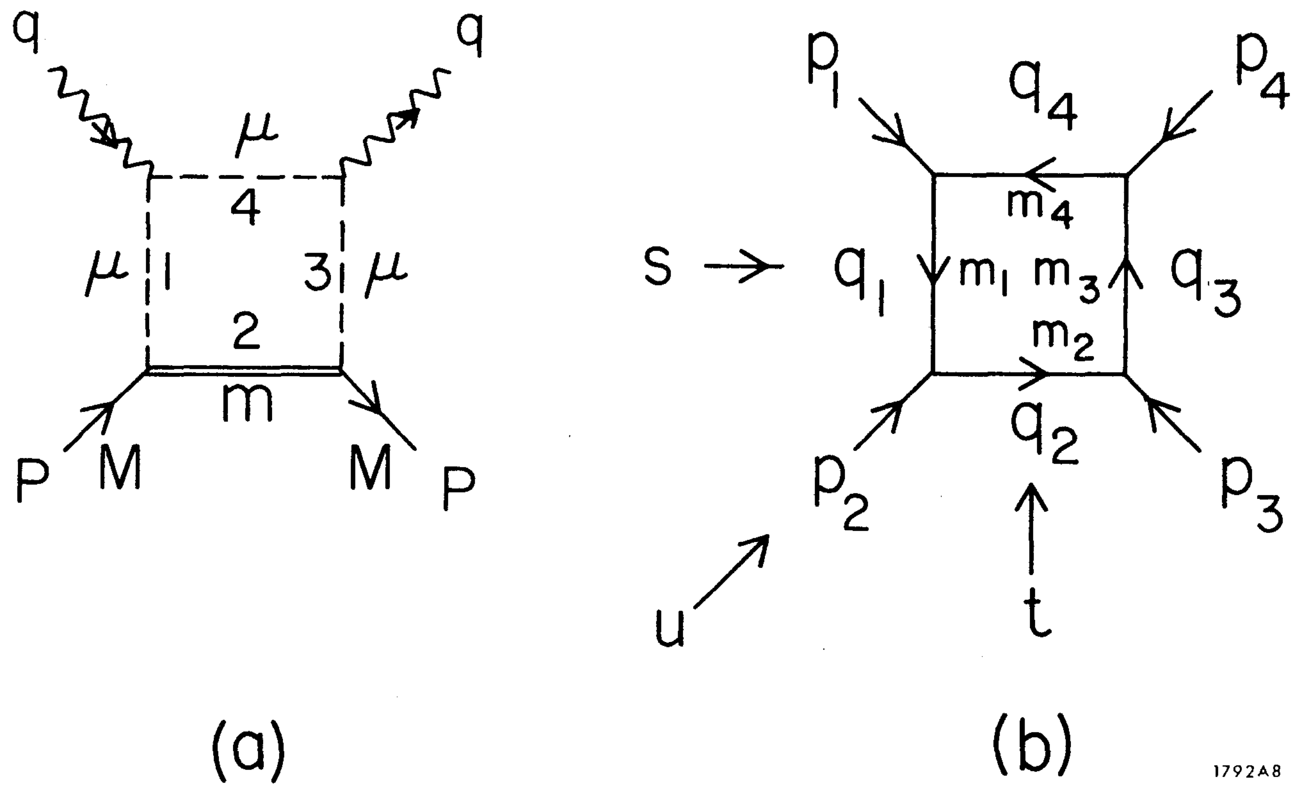

Fig. 8

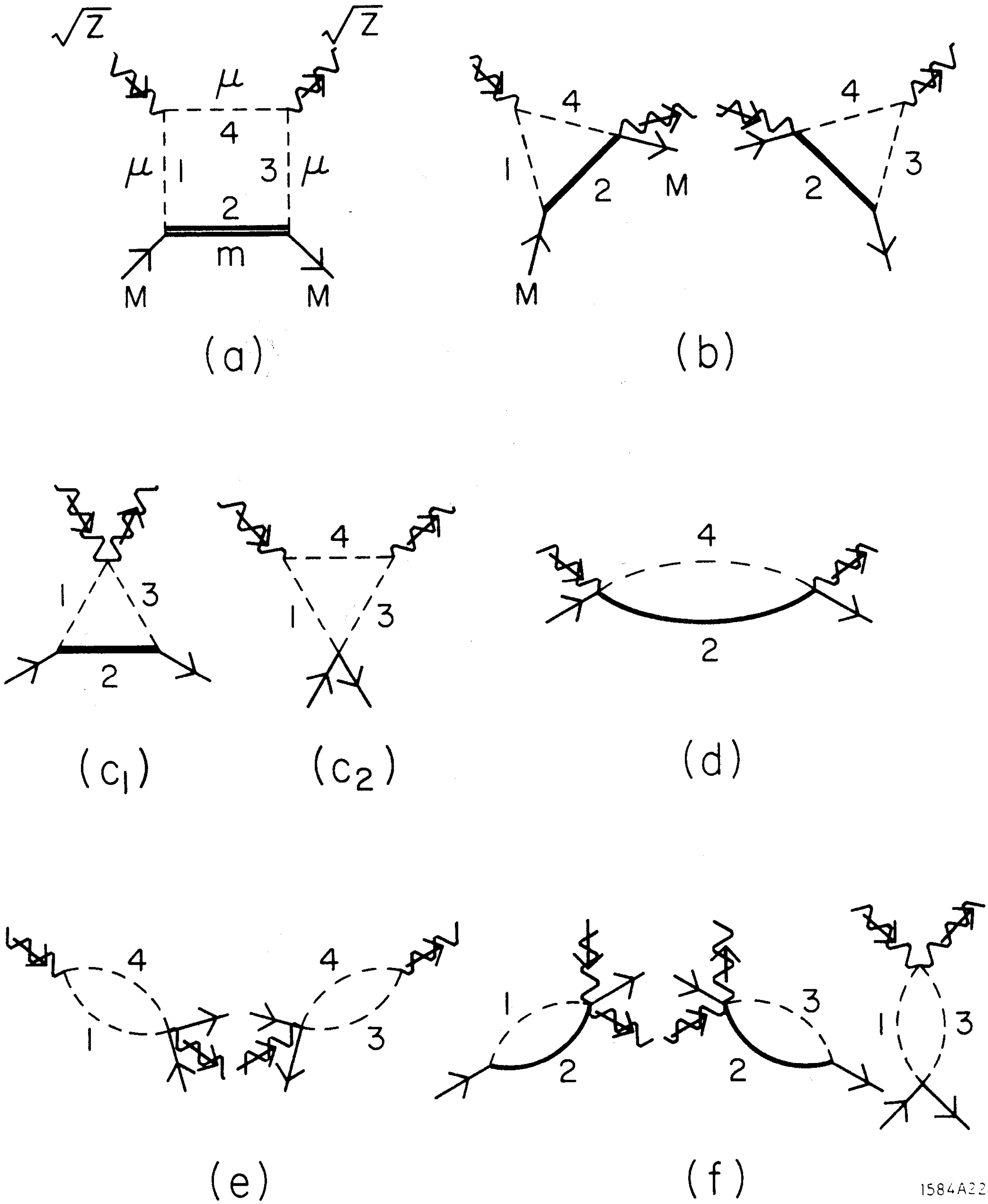

Fig. 9

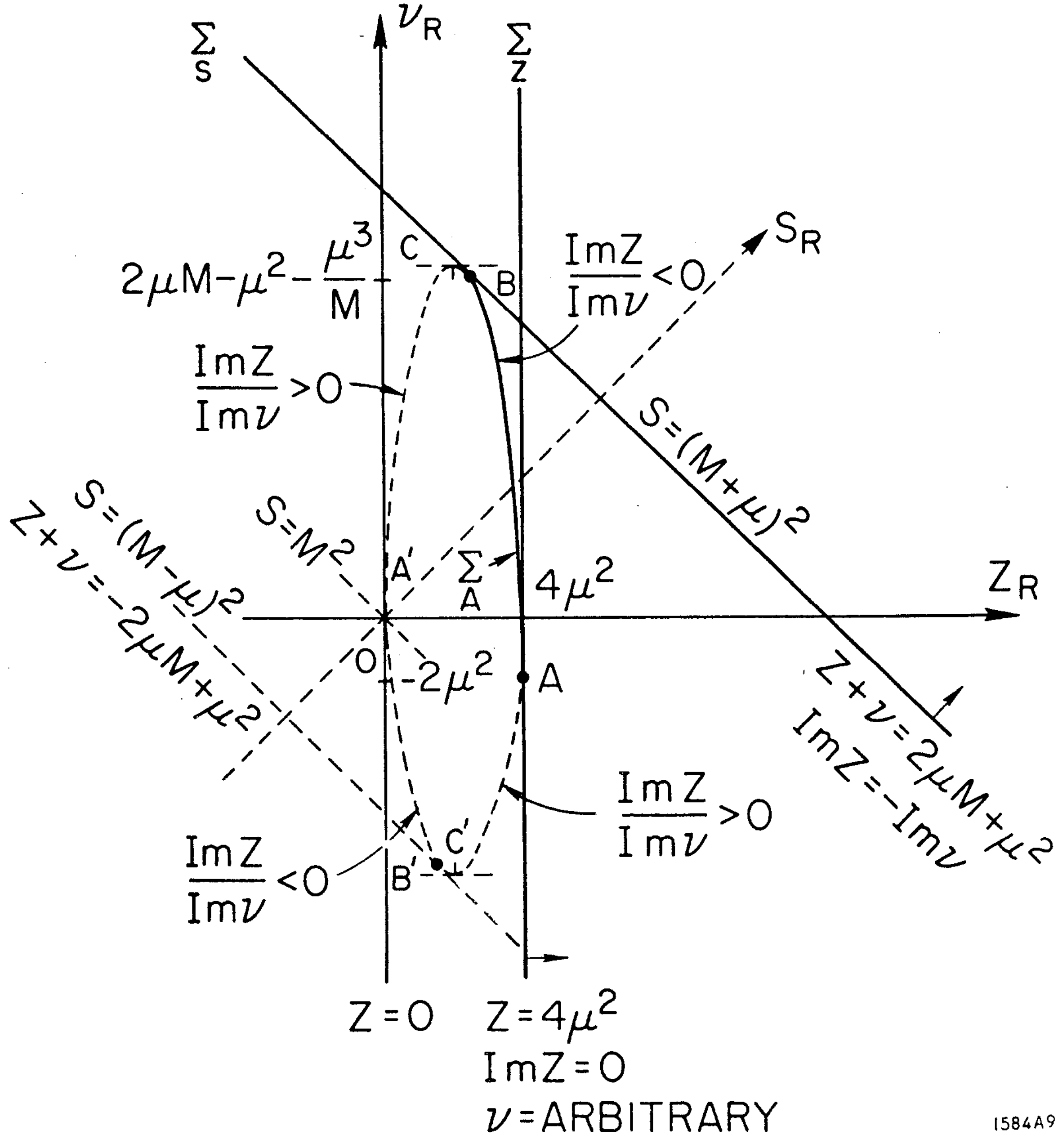

ν_R
Σ_S
Σ_Z
S_R
Z_R
$2\mu M-\mu^2-\frac{\mu^3}{M}$
C
B
$\frac{\mathrm{Im}Z}{\mathrm{Im}\nu}<0$
$\frac{\mathrm{Im}Z}{\mathrm{Im}\nu}>0$
$S=(M+\mu)^2$
$S=(M-\mu)^2$
$S=M^2$
$Z+\nu=-2\mu M+\mu^2$
A'
Σ_A
$4\mu^2$
O
$-2\mu^2$
A
$Z+\nu=2\mu M+\mu^2$
$\mathrm{Im}Z=-\mathrm{Im}\nu$
$\frac{\mathrm{Im}Z}{\mathrm{Im}\nu}>0$
C'
$\frac{\mathrm{Im}Z}{\mathrm{Im}\nu}<0$
B'
$Z=0$
$Z=4\mu^2$
$\mathrm{Im}Z=0$
ν=ARBITRARY
1584A9

Fig. 10

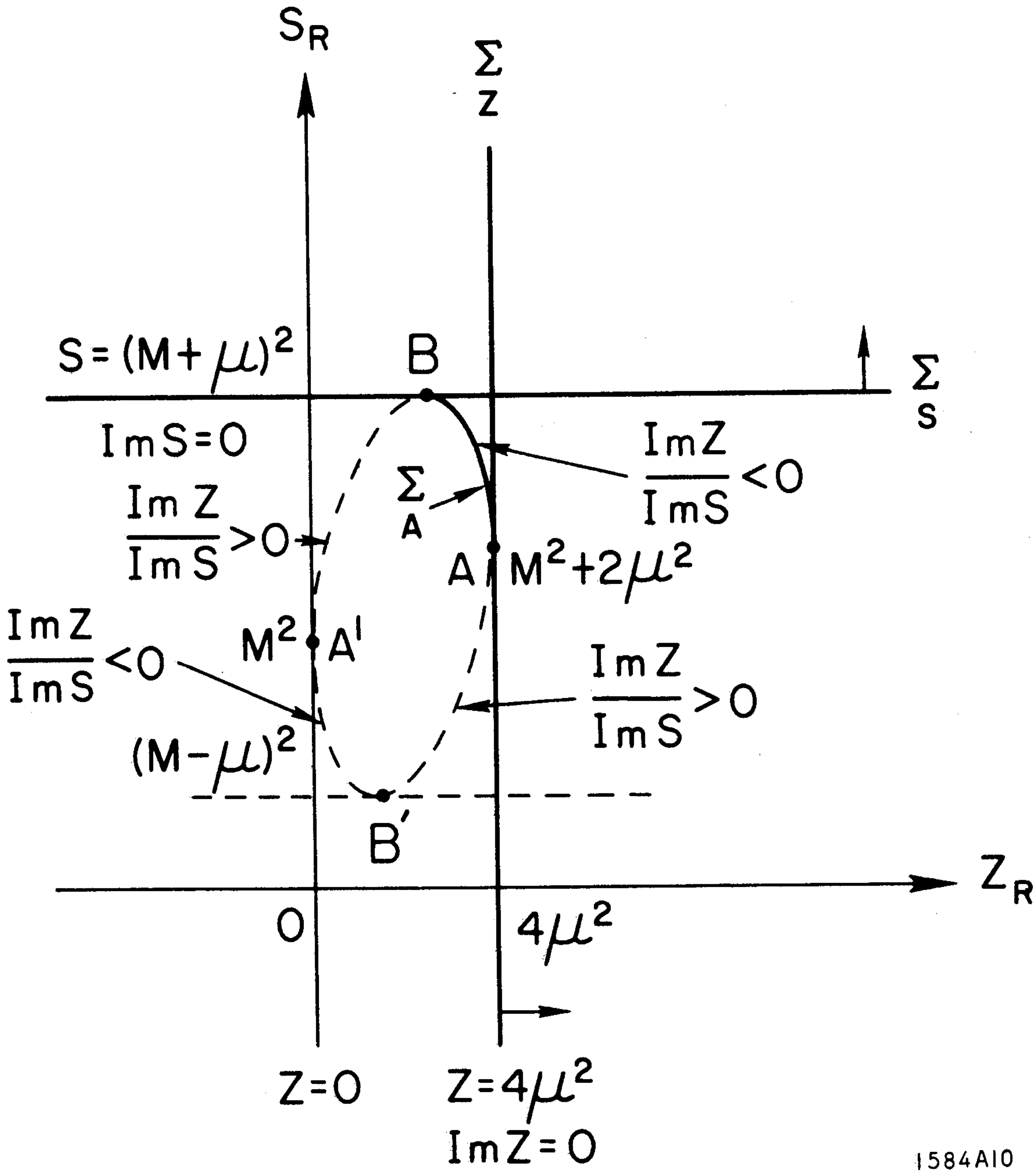

S_R
Σ_Z
$S=(M+\mu)^2$
B
Σ_S
$\mathrm{Im}S=0$
$\frac{\mathrm{Im}Z}{\mathrm{Im}S}<0$
Σ_A
$\frac{\mathrm{Im}Z}{\mathrm{Im}S}>0$
A
$M^2+2\mu^2$
$\frac{\mathrm{Im}Z}{\mathrm{Im}S}<0$
M^2
A'
$\frac{\mathrm{Im}Z}{\mathrm{Im}S}>0$
$(M-\mu)^2$
B'
Z_R
0
$4\mu^2$
$Z=0$
$Z=4\mu^2$
$\mathrm{Im}Z=0$
1584A10

Fig. 11

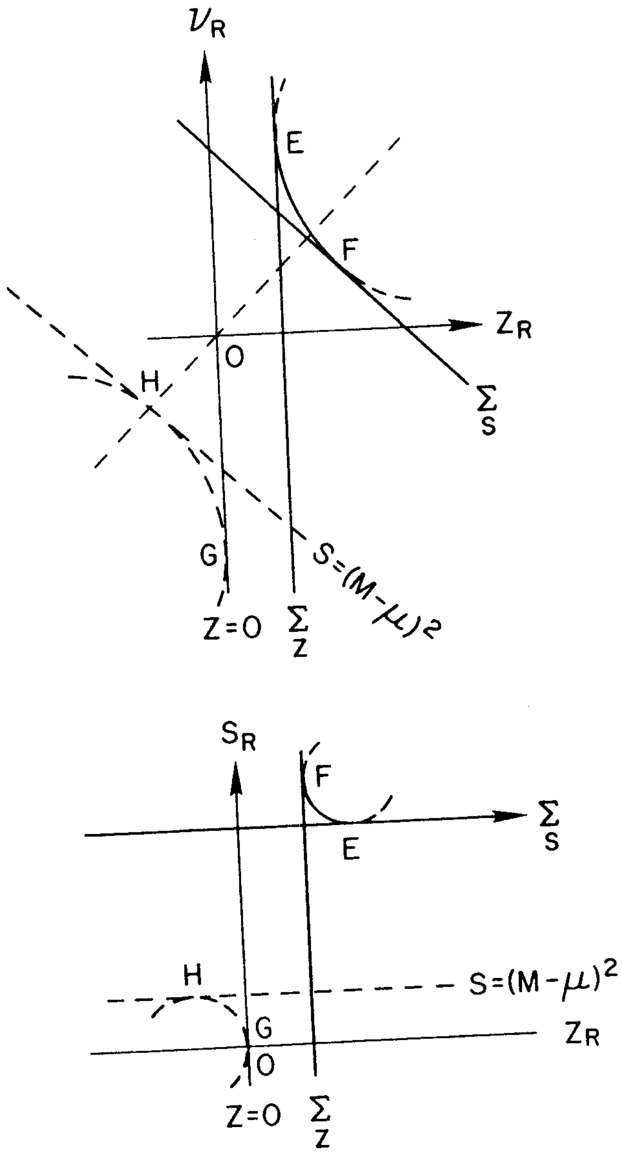

(a)

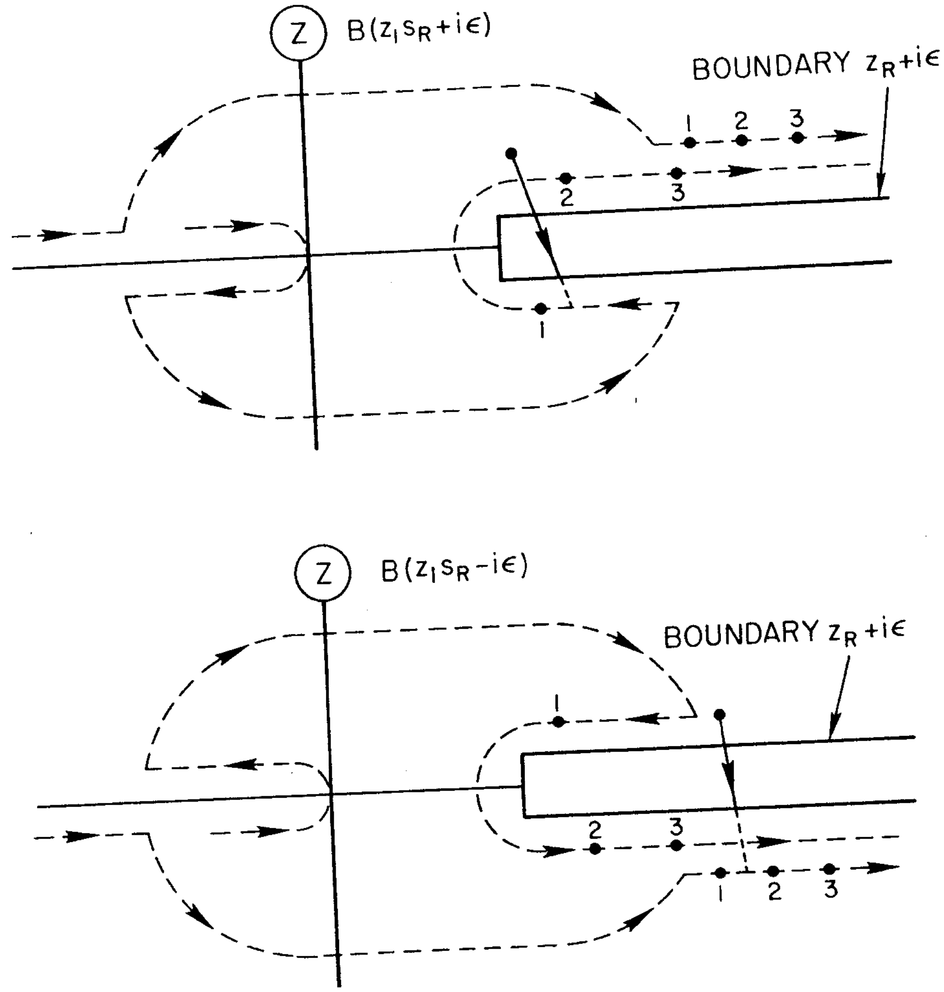

(b)

1792B12

Fig. 12

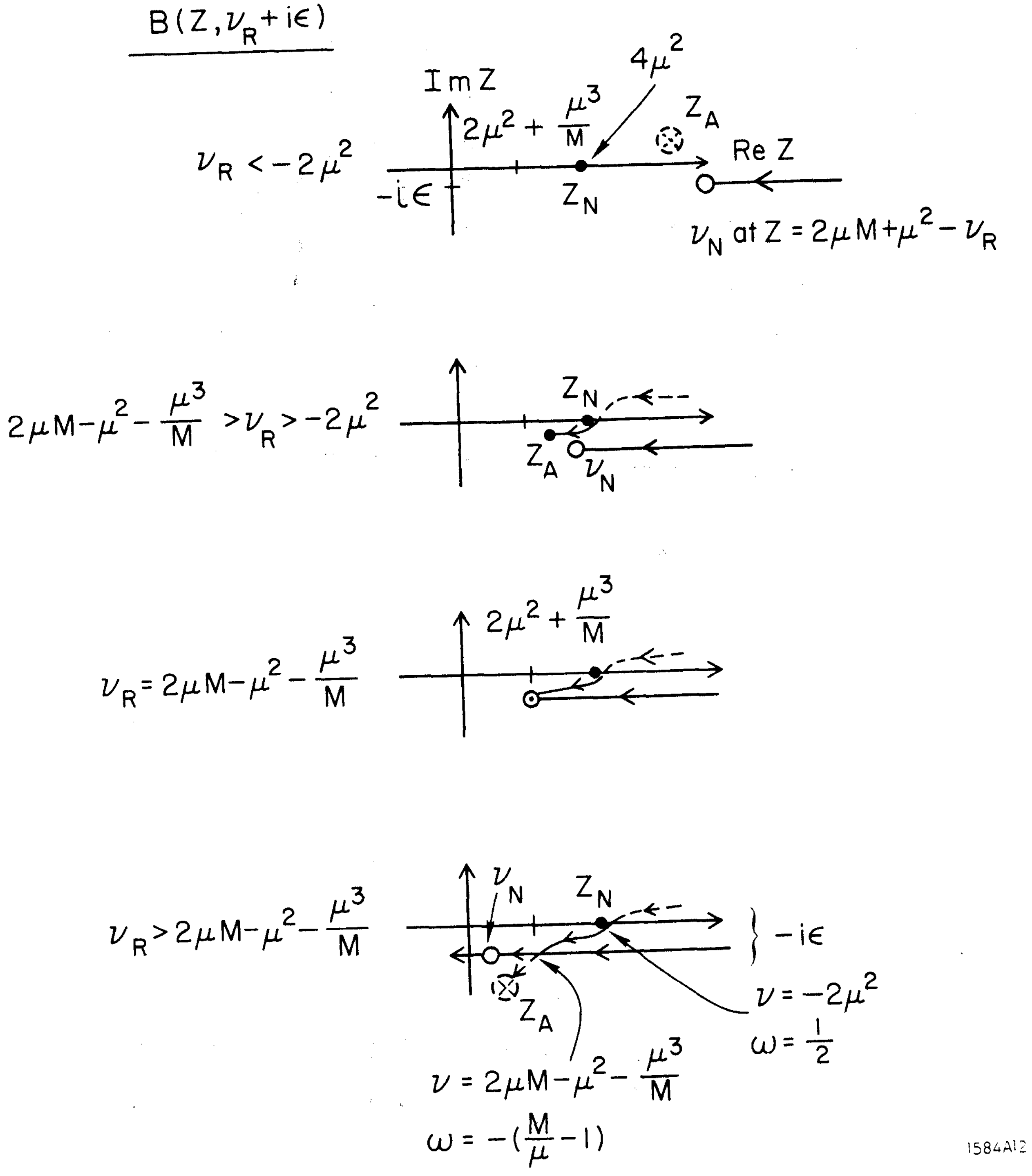

B(Z, ν_R + iε)
Im Z
4μ^2
2μ^2 + μ^3/M
Z_A
Re Z
ν_R < −2μ^2
−iε
Z_N
ν_N at Z = 2μM + μ^2 − ν_R
Z_N
2μM − μ^2 − μ^3/M > ν_R > −2μ^2
Z_A
ν_N
2μ^2 + μ^3/M
ν_R = 2μM − μ^2 − μ^3/M
ν_N
Z_N
ν_R > 2μM − μ^2 − μ^3/M
−iε
Z_A
ν = −2μ^2
ω = 1/2
ν = 2μM − μ^2 − μ^3/M
ω = −(M/μ − 1)
1584A12

Fig. 13A

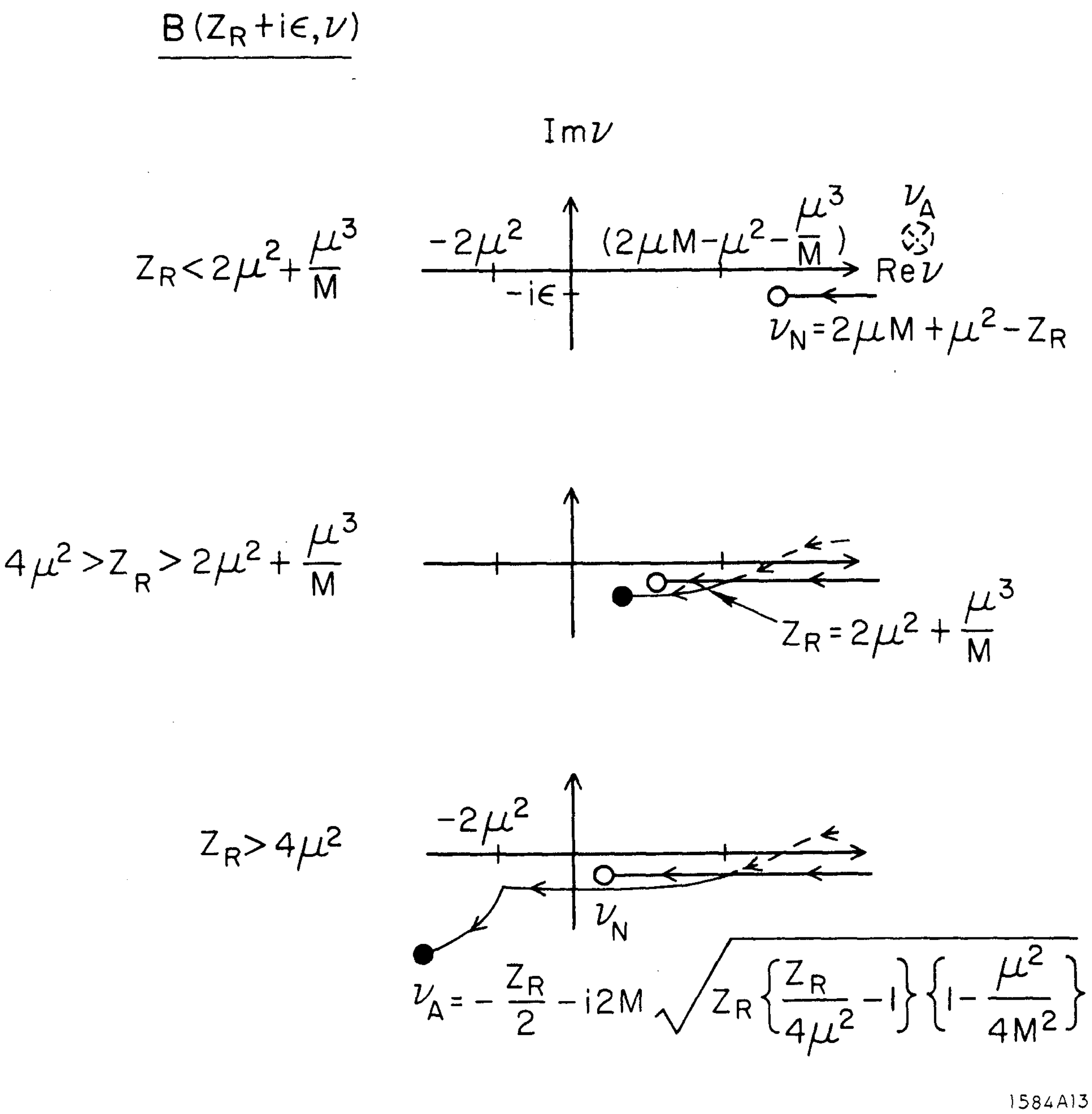

B(Z_R+iε,ν)
Imν
Z_R<2μ²+μ³/M
−2μ²
(2μM−μ²−μ³/M)
ν_A
Reν
−iε
ν_N=2μM+μ²−Z_R
4μ²>Z_R>2μ²+μ³/M
Z_R=2μ²+μ³/M
Z_R>4μ²
−2μ²
ν_N
ν_A=−Z_R/2−i2M√(Z_R{Z_R/4μ²−1}{1−μ²/4M²})
1584A13

Fig. 13B

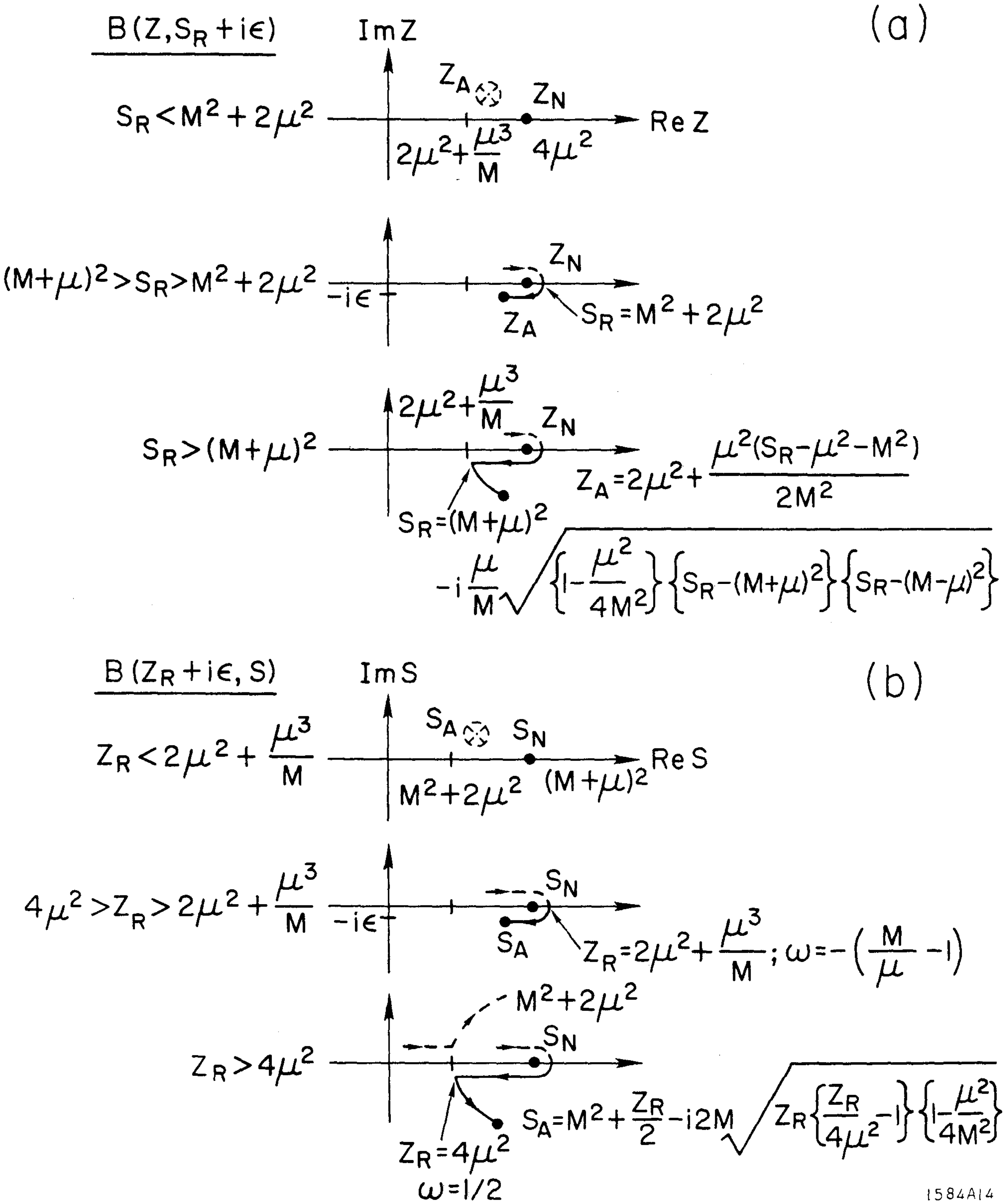

(a)
B(Z,S_R + iε)
Im Z
S_R < M² + 2μ²
Z_A
Z_N
Re Z
2μ² + μ³/M
4μ²
(M+μ)² > S_R > M² + 2μ²
-iε
Z_A
S_R = M² + 2μ²
S_R > (M+μ)²
2μ² + μ³/M
S_R = (M+μ)²
Z_A = 2μ² + μ²(S_R − μ² − M²)/2M² − i (μ/M) √({1 − μ²/4M²}{S_R − (M+μ)²}{S_R − (M−μ)²})
(b)
B(Z_R + iε, S)
Im S
Z_R < 2μ² + μ³/M
S_A
S_N
Re S
M² + 2μ²
(M+μ)²
4μ² > Z_R > 2μ² + μ³/M
-iε
S_A
Z_R = 2μ² + μ³/M ; ω = −(M/μ − 1)
M² + 2μ²
Z_R > 4μ²
S_N
S_A = M² + Z_R/2 − i2M √(Z_R {Z_R/4μ² − 1}{1 − μ²/4M²})
Z_R = 4μ²
ω = 1/2
1584A14

Fig. 14

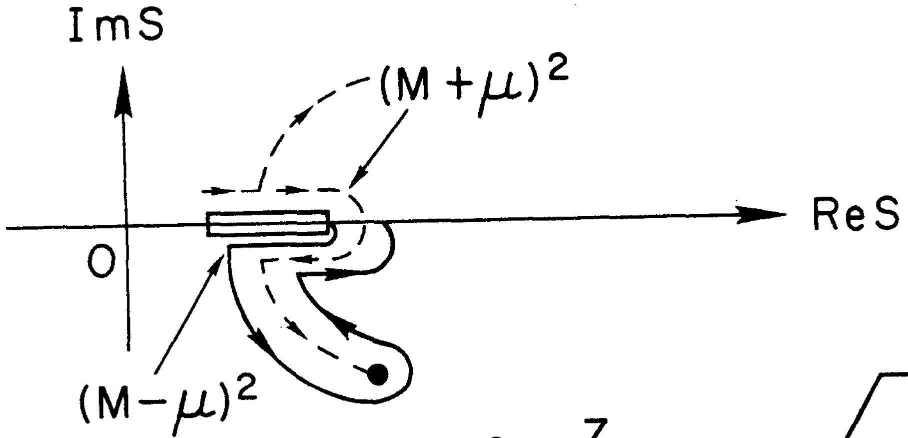

$$S = M^2 + \frac{Z}{2} - i2M\sqrt{Z\left\{\frac{Z}{4\mu^2}-1\right\}\left\{1-\frac{\mu^2}{4M^2}\right\}}$$

1584A15

Fig. 15

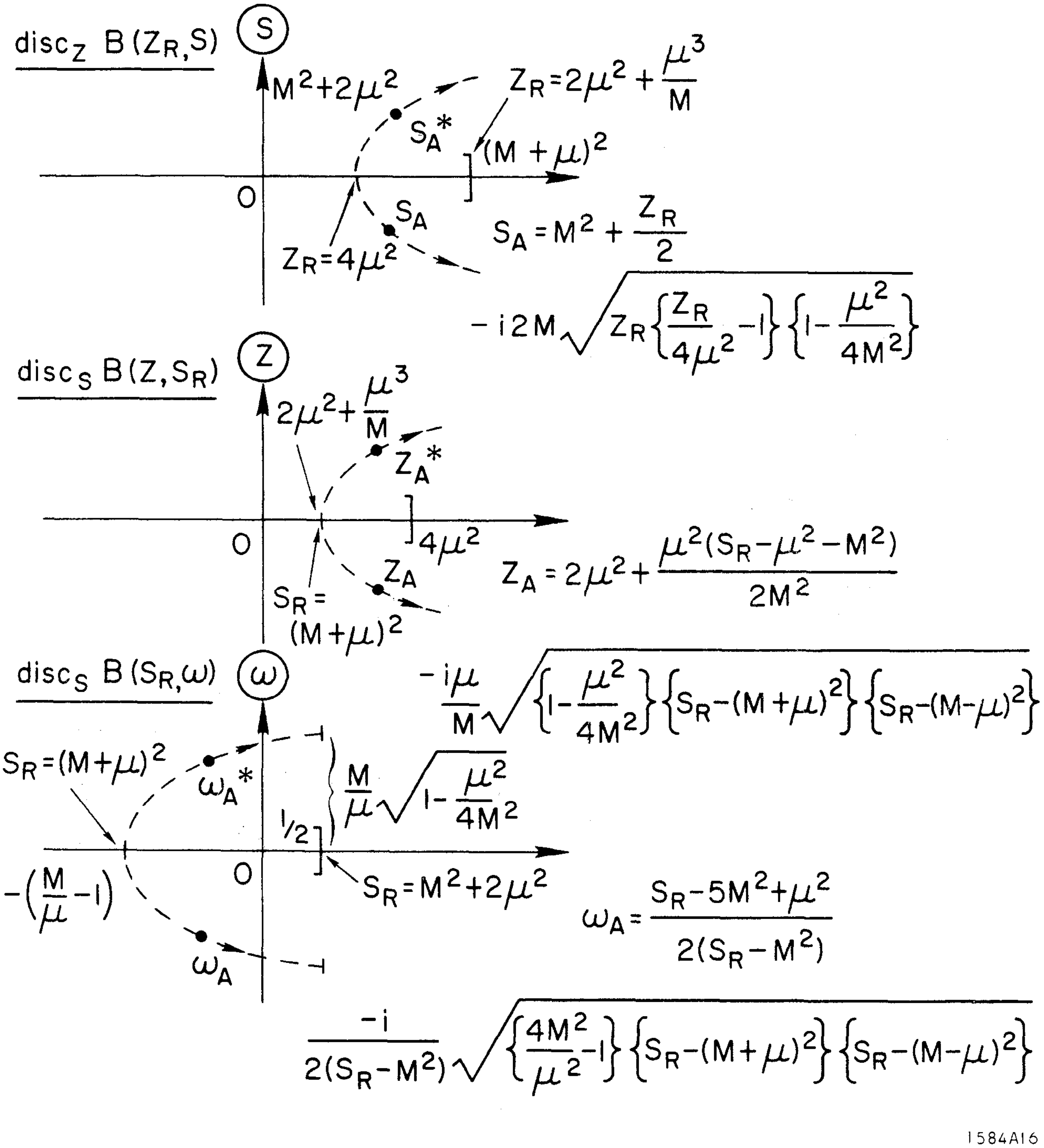

$\mathrm{disc}_Z\, B(Z_R, S)$
S
$M^2+2\mu^2$
$Z_R = 2\mu^2 + \frac{\mu^3}{M}$
S_A^*
$(M+\mu)^2$
0
S_A
$Z_R = 4\mu^2$
$S_A = M^2 + \frac{Z_R}{2}$
$-i2M\sqrt{Z_R\left\{\frac{Z_R}{4\mu^2}-1\right\}\left\{1-\frac{\mu^2}{4M^2}\right\}}$
$\mathrm{disc}_S\, B(Z, S_R)$
Z
$2\mu^2+\frac{\mu^3}{M}$
Z_A^*
0
$4\mu^2$
Z_A
$Z_A = 2\mu^2 + \frac{\mu^2(S_R-\mu^2-M^2)}{2M^2}$
$S_R = (M+\mu)^2$
$\mathrm{disc}_S\, B(S_R, \omega)$
ω
$-\frac{i\mu}{M}\sqrt{\left\{1-\frac{\mu^2}{4M^2}\right\}\left\{S_R-(M+\mu)^2\right\}\left\{S_R-(M-\mu)^2\right\}}$
$S_R = (M+\mu)^2$
ω_A^*
$\frac{M}{\mu}\sqrt{1-\frac{\mu^2}{4M^2}}$
$1/2$
$-\left(\frac{M}{\mu}-1\right)$
0
$S_R = M^2+2\mu^2$
$\omega_A = \frac{S_R-5M^2+\mu^2}{2(S_R-M^2)}$
ω_A
$\frac{-i}{2(S_R-M^2)}\sqrt{\left\{\frac{4M^2}{\mu^2}-1\right\}\left\{S_R-(M+\mu)^2\right\}\left\{S_R-(M-\mu)^2\right\}}$
1584A16

Fig. 16

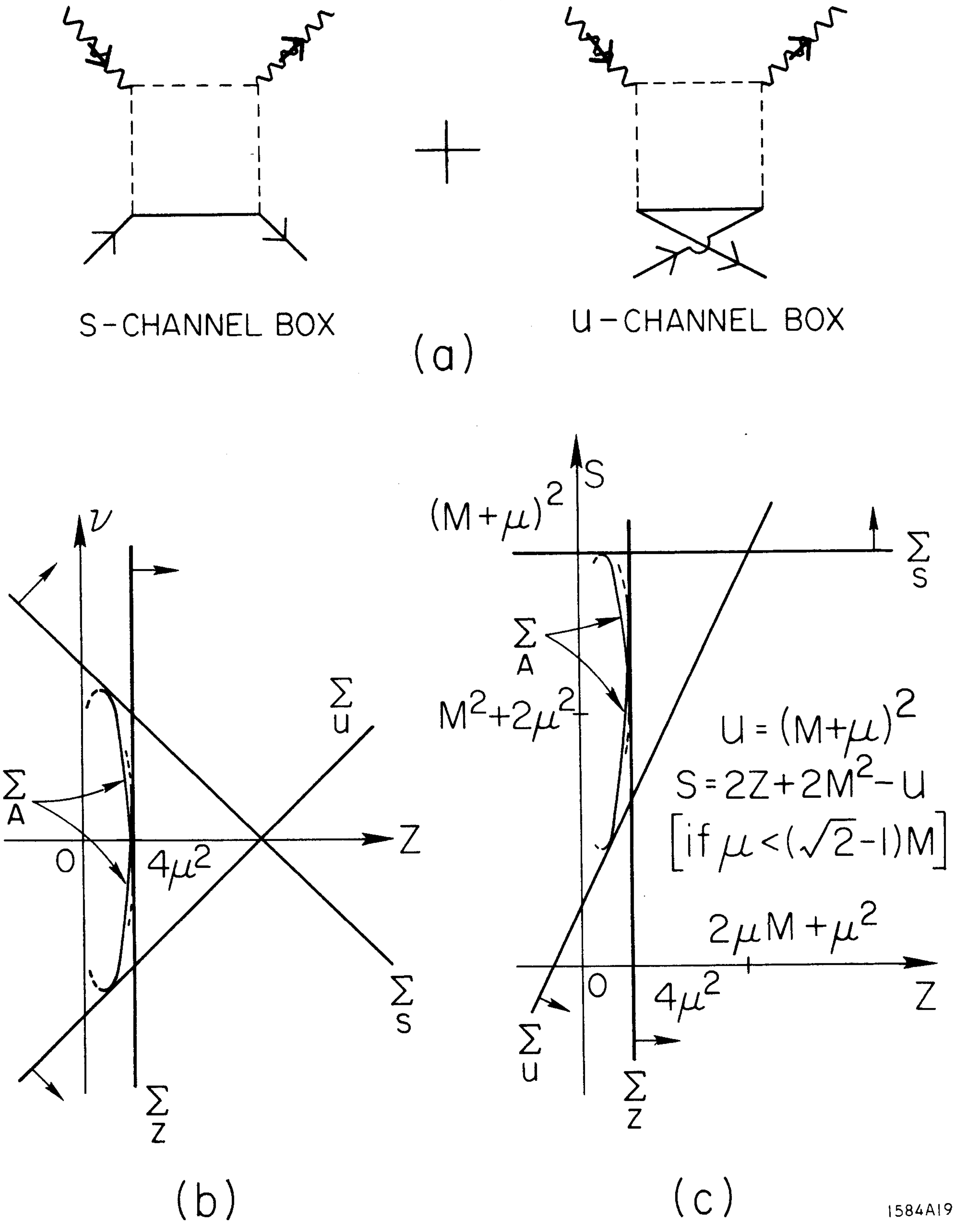

S-CHANNEL BOX
U-CHANNEL BOX
(a)
ν
Σ
u
Σ
A
0
4μ²
Z
Σ
s
Σ
z
(b)
S
(M+μ)²
Σ
s
Σ
A
M²+2μ²
U = (M+μ)²
S = 2Z+2M²−U
[if μ < (√2−1)M]
2μM+μ²
0
4μ²
Z
Σ
u
Σ
z
(c)
1584A19

Fig. 17

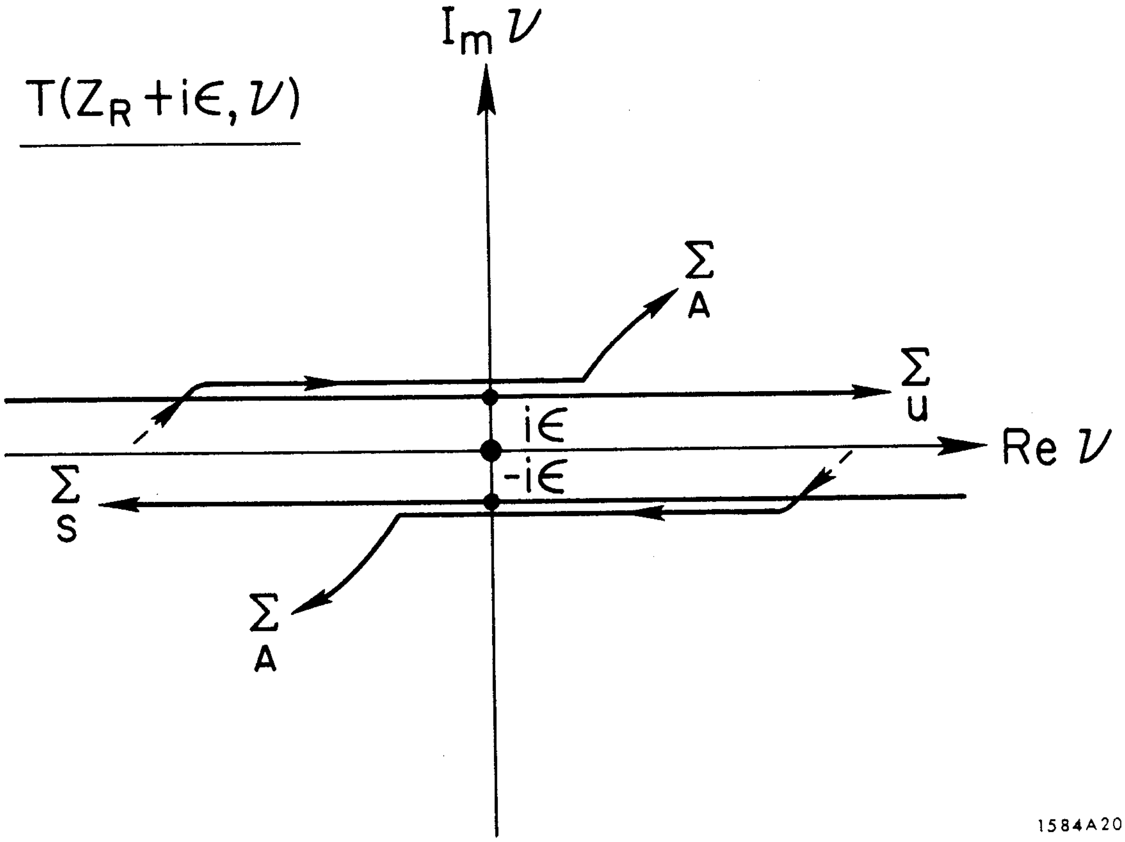

$T(Z_R + i\epsilon, \nu)$
$I_m \nu$
Σ_A
Σ_u
$i\epsilon$
Re ν
$-i\epsilon$
Σ_s
Σ_A
1584A20

Fig. 18

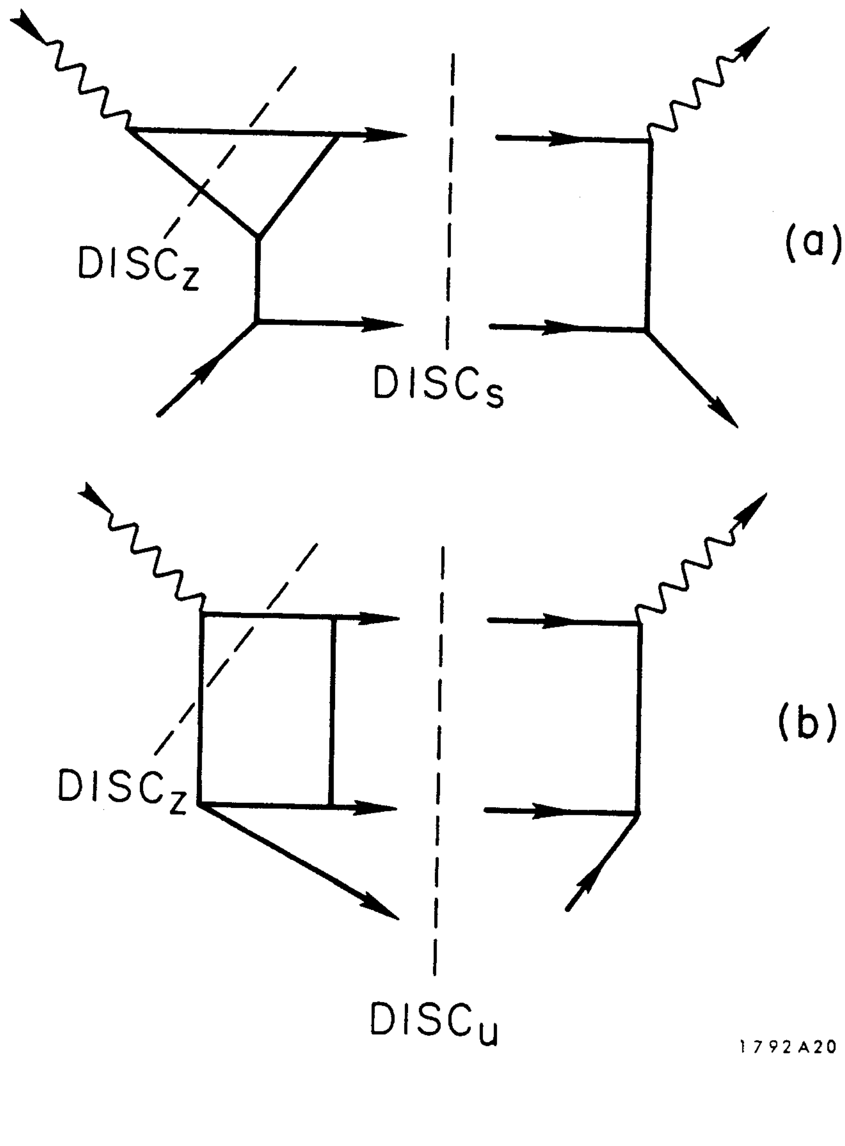

Fig. 19

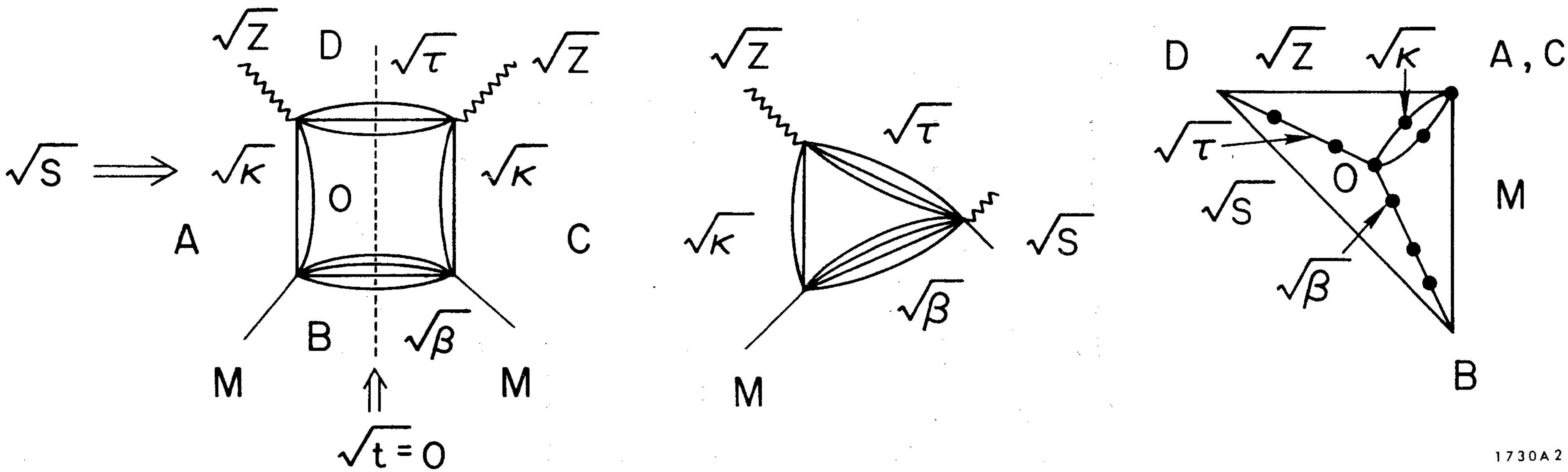
$\sqrt{Z}$
D
$\sqrt{\tau}$
$\sqrt{Z}$
$\sqrt{S}$
$\sqrt{\kappa}$
O
$\sqrt{\kappa}$
A
C
B
$\sqrt{\beta}$
M
M
$\sqrt{t} = 0$
$\sqrt{Z}$
$\sqrt{\tau}$
$\sqrt{\kappa}$
$\sqrt{S}$
$\sqrt{\beta}$
M
D
$\sqrt{Z}$
$\sqrt{\kappa}$
A, C
$\sqrt{\tau}$
O
$\sqrt{S}$
M
$\sqrt{\beta}$
B
1730A2

Fig. 20

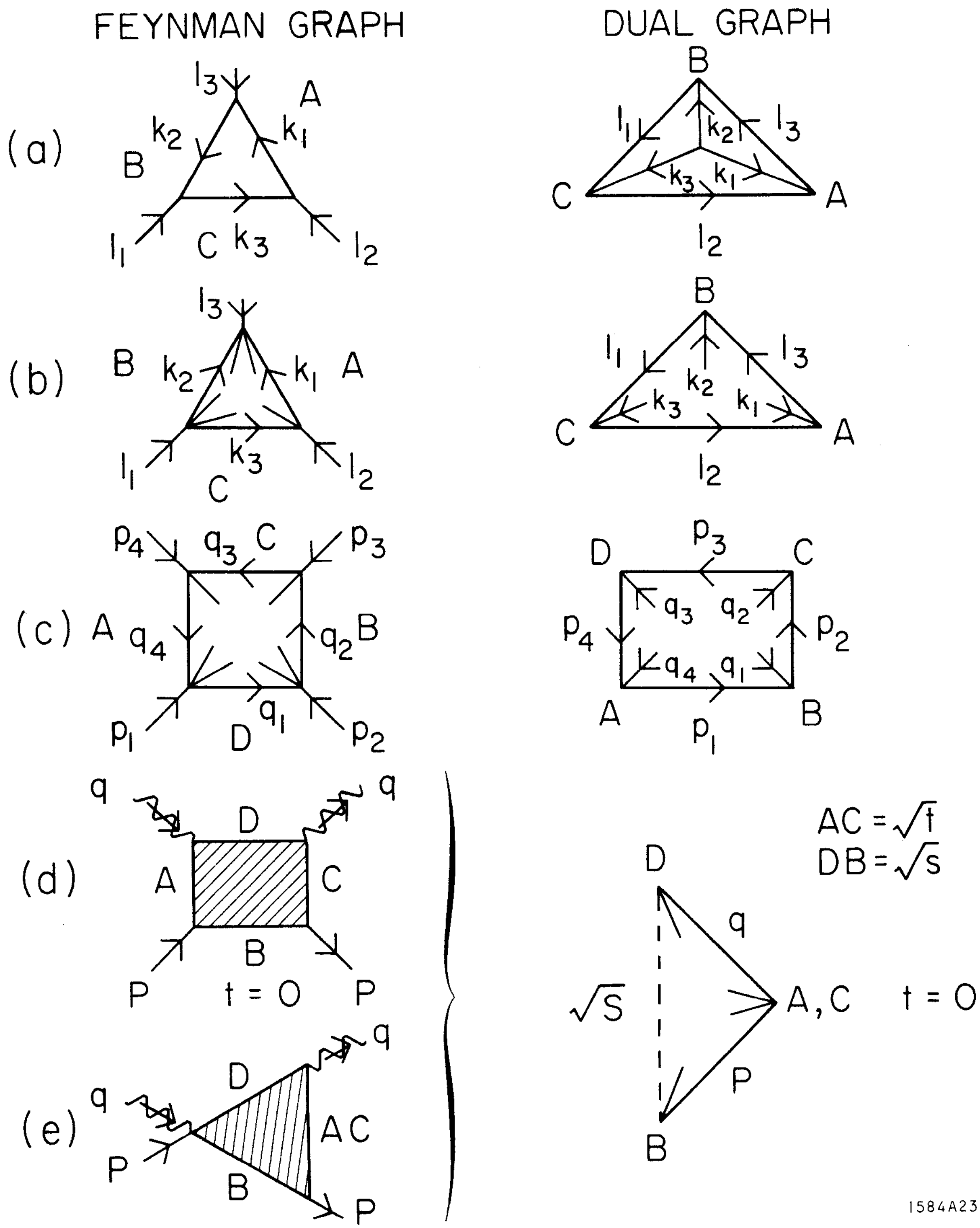

FEYNMAN GRAPH
DUAL GRAPH
(a)
(b)
(c)
(d)
(e)
$AC = \sqrt{t}$
$DB = \sqrt{s}$
$\sqrt{S}$
A, C
t = 0
1584A23

Fig. 21

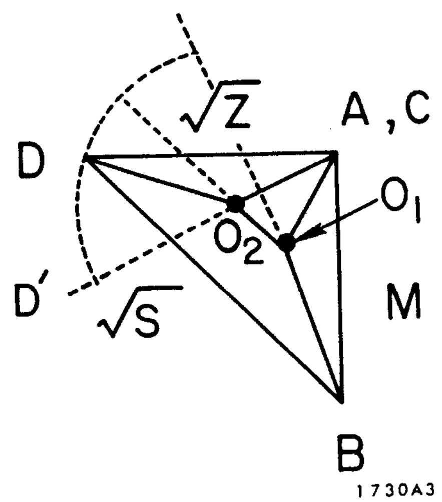

Fig. 22

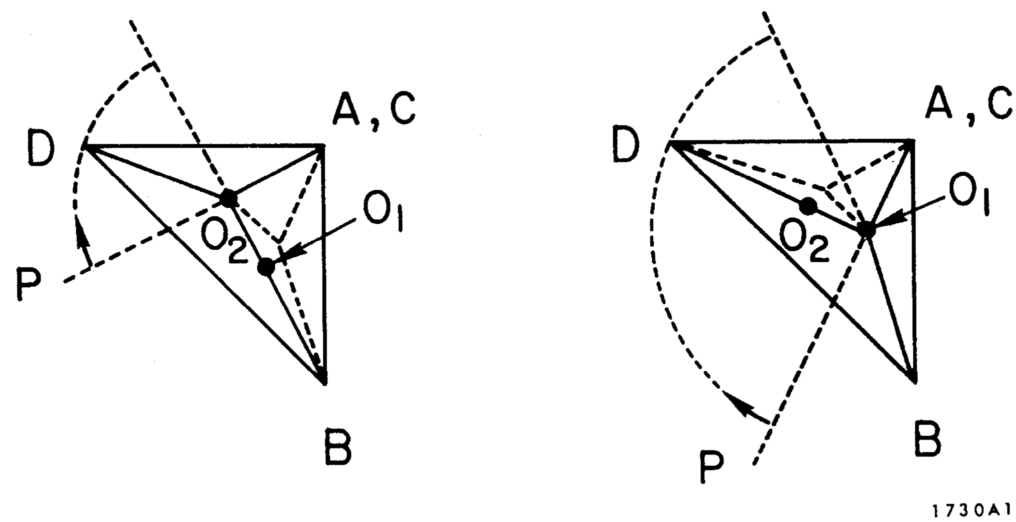

Fig. 23